An Energy Flow Simulation Tool for Incorporating Short-Term PV Forecasting in a Diesel-PV-Battery Off-Grid Power Supply System

Taskin Jamal[*], Craig Carter[*], Thomas Schmidt[#], GM Shafiullah[*], Martina Calais[*], Tania Urmee[*]

*College of Science, Health, Engineering and Education, Murdoch University, WA 6150, Australia

[#]DLR Institute of Networked Energy Systems, Energy Systems Analysis, 26122 Oldenburg, Germany

Abstract

One of the primary technical challenges of integrating high levels of PV generation into standalone off-grid power supply systems is their variable power output characteristics. In dealing with this issue, the integration of reliable PV forecasting techniques and preferably energy storage, are highly effective. Applying a short-term PV forecasting method, together with a compensatory controllable resource, can help in the management of system operation. This study incorporates the development of an energy flow modelling tool that has been used to analyse the benefits of 1-minute ahead PV forecasting and battery storage for different system configurations. Based on the five days of 1-minute ahead forecasting results analysed, it is found that PV forecasting enables the prosumer to install more than double the PV capacity, compared to the allowed installed PV capacity when no forecasting is employed. This additional PV capacity saves around 24-25% (on average) of diesel fuel per day for the diesel-PV-battery configuration. The outcomes evidently indicate that incorporating 1-minute ahead PV forecasting enables a significant increase of PV hosting capacity of the system, without compromising the reliability of the system.

Keywords: Energy flow modelling tool, Short-term PV forecasting, PV hosting capacity, PV penetration level, Standalone off-grid power supply system, remote area electricity

1. Introduction

Across the world, electricity access in remote and rural areas has always been economically and technically challenging due to the long distances between the load centres and their nearest power grid line and substation, low load densities and challenging topography [1]. Predominantly, diesel generators (DG) are used to meet the load demands for these areas due to their convenience and economic advantages [2, 3]. Nevertheless, solar PV systems are the most widely used and the fastest growing off-grid renewable energy technology (RET) deployed in these off-grid type power supply systems. This is due to the abundance of solar irradiance available in most parts of the world, and the rapidly decreasing cost of PV technologies [4].

One of the primary technical challenges of integrating PV systems into power supply systems is their variable power output characteristics. This variability is due to diurnal and seasonal impacts together with random cloud movements [1]. As it might be perceived as an inconsistent resource, PV power raises a grid integration concern, in particular, due to the difficulty of dispatching that energy [5]. Therefore, in dealing with this variable nature of PV output power, the integration of energy storage technologies and reliable forecasting techniques are essential.

The integration of distributed PV systems with centralised battery energy storage systems is gaining importance in remote area standalone off-grid power supply (SOPS) systems. A comprehensive study conducted by Blechinger et al. has revealed that PV-battery based systems along with DG based systems could be economically operated for almost 1,800 small islands worldwide with populations below 100,000 per island [6]. Cader et al. have remarked that in many regions around the world, the introduction of DG-PV-battery systems achieves significant reductions in the levelised cost of energy, compared to diesel-only systems [4].

Generally, a low spatial diversity of PV systems in a small area leads to very high PV power variability compared to dispersed PV systems. An isolated or island community can be fully or partially shaded or unshaded by ~~fast~~ fast-moving clouds in a time span ranging from a few seconds to minutes [7, 8]. Hence, to accommodate this variable nature of power output, there is a need to ensure power supply quality and network stability. Therefore, either DGs must offer sufficient flexibility or battery storage must be introduced to provide an adequate buffer against short-term PV power fluctuations. DG flexibility includes spinning reserve (SR, a

subset of operating reserve) and step load capability. If the DGs and storage systems do not offer enough flexibility, network operators have to limit the maximum PV penetration to certain levels, which adversely affects the uptake of PV systems [1]. Depending on the system control mechanism, batteries can also provide grid-forming and black start capability. They can be seen by the system as a synchronous generator and can provide frequency support by acting as a "virtual generator". They can also detect and clear faults across the entire network, as well as providing synthetic inertia to the system [9].

Proper control of PV power output can facilitate stable, reliable and effective operation of the system. The motion of clouds affects the performance of PV systems and therefore must be forecast to avoid undesired technical issues and costs [10]. To manage the PV power output variability, system operators need knowledge of cloud movement prediction. Power utilities are always concerned with meeting the minimum requirement of operating reserve (OR) at every instant, to ensure high reliability of operation at a minimal cost. Applying a short-term PV forecasting method, together with an alternative compensatory controllable resource, can help in the management of system operation in maintaining the system stability while increasing PV penetration level [11-15]. This is discussed in detail in later sections. However, the benefit of short-term PV forecasting varies with the network's specific design and control mechanism.

Solar irradiance and PV output forecasting is not a new concept in power systems operation. Different methods are used for solar PV forecasting depending on application level, forecast horizon and cloud conditions [8, 16]. The forecast accuracy depends on the area of the site, and whether forecasting is performed for a single, small location or a large area. Short-term PV forecasting using ground-based sky imagery mechanisms demonstrates clear advantages over other well-known, conventional methods. These include numerical weather prediction (NWP), satellite imaging and ~~statistical~~ statistical-based methods [8, 17]. Complex configurations of clouds and the associated small scale dynamics limit the application of modern-day NWP models. These models also lack the necessary temporal and spatial resolution to predict small scale atmospheric phenomena precisely. Hence, very high-resolution sensors are required.

Ground-based sensors, i.e. sky imagery mechanisms, provide useful and continuously updated information on current sky conditions. A depiction of the future sky can be achieved through observing and analysing subsequent images captured by the sky-facing camera. This

technique fills the forecasting gap mentioned above by providing sub-kilometre resolution of cloud coverage. This can be combined with measures of solar irradiance, cloud height above ground and basic geometrical considerations, with further support from machine learning and maps of the local surface, yielding a sufficiently accurate irradiance prediction [8, 12, 14-19].

To improve the PV penetration levels in a remote area DG-PV-battery based SOPS system, it is essential to offset the uncertainties of the PV output variability as much as possible using high-resolution data computation. In these types of systems smaller sized DGs of a few hundred kilowatts capacity usually take roughly around a minute to go to full load from a cold start. Hence, this calls for an assessment of 1-minute-level DG scheduling to ensure adequate system operating reserve. On the other hand, the PV forecast period should be adapted to the system size. Smaller sized power systems have similar array areas and therefore have higher fluctuation probabilities and need higher resolution forecasting. Currently, there is no study available in the literature on the optimal temporal resolution of PV forecasting. The effect of various temporal resolutions cannot be quantified. Thus, the data computation resolution of a 1-minute window for PV forecasting and DG-battery dispatch represents a sensible approach and hence, this study investigates the benefit of 1-minute–level PV forecasting to enable high PV penetration into a diesel-PV-battery based SOPS system. The study considers PV irradiance forecast resolutions as high as 1-second but averaged to 1-minute for better computing performance.

Most well-known and commercially available microgrid and renewable ~~energy~~ energy-based system simulation software tools used for energy flow modelling do not accurately simulate minute-level system operation. For example, HOMER Pro by HOMER Energy [20], RETScreen Expert by Natural Resources Canada [21], and the System Advisor Model (SAM) by the US National Renewable Energy Laboratory (NREL) [22] can perform system simulations at an hourly resolution. Therefore, to incorporate 1-minute ahead PV forecasting into the energy flow of a system, a Microsoft Excel-based energy flow simulation tool is developed in this study to assess the performance of a test SOPS system. The core novelty offered in this study can thus be summarised as follows:

- Development of an energy flow simulation tool that simulates 1-minute resolution real power flow, using a customizable generation dispatch strategy to meet the system reliability objectives

- Development of an algorithm for the application of sky camera-based 1-minute ahead PV forecasting data and
- Assessment of short-term (1-minute) PV forecasting benefits in relation to system performance

The remainder of the article comprises: Section 2, which provides key background information; Section 3, which describes the methodology; Section 4, which sets out the development of the tool; Section 5, which describes the application of the tool to assess PV forecasting benefits; and finally Section 6, which presents the conclusions reached by the study.

2. Issues and opportunities of PV forecasting into diesel-PV-battery SOPS systems

The integration of PV generators and batteries into SOPS systems is gaining popularity among stakeholders. In many remote, rural and off-grid communities around the world, there are now ample numbers of DG-PV-battery-based SOPS systems being used for electricity supply [23, 24]. For example, the former Chief Executive Officer (CEO) of Australian Renewable Energy Agency (ARENA) mentioned in a speech that, "*In off-grid locations, renewable energy has unique advantages over the incumbent fossil fuels. Many remote Australian communities rely on diesel generators that are expensive to run and which create energy uncertainty due to the volatility of fuel prices ... So unpredictable diesel costs, falling renewable generation costs and increased energy security can all provide motivators for the adoption of renewables … Regional Australia's Renewables – Industry (I-RAR) has a fairly wide remit, focussing on developing renewable energy solutions for remote areas where fossil fuels are currently or would otherwise be used to generate electricity*" [25]. This illustrates the significant interest remote utilities have to improve system components so as to facilitate the use of more renewables in power systems.

Battery storage systems, along with other smart control mechanisms, are offering better solutions to many of the technical challenges posed by variable PV generators. A recent study has found that academics, industry experts and consultants now agree that DG-PV-battery systems are superior to DG-PV or DG-only systems for remote off-grid communities, considering the economic and technical issues involved [26]. Cader et al. have used a novel research framework to form an overview of the overall potential of DG-PV-battery based systems worldwide [4]. According to that study, where there were higher shares of PV, a

centralised battery bank (BB) was used for load shifting and reduced diesel consumption. This required substantial initial capital investment but operation and maintenance costs were decreased compared to the DG-only scenario.

Where batteries are incorporated into SOPS system, the response time and sizing are critical. Bass et al. [27] have determined the power and energy capacity of the centralised battery bank for a rural type feeder in Portland, OR, USA. The centralised BB control mechanism enabled the feeder to integrate a higher share of PV output (30-55% of the average maximum feeder load) [27]. The Hornsdale Power Reserve in South Australia owns a substantial capacity 100MW and 129MWh Li-ion battery. The power output of the BB can rise from zero to 30 MW, or drop from 30 MW to zero, within a few milliseconds [28].

A well-developed DG-PV-battery SOPS system model incorporating robust generation dispatch strategies provides a more reasonable estimate of fuel and cost savings. Employing a load-following DG dispatch strategy showed that the DG-PV-battery model could achieve 73-77% fuel savings in winter and 80.5-82% fuel savings in summer, compared to the DG only scenario [29]. A study based on an Indonesian island has shown that the gradual reduction of the number of online DGs by employing more PV-battery systems still results in low initial capital expenditure [30]. A review by Salas et al. of current techniques used in off-grid DG-PV-battery systems has demonstrated that for low PV penetration (<20%) no extra control or energy storage is required [31]. However, it has also shown that for medium (20-65%) and high PV penetration (65-100%) systems, support from energy storage and a robust control management system is required [31].

In order to incorporate more PV systems into electricity supply systems, detailed PV power output information and knowledge of power fluctuation patterns are very important. Elsinga et al. [32] commented that solar irradiance forecasting is an essential component in economic realisation for high levels of PV penetration. Their study utilised a short-term, intra-hour solar forecasting method and found that during the highly variable days, this method had superior performance to the persistence method [32]. In [33], the researchers successfully demonstrated the management of system with a high penetration of PV generation in a smart grid using 15-minutes ahead PV power forecasting. Litjens et al. [34] developed and assessed forecasting methods using 5-minute resolution data to predict PV yield in order to improve self-consumption of PV power, decrease curtailment losses and improve revenues. Another study has shown that integration of batteries and solar irradiance forecasting into the system

has higher potential to relieve the network than a system which only maximises self-consumption [35]. Analysis of a German residential demand profile has shown that 26% more PV capacity can be added to the grid using PV-battery systems with persistence forecast algorithms [35]. Angenendt et al. [36] looked into forecast-based operation strategies to increase BB lifetime and reduce PV curtailment. Liu et al. [13] incorporated solar prediction interval and deterministic point predictions into their algorithm, resulting in a better performance than conventional forecast methods.

PV forecasting yields benefits to the power system in various ways by addressing the technical challenges of high levels of PV penetration. A short-term PV forecasting mechanism using "Sky Camera" (sky imager) images has been used to forecast the solar irradiance levels in these several research works [15, 16, 18, 37]. The authors' previous research has revealed that the application of sky ~~imagery~~ imagery-based short-term PV forecasting enables the system to integrate high levels of PV penetration without adversely affecting system stability. It offers favourable outcomes during high net load fluctuations caused by abrupt PV and load variations. Schmidt et al. [7] investigated the possibility of reducing spinning reserve requirements under constant clear sky conditions with high levels of PV penetration in the network. This study mentioned ~~concluded~~ that "*the accurate prediction of changes in solar irradiance in the 2-5 min time window is of importance rather than the accurate prediction of irradiance at a specific point in time and space*".

Mazzola et al. assessed the potential benefit of PV forecasting and revealed that cost savings could vary from 2-7% depending on the forecast quality and the composition of the microgrid [38]. Liandrat et al. [17] utilised a thermal-infrared sky imager for PV forecasting to optimise the hybrid DG-PV system. Their study considered a relatively high PV penetration level of 30% and 10-minutes ahead irradiance forecasting for an island in France. However, the study case was limited to considerations of a constant load throughout the analysis period. Also, the efficiencies of PV and DG were 100%, and all DGs were always operating at their nominal output. The results revealed that compared to the 'no forecast' scenario, the inclusion of forecasting in the system control reduces the overall fuel consumption, helps to inject more PV into the network and reduces the potential number of blackout events. The estimated cost reduction was around US$97,000 per year [17]. However, the consideration of load dynamics, realistic efficiency curves for PV and DGs and dynamic control of DG output would result in a different cost estimation.

A recent study [39] concentrated on the use of a binary prediction model for PV forecast to eliminate the use of batteries in the network. The study showed that the elimination of battery storage is the most economical option only when the annual percentage of an average number of cloudy days does not exceed the percentage share of battery costs within the overall operation & maintenance costs of a DG-PV system. This is not always the case for the majority of remote and rural areas.

In light of the discussion above, it is apparent that to facilitate high levels of PV penetration in a SOPS system, the following issues need to be considered:

- BB dispatch and control mechanism to address stability issues
- DG dispatch strategies to reduce fuel consumption
- Real-time irradiance measurement to improve performance of PV forecasting
- Selection of a time window to accurately predict changes in solar irradiance

To address the above issues, sky camera-based 1-minute ahead PV forecasting is applied in this study, enabling the system to integrate a high level of PV penetration without adversely affecting system stability. The dispatch strategy followed in this study provides the potential for higher reductions of CO_2 emissions from fossil fuel-based power generation, as self-consumption of PV energy by the prosumers is maximised.

3. Methodology

The overall methodology of this study is displayed as a flowchart in Figure 1. The work is carried out in three steps. Step 1 describes the design and specification of the SOPS system. Step 2 explains the development of the energy flow simulation tool and step 3 discusses the application of the tool to assess the PV forecasting benefits for SOPS systems in remote areas.

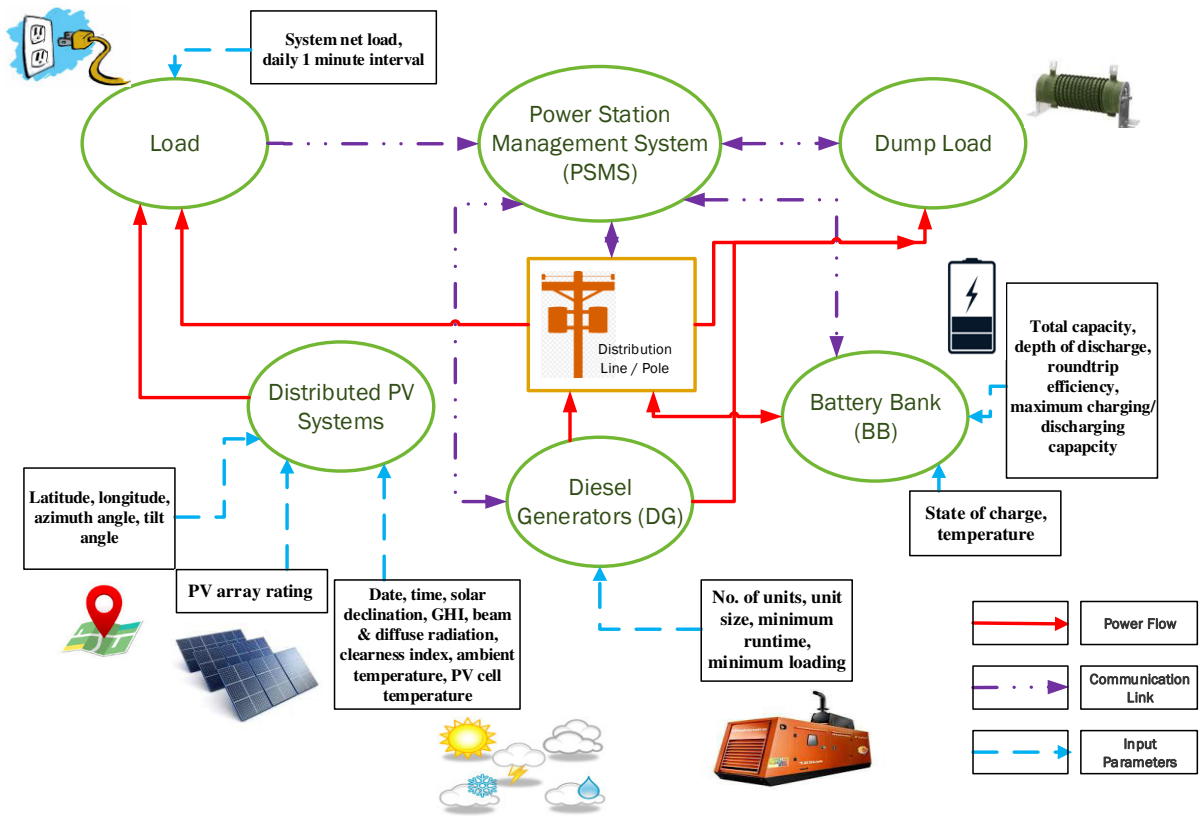

Figure 1: The infrastructure of the SOPS system and the system components used in the tool

3.1 *Step 1: Design of the SOPS System*

A meaningful operational strategy must be grounded in a reasonable estimate of how the SOPS system would operate in reality. System design, operational strategies and selection of load profiles are discussed in some of our previous studies [2, 40]. For this study, the SOPS system is assumed to be located in a remote town where central grid expansion is not feasible, and where the community is keen to install distributed PV systems and centralised battery systems, alongside the currently operating DGs. The model takes weather information from the city of Oldenburg in the state of Lower Saxony, Germany. The study considers the integration of a high PV share into the SOPS system which is distributed throughout the town and is assumed to comprise rooftop installations on residential and commercial settlements. However, to avoid technical and social complexities, it is assumed that the battery systems are not distributed, but rather that there is a battery bank (BB) at the power station. The system considers a generic load profile of a standard remote community. The SOPS system has six DGs, the maximum available. Each has a capacity of 170kVA to meet the daily total electricity demand of 8823.06 kWh. The PV systems are distributed along the three

distribution feeders in the town. Figure 2 presents the 24-h load profile that is employed in the tool for simulation. Table 1 shows the important system parameter values considered for DGs, PV and battery.

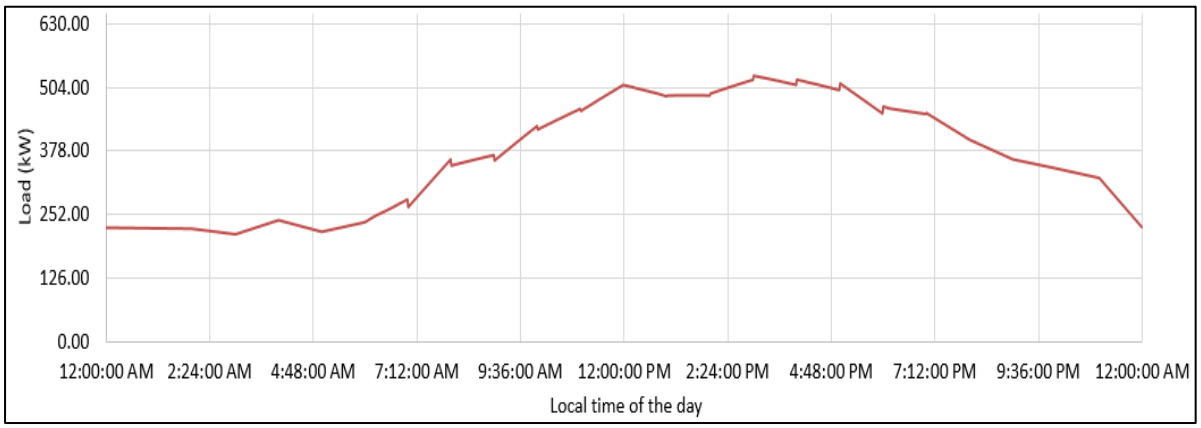

Figure 2: Daily load profile

Table 1: System component parameter values

Item	Parameter	Unit	Value
Gross load	Maximum	kW	527
	Minimum	kW	266
	Average	kW	368
DG	Unit capacity	kW	140
	Maximum allowable loading	%	90
	Minimum loading	%	30
	Minimum runtime	minute	30
PV	Slope of surface (Tilt)	degree	53
	PV derating factor	%	95
	Max power point efficiency under standard test conditions (STC)	%	13.5
Battery	Technology		Lithium Ion
	Battery charge efficiency	%	95
	Battery discharge efficiency	%	95
	Power rating	kW	140

3.2 *Step 2: Development of the Energy Flow Simulation Tool*

As stated earlier, 1-minute-level resolution profile of the generator scheduling and OR is essential to assess the benefits of the 1-minute-level short-term PV forecasting feature. To

address this issue, the tool has been developed utilising a 1-minute simulation time step, as it enables adequate representation of the energy flow and generator dispatch. Other commercially available pre-feasibility analysis software tools do not provide in concise form the 1-minute-level resolution simulation outcome needed by the significant number of stakeholders who lack technical understanding and related knowledge. This causes a slow and delayed uptake of PV systems in remote and rural areas all around the world [26]. Considering these issues, a tool is required which is handy and useful for this group of stakeholders. The study has fulfilled this gap by developing the tool using Microsoft Excel. The uniqueness of the tool lies in the fact that all the worksheets are observable and each of the steps is transparent during the execution of the logical algorithm. The algorithm addresses the objective functions of the problem using simple linear programming techniques. The tool offers two types of outcomes: (i) the generation of 1-minute resolution power generation and operational reserve profiles of the SOPS system using the user-defined operational algorithm, and (ii) the use of the PV forecast data to determine the DG operational profile and consequent fuel savings. Figure 3 presents an overview of the tool, showing the parameters required as input and the expected output from the tool. Figure 4 shows the schematic representation and the single line diagram of the SOPS system.

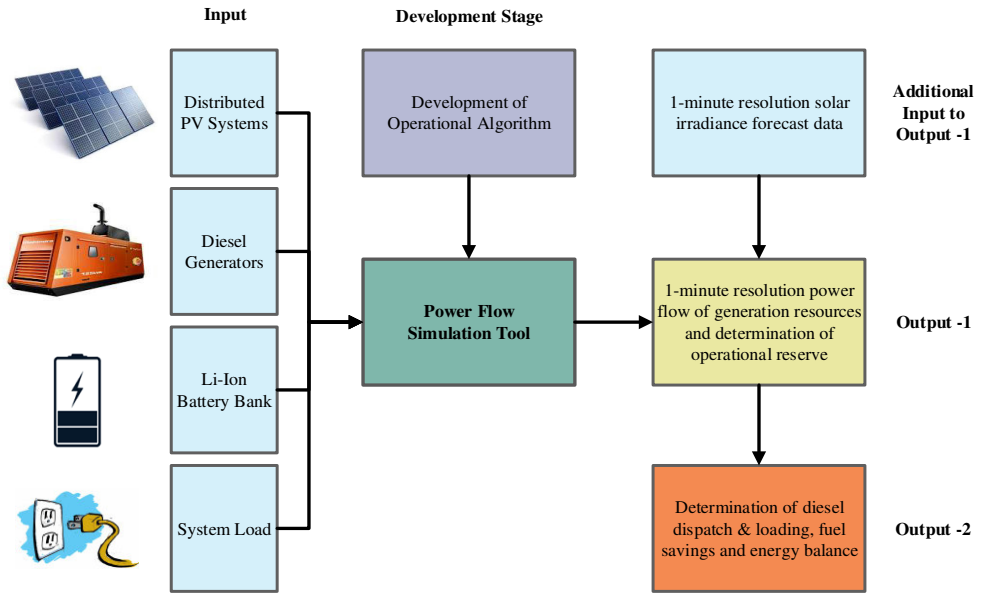

Figure 3: Flowchart showing the inputs and outputs of the energy flow simulation tool

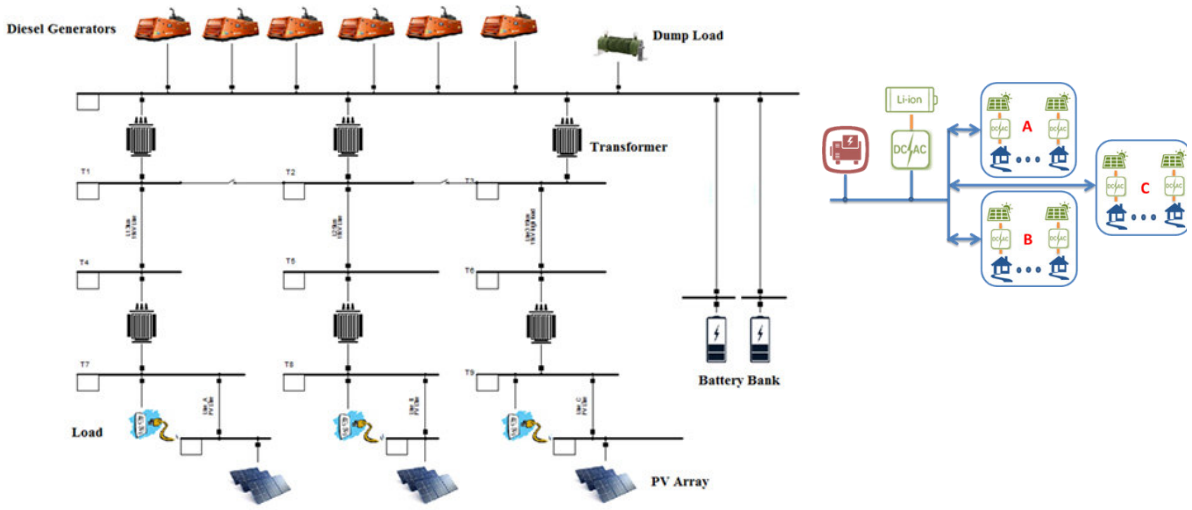

Figure 4: Block Diagram of a sample SOPS system for three rural type feeders: A, B and C

3.3 *Step 3: Assess PV Forecasting Benefits using the tool*

The tool can be used to assess the benefits of 1-minute resolution short-term PV forecasting for the specified SOPS system. Figure 5 shows the logical sequence followed for this application. The 1-minute ahead irradiance forecast data acquired from the image and irradiance processing software is applied to the energy flow simulation. A discussion based on several case studies is presented in section 5 and includes details of image acquisition and processing for the software.

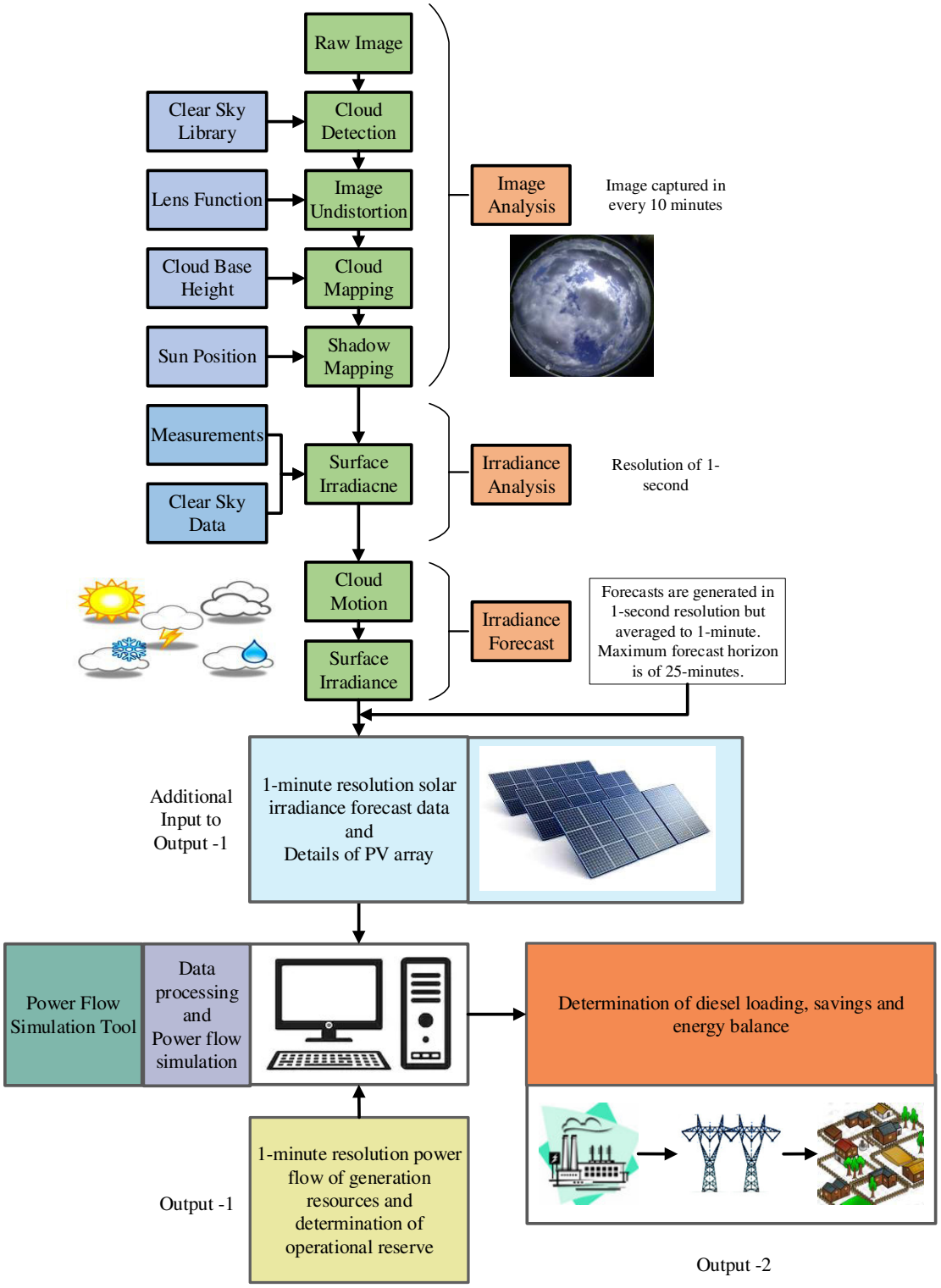

Figure 5: Stages and strategies of the approach leading to tool development

4. Description of the Energy Flow Simulation Tool

A distinguishing feature of the tool is that it takes 1-minute data as inputs to simulate 1-minute output. The specific inputs are: system load profile of 1-minute resolution, PV array information, DG capacity, battery capacity and location-specific information. The DGs and the BB are operated in automated control mode. PV systems are assumed to be distributed on the rooftops of the community buildings and households. An automatic 'Power Station Management System' (PSMS) communicates with 'Generator Supervisory Systems' on each of the DGs and the BB controller, and schedules them to supply the consumer loads. The whole battery bank is divided into two individual systems – the BB regular response (BB-RR) system and the BB emergency response (BB-ER) system. There is no advisory control imposed on the distributed PV systems. This section discusses the mathematical modelling of the components and the logical algorithms used to develop the energy flow simulation tool.

4.1 PV Array Modelling

The essential inputs required to calculate the PV array output include day of the year, location-specific information (e.g. latitude, longitude), weather information (e.g. solar irradiance), ambient temperature, clearness index and PV systems related information (e.g. the orientation of the array and array size). Some performance-related characteristics are also required, such as the PV inverter's manufacturer specifications. The total (global) irradiance incident on the horizontal surface of a PV array (plane of array) is the arithmetic sum of the direct (beam) and diffuse irradiance components incident on a horizontal surface, as shown in Eq. (1):

$$E_{POA} = E_b + E_d \quad (1)$$

Where, E_{POA} is the total irradiance incident on the plane of array (kW/m^2), E_b is the direct irradiance incident on a horizontal surface (kW/m^2) and E_d is the diffuse irradiance incident on a horizontal surface (kW/m^2)

To determine the irradiance incident on the array for each time step, the global horizontal irradiance is calculated from the beam and diffuse components. The diffuse component can be determined from the clearness index using Eq. (2) and Eq. (3) [41]. Clearness index is the ratio of the irradiance on the plane of the array to the extraterrestrial irradiance, as shown in Eq. (2):

$$kt = {}^{E_{POA}}/_{E_O} \tag{2}$$

$$\frac{E_d}{E_{POA}} = \begin{cases} 1.0 - 0.09kt, & kt \leq 0.22 \\ 0.9511 - 0.1604kt + 4.388kt^2 - 16.638kt^3 + 12.336kt^4, & 0.22 < kt \leq 0.80 \\ 0.165, & kt > 0.80 \end{cases} \tag{3}$$

Where kt is the clearness index and E_O is the extraterrestrial irradiance on a horizontal surface (kW/m^2)

The ideal performance of a PV module is achieved when the connected solar inverter is operating at the maximum power point (MPP). The model assumes that solar inverters have maximum power point tracking (MPPT) capability. MPPT is a performance characteristic which inverters and charge controllers use to harness the maximum power from the PV array at a particular time. They do this by operating at the point when the output power (i.e. the product of the output current and output voltage) is maximised for a given irradiance or cell temperature [42]. The global irradiance incident on the PV array (E_t) is dependent on the beam irradiance, diffuse irradiance, anisotropic index, slope of the array surface (tilt angle), zenith angle and global horizontal irradiance on the earth's surface. The total power generation from a PV array is determined using Eq. (4):

$$P_{PV} = P_{PVRated} \times DF_{PV} \left(\frac{E_t}{E_{t,STC}}\right) \times \left[1 + \alpha_{temp}\left(T_{cell} - T_{cell,STC}\right)\right] \tag{4}$$

Where, P_{PV} is the output power of the PV array (kW), $P_{PVRated}$ is the rated capacity of the PV array at STC (kW), DF_{PV} is the PV derating factor (%), E_t is the total global irradiance incident on the PV array (kW/m^2), $E_{t,STC}$ is the solar irradiation incident at STC (1 kW/m^2), α_{temp} is the temperature coefficient of power (%/°C), T_{cell} is the PV cell temperature at the current time step (°C) and $T_{cell,STC}$ is the PV cell temperature at STC (25°C)

PV cell temperature depends on factors, such as air temperature, irradiance, wind speed, and module materials. In each time step, Eq. (5) is used to calculate the PV cell temperature:

$$T_{cell} = \frac{T_{amb} + \left(T_{cell,NOCT} - T_{amb,NOCT}\right)\left(\frac{E_t}{E_{t,NOCT}}\right)\left[1 - \frac{\eta_{mp,STC}\left(1 - \alpha_{temp}T_{cell,STC}\right)}{\tau\alpha}\right]}{1 + \left(T_{cell,NOCT} - T_{amb,NOCT}\right)\left(\frac{E_t}{E_{t,NOCT}}\right)\left(\frac{\alpha_{temp}\eta_{mp,STC}}{\tau\alpha}\right)} \tag{5}$$

Where, T_{cell} is PV cell temperature (°C), T_{amb} is ambient temperature (°C), $T_{cell,NOCT}$ is the PV cell temperature at Nominal Operating Cell Temperature (NOCT) (°C), $T_{amb,NOCT}$ is the ambient temperature at NOCT (°C), E_t is the total global irradiance incident on the PV array (kW/m^2), $E_{t,NOCT}$ is the total global irradiance incident on the PV array at NOCT (kW/m^2), $\eta_{mp,STC}$ is the maximum power point efficiency under STC (%), α = solar absorptance of the array (%), α_{temp} is the temperature coefficient of power (%/°C) and $T_{cell,STC}$ is the PV cell temperature at STC (25°C)

4.2 Diesel Generator (DG) Modelling

Generators are usually of two types: engine-generator and electric generator. Diesel generators are classified as engine-generators. Diesel engines running below a recommended minimum loading level for an extended period result in low efficiency and cylinder bore glazing. This reduces engine operating life, therefore increasing the annual operational and maintenance costs. It should also be noted that the specified minimum loading for diesel generators varies from manufacturer to manufacturer [1]. Generator power output is given by Eq. (6). Generator fuel curve defines the required amount of fuel consumed to meet the demand. Eq. (7) gives the generator's fuel consumption in litres/h.

$$P_{DG^{min}} \geq P_{DG}(i) \geq P_{DG^{rated}} \tag{6}$$

$$F = F_0 + F_1 P_{DG} \tag{7}$$

Where, P_{DG} represents instantaneous power from the DG unit, $P_{DG^{min}}$ and $P_{DG^{rated}}$ represents minimum allowable power output from the DG unit and the rated power of the DG unit, respectively, F is total fuel consumption (L/h), F_0 is fuel curve intercept coefficient in L/h/kW, and F_1 is fuel curve slope in L/h/kW

4.3 Battery Bank (BB) Modelling

A battery model based on Li-ion technology is used in this tool. It takes as inputs the battery string size (Wh), the initial and minimum state of charge (SOC) of the battery bank and specified roundtrip efficiency. The current energy capacity of the BB is calculated using Eq. (8) and Eq. (9). During charging/discharging, the SOC limit is always checked for both the battery systems using Eq. (10).

$$E_{BB-RR}(i+1) = E_{BB-RR}(i-1) + E_{BB-RR}(i) \quad (8)$$

$$E_{BB-ER}(i+1) = E_{BB-ER}(i-1) + E_{BB-ER}(i) \quad (9)$$

$$BB_{SOC}{}^{min} \geq BB_{SOC}(i) \geq BB_{SOC}{}^{max} \quad (10)$$

Where, $E_{BB-RR}(i)$ represents the BB-RR energy at time instant 'i', $E_{BB-RR}(i+1)$ represents the BB-RR energy at the next time instant, $E_{BB-RR}(i-1)$ represents the BB-RR energy at the previous time instant 'i-1', $E_{BB-ER}(i)$ represents the BB-ER energy at the current time instant 'i', $E_{BB-ER}(i+1)$ represents the BB-ER energy at the next time instant, BB_{SOC} is the SOC at any time instant, $BB_{SOC}{}^{min}$ is the minimum level of SOC allowed and $BB_{SOC}{}^{max}$ is the maximum level of SOC allowed when battery gets charged

4.4 Inverter Modelling

It is assumed in the modelling that all the inverters are integrated with the individual system components. The inverters dedicated to the battery banks are bi-directional grid-tied inverters, and the dedicated inverters that are coupled to the PV arrays are grid-tied PV inverters. Eq. (11) and Eq. (12) show the basic mathematical expressions used for measuring an inverter's uni-directional input and output power.

$$P_{inv-BB}(i) = P_{BB}\ (i) \times \eta_{inv} \quad (11)$$

$$P_{inv-PV}(i) = P_{PV}\ (i) \times \eta_{inv} \quad (12)$$

Where, P_{PV} is the output power of the PV array (kW), P_{BB} is the output power of the BB (kW), P_{inv-BB} is the input/output power of the battery inverter, P_{inv-PV} is the input/output power from the solar inverter and η_{inv} is the inverter efficiency

4.5 Operation of the PV systems and the Battery Bank

It is assumed that the daytime gross load demand will be offset by the electricity generated by the PV systems, and that any excess of generation will be used to charge the battery in order to prevent the DGs from under-loading. In all cases, at least one DG will remain connected for grid forming and supplying electricity to the grid (system). The net system load seen by the PSMS is the estimated net load (based on historical statistics) and the forecasted net load, measured using Eq. (13) and Eq. (14). Eq. (15) and Eq. (16) represent the calculation of gross

load when the DGs are in regular operation, in cases where one source is not generating power. The algorithm used in this tool assumes the maximum loading (δ) and the minimum loading (∂) of each DG unit to be 90% and 15%, respectively. The PSMS continuously sends the BB a power set point limit, ensuring that preselected minimum loadings of all online DGs are maintained. The PV systems' short-term power fluctuations are smoothed out by BB-RR which acts as an energy buffer, absorbing excess PV energy and topping up during periods of cloud cover. BB-ER is dedicated to responding only in emergencies. It corresponds to the immediate action required to provide grid stability and take up the load in cases of sudden failure of an online DG. The algorithm used in this tool regards 85% of the whole BB capacity as dedicated to BB-RR and the remaining 15% capacity as BB-ER (see Eq. (17), where $\boldsymbol{\rho} = 0.85$ and $\boldsymbol{\sigma} = 0.15$).

$$Net\ Load\ (i) = Gross\ load\ (i) - P_{PV}(i) \tag{13}$$

$$Net\ Load\ (i) = \sum_{DG=1}^{n} P_{DG}\ (i) + P_{BB-RR}(i) \tag{14}$$

$$\partial * P_{DG^{rated}} \leq P_{DG}(i) \leq \delta * P_{DG^{rated}} \tag{15}$$

$$Gross\ Load\ (i) = \begin{cases} P_{PV}(i) + \sum_{DG=1}^{n} P_{DG}\ (i)\ ; when\ P_{BB-RR}(i) = 0 \\ \sum_{DG=1}^{n} P_{DG}\ (i) + P_{BB-RR}(i)\ ; when\ P_{PV}(i) = 0 \\ \sum_{DG=1}^{n} P_{DG}\ (i)\ ; when\ P_{PV}(i) = P_{BB-RR}(i) = 0 \end{cases} \tag{16}$$

$$E_{BB-RR} = \rho\ \times E_{BB}\ and\ E_{BB-ER} = \sigma \times E_{BB} \tag{17}$$

Where P_{PV} represents instantaneous power from PV array, P_{DG} represents instantaneous power from DG, P_{BB-RR} represents instantaneous power from BB-RR, $P_{DG^{min}}$ means minimum DG loading capability, $P_{DG^{rated}}$ represents the rated power of a DG unit

The PSMS maintains the BB's power flow (negative when importing, positive when exporting) at a determined power set point. To do this, it also takes into account the net load fluctuation and minimum diesel loading. Figure 6 shows the logical sequences followed by the PSMS for generation dispatch to meet the load demand. This follows Eq. (16).

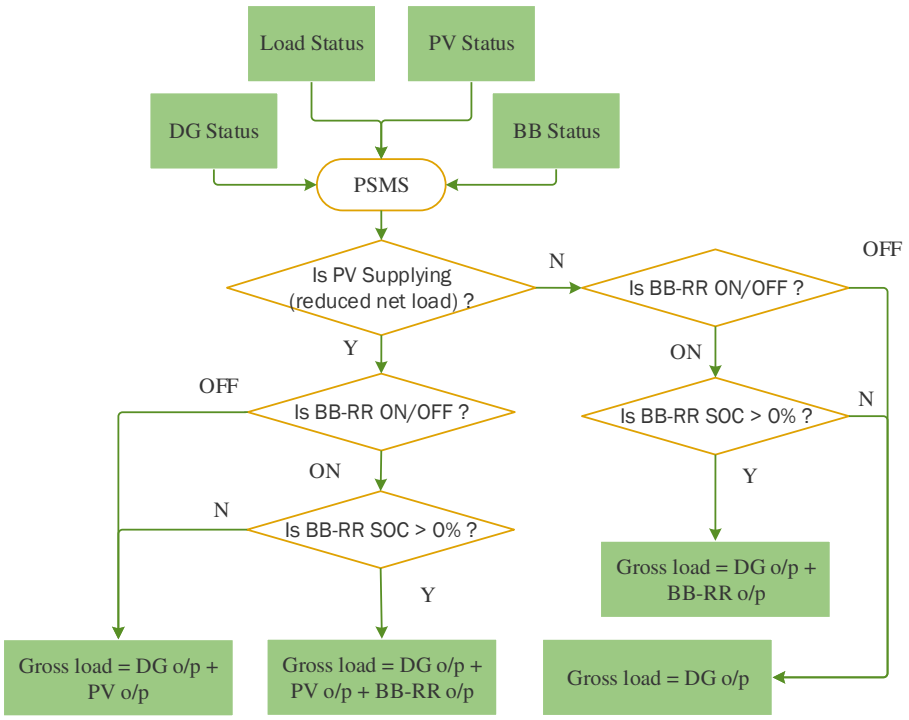

Figure 6: Generation dispatch method to meet the load demand

4.6 DG Plant Schedule and Operating Reserve

The system has enough DG capacity to provide an operating reserve sufficient to cover the net system load at every time step for specified contingency events such as sudden cloud cover, sudden load increase or loss of generation capacity. The DG units' dispatch priority depends on user preference. An additional DG is scheduled ON when an increasing net system load plus a specified margin covering the loss of a DG equals the sum of the de-rated power ratings of on-line DGs. The BB-ER system always keeps a pre-determined energy reserve. If this reserve is capable of discharging the same power that the biggest de-rated DG unit can supply, then BB-ER capacity is considered to be the operating reserve equivalent to the biggest de-rated DG, see Eq. (18). If the BB-ER system does not take part in providing an operating reserve, then the PSMS brings on one or more additional DGs to provide the minimum operating reserve. This is equal to the capacity of the biggest DG unit, see Eq. (19). The overall operating reserve at any instant also covers a certain range of load and PV output fluctuations, neither of which should exceed the capacity of one DG unit. The BB-ER system maintains a minimum stored energy of 5kWh to cover the loss of a DG unit for at least two minutes. The minimum runtime for a DG unit is assumed to be thirty minutes, see Eq. (20). When the supervisory system of any DG unit receives a signal to turn it off, it checks for the minimum runtime constraint before responding to the command. A DG unit is scheduled OFF

when a reducing total net load plus the required minimum operating reserve margin drops below the sum of the de-rated power ratings of those DGs that are to remain in service. The DG to be scheduled OFF is first changed by the PSMS from operating in isochronous frequency to frequency droop control. The PSMS then lowers the DG's power set point to near zero, disconnects it from the generator busbar, and runs it for a further few seconds to cool the unit. Figure 7 shows the diesel generator dispatch algorithm which follows Eq. (18) – Eq. (20).

$$P_{BB-ER}{}^{max}(i) = P_{DG}{}^{rated}(i) \tag{18}$$

$$OR\ (i) = \begin{cases} OR_{BB-ER}(i)\ ; when\ E_{BB-ER}(i)\ \geq 5kWh \\ SR_{DG}(i)\ ; when\ \ E_{BB-ER}(i)\ < 5kWh \end{cases} \tag{19}$$

$$t_{P_{DG}}^{min} = 30\ minute \tag{20}$$

Where $P_{BB-ER}{}^{max}$ represents the maximum deliverable power from BB-ER, OR means operating reserve of the system, OR_{BB-ER} represents the operating reserve contribution from BB-ER, SR_{DG} represents spinning reserve contribution from DG units and E_{BB-ER} represents the energy capacity of BB-ER

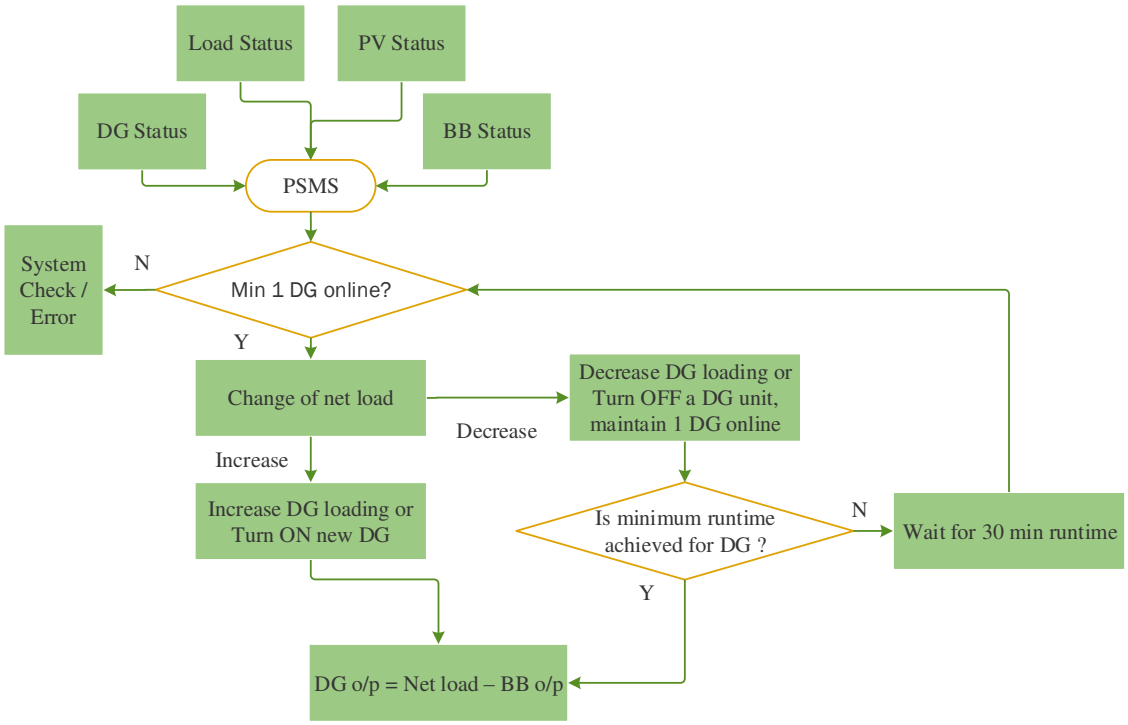

Figure 7: Diesel generator dispatch algorithm

4.7 Operational Steps

The system net load increases when the load demand increases and (or) the total PV output from prosumers decreases for every time step, and vice versa. With rising PV output, DGs may face an under-loading situation or even a reverse power condition. During these periods of excess energy arising from high PV penetration or under-loading of DGs, the PSMS sends a power setpoint signal to the BB-RR to stop discharging immediately and to start charging and boosting the state of charge (SOC), see Eq. (21) – Eq. (23). As soon as the excess electrical power becomes zero, according to Eq. (21), the BB-RR resumes its normal discharging function in accordance with the regular instructions from the PSMS. If the BB-RR hits the maximum SOC level, then to prevent the DGs from going to an under-loading condition to meet the energy balance scenario, a short-term dump load is activated. The dump load has to be employed to maintain system stability and energy balance by avoiding the DGs going to a reverse power condition. The PSMS monitors the SOC levels of the BB-RR and BB-ER, according to Eq. (22). Between these levels, PSMS sends a signal to the BB-RR in an effort to sustain diesel loading at the specified minimum loading and, at the very least, to keep DGs out of overload (for example, after a DG trip). It corrects for overcharging (excess

PV power) by adjusting the power set point of the dump load and it corrects for undercharging by stopping BB-RR from discharging any further. It also controls the BB-RR system such that it does not discharge during the off-PV generation period. Battery discharge is allowed only during the sunshine hours, up to 19:00, see Eq. (24) – Eq. (25). Simultaneous charging and discharging processes of the BB are avoided using a binary decision variable, β_{BB}, see Eq. (26). Figure 8-9 shows the battery bank charging and discharge algorithms, respectively.

$$Excess\ Power\ (i) = \begin{cases} 0\ ; when\ Gross\ load\ (i)\ \geq\ P_{PV}(i) + P_{DG}(i) + P_{BB}(i) \\ P_{PV}(i) + P_{DG^{min}}(i) - \ Gross\ load\ (i)\ ; when\ P_{PV}(i) + P_{DG^{min}}(i) >\ Gross\ load\ (i) \end{cases} \quad (21)$$

$$BB - RR_{SOC^{min}} \leq BB - RR_{SOC}(i) \leq BB - RR_{SOC^{max}} \quad (22)$$

$$P_{BB-RR^{max}}\ (i) = P_{DG^{rated}} \quad (23)$$

$$P_{BB-RR}\ (i) = \begin{cases} P_{BB-RR^{-}}\ (i);\ charging\ \ when\ Excess\ Energy\ (i) > 0\ \ and\ also\ 00{:}00 < i < 06{:}00 \\ P_{BB-RR^{+}}\ (i); discharging\ when\ BB - RR_{SOC}(i)\ >\ BB - RR_{SOC^{min}}\ and\ i = sunshine\ hrs, upto\ 1 \end{cases} \quad (24)$$

$$P_{BB-ER}(i) = \begin{cases} P_{BB-ER^{-}}\ (i);\ charging\ \ when\ E_{BB-ER}(i)\ < 5kWh\ \ and\ Emergency\ Situation = OFF \\ P_{BB-ER^{+}}\ (i); discharging\ when\ Emergency\ Situation = ON \end{cases} \quad (25)$$

$$0\ \leq\ P_{BB-RR^{+}}\ (i) \leq\ \beta_{BB} \times P_{BB-RR^{max}}\ (i) \quad (26)$$

$$0\ \leq\ P_{BB-RR^{-}}\ (i) \leq (1 - \beta_{BB}) \times P_{BB-RR^{max}}\ (i)$$

Where, $BB - RR_{SOC}$ represents the SOC of BB-RR, $P_{BB-RR^{max}}$ represents the maximum absorbed or deliverable power from BB-RR, $P_{BB-RR^{+}}$ represents discharging state and $P_{BB-RR^{-}}$ represents charging state

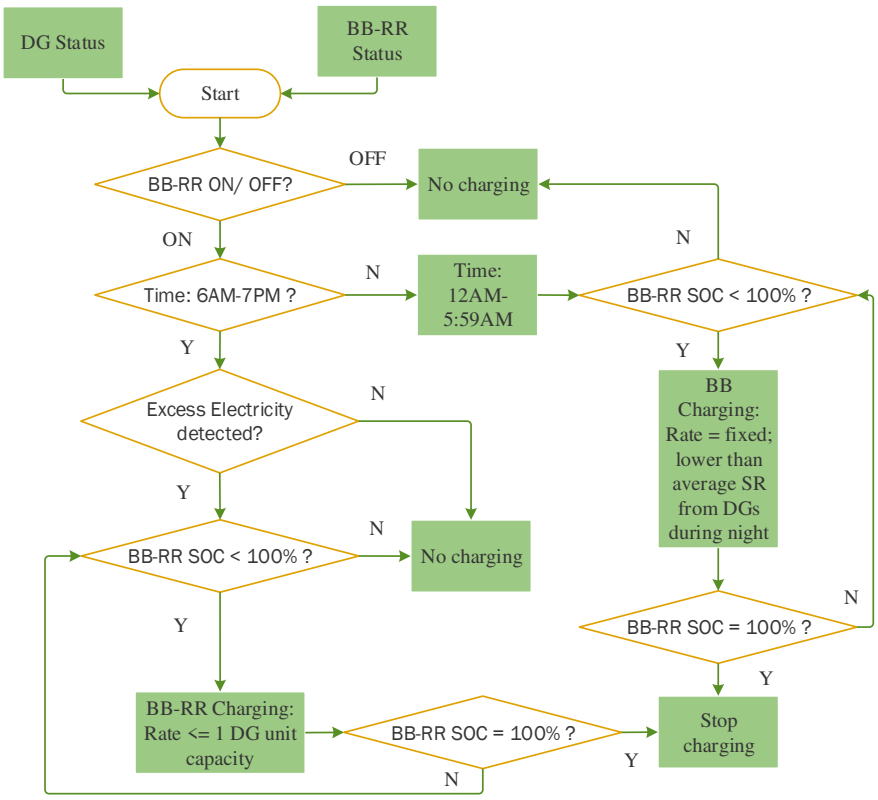

(a)

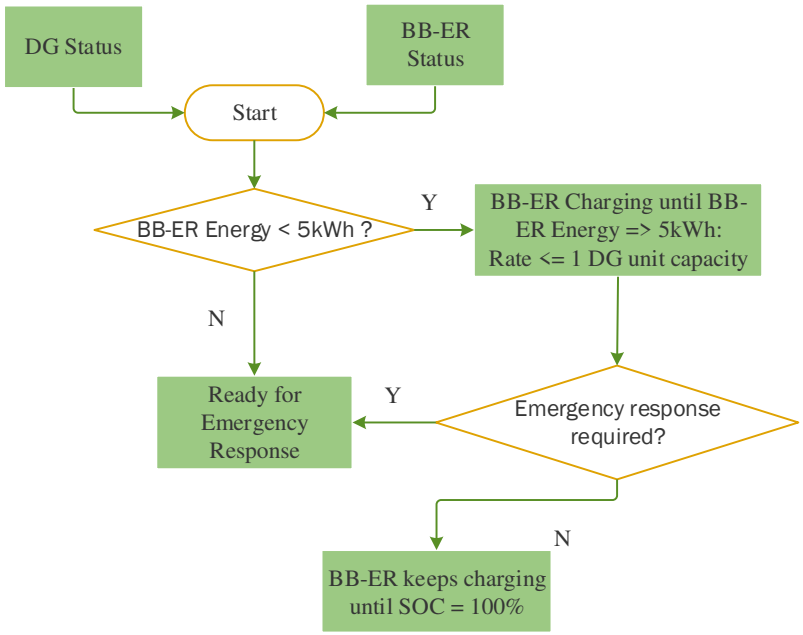

(b)

Figure 8: Battery bank charging algorithm: (a) for BB-RR and (b) for BB-ER

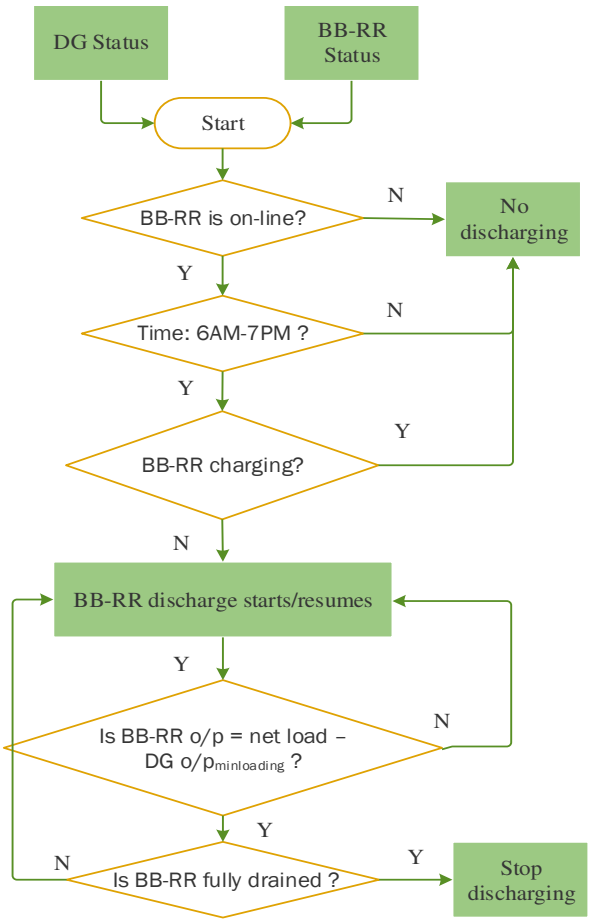

Figure 9: Battery bank discharge algorithm

4.8 Operating Reserve provided by the BB

As stated earlier, the capacity of the BB-ER is always kept at such a level that there remains sufficient reserve contribution to cover the loss of the biggest DG unit of the system. To illustrate the BB system division and minimum storage capacity determination of the BB-ER system, we can consider the example where the BB has a total capacity of 100kWh, according to Eq. (17), and BB-RR and BB-ER have capacities of 85kWh and 15kWh, respectively. This corresponds to a low power/high energy system for BB-RR and high power/low energy system to represent BB-ER's activity. The maximum charge and discharge rate are set equal to the largest DG capacity (e.g., 140kW) so that the BB is equivalent to, but not greater than, the largest DG capacity. When the BB-ER is required to respond, it can discharge at a maximum rate equal to the largest DG capacity of 140kW for enough time to allow DG to turn ON and maintain the N+1 redundancy criterion. The minimum capacity of the BB-ER is maintained according to the Eq. (19). Figure 10 shows the working principle of the BB-ER system as an operating reserve.

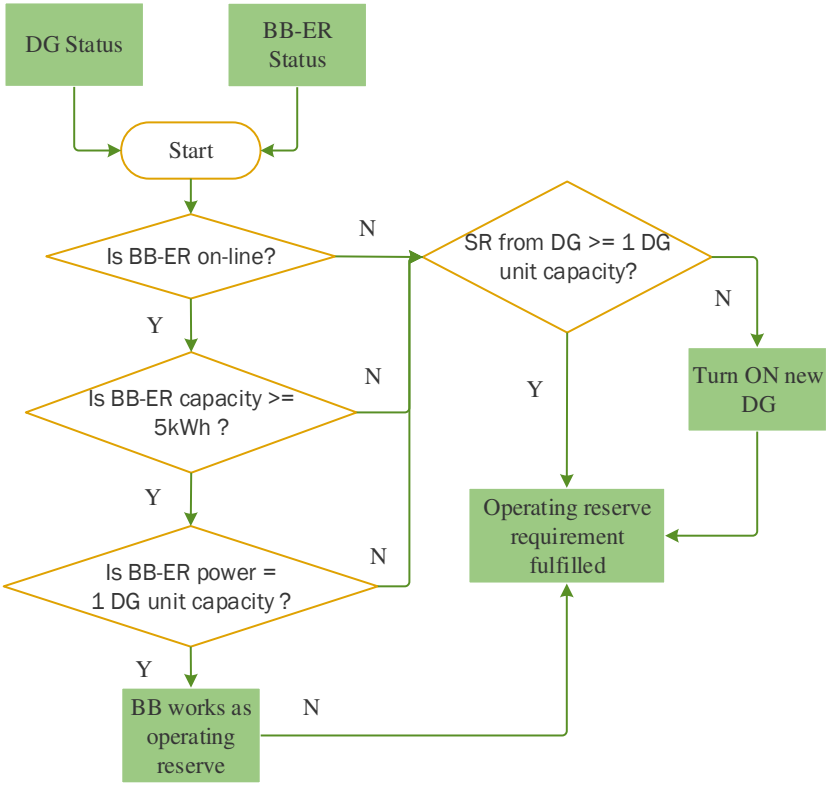

Figure 10: Operating reserve management from the BB-ER system

4.9 System Operation with Battery Bank Offline

When the BB (i.e. the BB-RR and BB-ER) is off-line, it does not contribute to any smoothing or the system operating reserve capacity. In this situation, all frequency and voltage controls are provided by the DGs. Because the net load fluctuations (assumed to be the same as the PV systems output variability) are not being managed by the BB, a dump load has to be employed.

4.10 Computation of Minimum Number of DGs Required Online

For different scenarios based on the available energy resources, the computation of the minimum number of DGs required to be online for every time instant follows Eq. 27-30.

Scenario 1: DG-PV system, no PV forecasting applied:

In this scenario, no BB is active. Therefore, DG provides support for the operating reserve, see Eq. (27).

$$N_{\min\_DG}(i) = Roundup\left\{\frac{\left(Gross\ load\ (i-1) - P_{PV}(i-1) + Min\_OR\ (i)\right)}{\delta * P_{DG^{rated}}}\right\} \quad (27)$$

Where, $N_{\min\_DG}$ represents the minimum number of DGs required online in the current time, $Min\_OR\ (i)$ represents the minimum amount of operating reserve required in kW in the current time which is equal to 140kW.

Scenario 2: DG-PV-BB system, no PV forecasting applied:

In this scenario, the BB is active and BB-ER provides support for the operating reserve, see Eq. (28).

$$N_{min\_DG} = Roundup\left\{\frac{\left(Gross\ load\ (i-1) - P_{PV}(i-1)\right)}{\delta * P_{DG^{rated}}}\right\};\ when\ Min_{OR}(i) = OR_{BB-ER}(i) \quad (28)$$

Scenario 3: DG-PV system, with 1-minute ahead PV forecasting applied:

In this scenario no BB is active. Hence, DG provides support for the operating reserve. In addition, in this step 1-minute ahead PV forecasting is applied, see Eq. (29).

$$N_{\min\_DG} = Roundup\left\{\frac{\left(Gross\ load\ (i) - P_{PV}(i+1) + Min\_OR\ (i)\right)}{\delta * P_{DG^{rated}}}\right\} \quad (29)$$

Scenario 4: DG-PV-BB system, with 1-minute ahead PV forecasting applied:

In this scenario, the BB is active and BB-ER provides support for the operating reserve. In addition, in this step 1-minute ahead PV forecasting is applied, see Eq. (29).

$$N_{min\_DG} = Roundup\left\{\frac{\left(Gross\ load\ (i) - P_{PV}(i+1)\right)}{\delta * P_{DG^{rated}}}\right\};\ when\ Min_{OR}(i) = OR_{BB-ER}(i) \quad (30)$$

The above formulae determine the minimum number of DGs required online for various scenarios. However, the current minute generation of the required online DGs added to the current minute BB generation (where the BB is included and online) equals the current minute gross load less the current minute PV power, see Eq. (13) and Eq. (14).

4.11 Advantages and Limitations of the Tool

In the next section, the tool will be applied to some case-based scenarios. This will demonstrate some significant advantages of the tool, specifically:

- It uses as input a minute-level resolution data from various available sources. The tool provides insight into the issues that need to be addressed on a minute by minute basis in order to apply them to the control mechanism of the power system to assess benefits.
- Short-term PV forecasting can forecast as little as 1-minute ahead solar irradiance levels. Therefore, this application requires a tool that can simulate minute-level resolution power flows. The tool achieves this and computes the overall fuel consumption, fuel savings and operational reserve requirements for any period considered.
- The dispatch algorithm can be customised, and every step is visible and transparent. This is an outstanding feature of the tool. A techno-economic analysis is recommended before using this tool, in order to learn about the economic configuration of any particular power supply system.

However, by their inherent nature, energy flow models have limitations. These are:

- They do not consider reactive power, frequency or voltage as technical parameters in making any decisions.
- The line loss calculation is omitted while dispatching power to the loads.
- They assume that the speed of completing a charging/discharging cycle has no negative impact on battery operation and lifetime.
- They do not consider cost functions as a decisive factor.

5. Assess PV forecasting benefits

This section assesses the benefits of short-term PV forecasting using the tool in order to allow higher shares of PV generation into the SOPS system. The current study focuses on the application of 1-minute ahead PV forecasting of irradiance data acquired by the “sky camera” (sky imager) device and image processing software.

A complex configuration of hardware is set up at the University of Oldenburg (53.15232 °N, 8.166022 °E) in Oldenburg, Germany. The sky imager used is a commercial network camera Vivotek FE8172V, equipped with a fisheye lens [8]. The essential specifications for this camera are a circular fisheye frame in a 1920*1920 pixels image plane and a full 180° view field. This takes images every 10 seconds from sunrise to sunset. A Python-based interface was developed to control most of the settings automatically. For this research, the maximum field of view for the camera has been set to 160° (±80° of the zenith angle). The experimental setup is presented in figure 11 [8]. The focus is on forecasts of global horizontal irradiance (GHI), measured at the location of the camera. Sky imagers take consecutive images of the sky and record the current cloud positions adjacent to and cover the camera location. An image processing mechanism is used to measure the cloud movement and determine the direction relative to the sun's position [8].

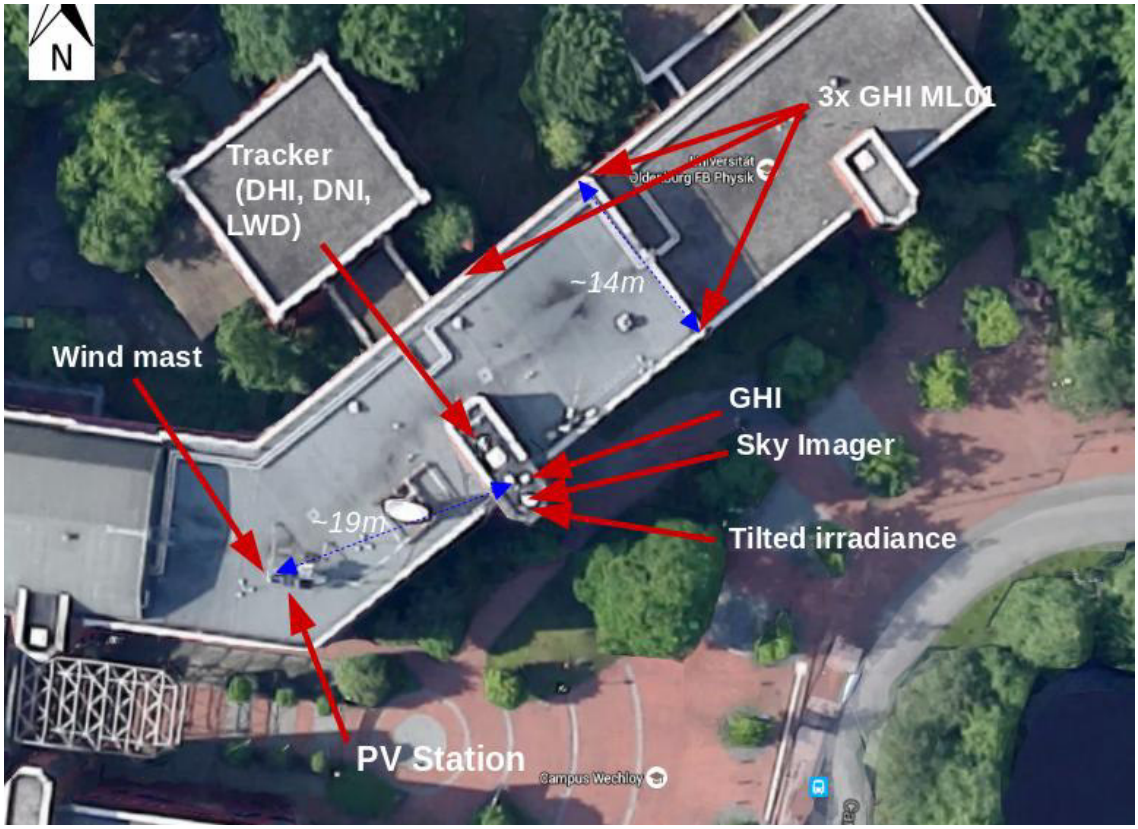

(a)


SunTracker with DHI und DNI sensors


Vivotek camera


PV module

(b)

Figure 11 (a): Top view of energy meteorology station at the University of Oldenburg. Measuring equipment for three main horizontal irradiance components are located together with a sky imager above the staircase of the building. A PV station with wind measurements is located about 19 meters nearby. A triangle of GHI measurements with photodiodes for cloud motion estimation is also located on the rooftop. Background source: Google. (b): Shows the sensors, camera and the PV module used in the experimental setup [8].

These images are then processed to obtain 1-minute ahead PV forecasting. For comparative analysis, a GHI forecast using perfect forecast data is also obtained. The perfect forecast method is characterised by the assumption of zero error in the irradiance forecast for the next time step. In forecasting applications where timing can be neglected (for example, predicting 10-min averages of variability), the sky imager technique outperforms the persistence forecasts. The persistence forecast method assumes the forecast GHI to be the same as the current GHI measurement in the next time instant. In clear-sky or overcast homogeneous sky conditions, persistence forecasts typically show low forecast errors [8]. Even if there are forecast errors, the sky imager-based techniques, making use of visible sky information, can predict cloud events. In these situations, other statistical models based on time series analysis fail due to the non-periodic nature of cloud coverage. Here lies the novelty of the sky-imagery-based short-term PV forecasting mechanism.

Single point measurement of solar irradiance, together with single sky camera image recordings and processing of cloud events, mean that any geographic diversity of solar irradiance due to intermittent cloud cover is not taken into account. Consequently, the

'smoothed' net total of solar PV power coming from geographically dispersed prosumer PV systems during intermittent broken cloud cover is not taken into account. The sky camera will tend to predict a 1-minute ahead forecast drop in PV power that would only arise when the entire town is blanketed by a rapidly moving large cloud within one minute. Therefore, the sky camera forecast of a drop in PV power caused by cloud cover will generally be a worst-case forecast, unless the sky camera does not forecast a minute ahead cloud cover event.

5.1 Application of PV Forecasting

This section describes the strategies used to assess the system performance, using 1-minute ahead PV forecasting. The energy flow model developed in the study is used to analyse the strategies, given in Table 2. Three system configurations are each assessed in relation to three forecasting strategies when PV systems are integrated. The base case scenario has been chosen as the DG-only operation scenario for the SOPS system (see Table 2).

The application successfully addresses all the issues mentioned in section 2. All technical constraints are thoroughly checked and adhered to in every time instant, while the tool is running. This helps the system to reduce the potential number of events where the N+1 redundancy criterion is violated. In addition, this study proposes a strategy to calculate the maximum allowed PV hosting capacity, when the PV forecasting mechanism is not applied. It assesses the benefits of 1-minute ahead PV forecasting of increasing the allowed PV hosting capacity and therefore the PV energy injection and then assesses the system performance in terms of fuel savings and PV share in the overall generation requirements.

In order to maintain simplicity in the analysis, the seasonal variations in the load profile are ignored (Figure 2) for the days on which the analysis has been performed.

Table 2: System configuration for application of PV forecasting

Case No.	System Configuration	PV Forecast Strategy	Remarks
1	DG-only (base case scenario)	N/A	• DGs are employed to meet the net load and try to maintain adequate OR.
2	DG-PV	2.1 No forecasting 2.2 1-minute ahead PV forecasting 2.3 Perfect forecasting	• DGs are employed to meet the net load and try to maintain adequate OR. • PV system hosting capacity is affected by PV forecast strategy. • BB is not employed.

Case No.	System Configuration	PV Forecast Strategy	Remarks
3	DG-PV-BB BB = 100kWh	3.1 No forecasting 3.2 1-minute ahead PV forecasting 3.3 Perfect forecasting	• DGs are employed to meet the net load and try to maintain adequate OR. • PV system hosting capacity is affected by PV forecast strategy. • BB is employed which comprises BB-RR and BB-ER (dual battery system).
	DG-PV-BB BB = 50kWh	3.4 No forecasting 3.5 1-minute ahead PV forecasting 3.6 Perfect forecasting	

5.2 Selection of the days

Five days, covering the primary seasonal and solar irradiance variations, have been selected for the assessment. The choice of days is based on comparatively superior values for some essential metrics such as 'forecasting skill' score and root mean square error (RMSE) of the forecast irradiance compared to the measured irradiance according to the Eq. (31) and Eq. (32) [8, 12]. However, it is to be noted that the primary emphasis in this research is given on the development of an algorithm on how to use the PV irradiance forecasted data and the application of forecasting mechanism. Hence, the metrics values for different days throughout the year would have no impact on the methodological approach but DG scheduling and the consequential fuel savings.

$$RMSE_{\%}(FH) = \frac{\sqrt{\sum_{i}^{N} \left(M_i(FH) - F_i(FH)\right)^2 / N}}{\overline{M(FH)}} \tag{31}$$

$$FSS_{\%} = \left(1 - \frac{RMSE_{Forecast}}{RMSE_{Persistence}}\right) \tag{32}$$

Where, RMSE = Root-mean-square error, FSS = Forecast skill score, FH = Forecast horizon, M_i = Measurement at i-th instant, F_i = Forecast at i-th instant.

One of the selected days is a clear sky day, one is an overcast day, while the others are intermittent cloudy days, where random cloud movements have been observed. Table 3 sets out the values of the essential metrics and describes each day. The forecast root mean square error can be seen to be higher in summer than in winter, while the mean bias error represents the average deviation. The forecast skill is computed by comparing the one minute ahead

forecast with the persistence forecast. The cloud coverage represents the percentage of cloud presence in the sky, and the standard deviation indicates the variability. Figure 12 shows the measured GHI, clear sky GHI, forecast GHI, forecast DNI, forecast DHI, and persistence GHI value for all five days.

Table 3: Selection of days and weather description

Date	Root mean square error	Mean bias error	Forecast Skill	Cloud coverage (0-100)	Standard deviation of cloud coverage	Sky cloud condition	Season at Oldenburg
26 January	4.796	0.143	0.491	99.536	0.137	Overcast, cloudy	Winter, coolest month
25 February	138.503	66.706	-0.580	57.630	36.179	Mixed: overcast in the afternoon, clear in the morning	Winter, driest month
18 April	81.745	15.928	0.124	5.921	4.866	Clear sky with few irradiance drops	Spring
6 June	168.544	41.305	0.120	48.297	41.861	Mixed day with a high overcast part in the morning and clear in the afternoon	Spring, wet month
19 August	166.641	20.859	0.175	70.965	14.143	Mixed, irradiance drop throughout the day	Summer, warmest month

26 January

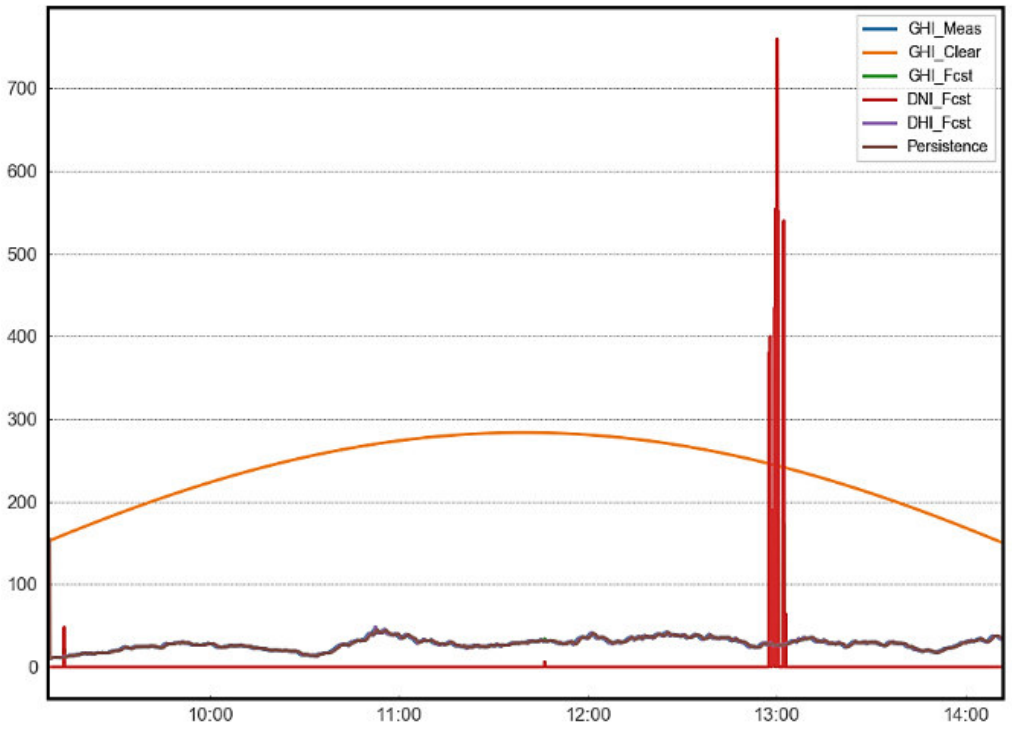

25 February

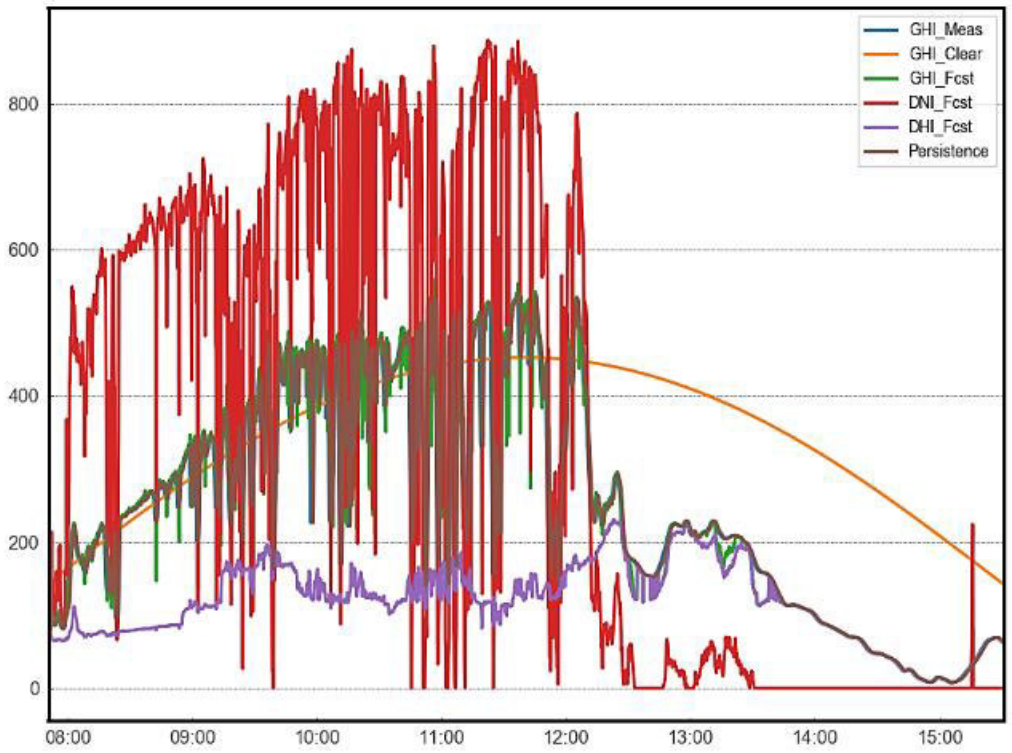

18 April

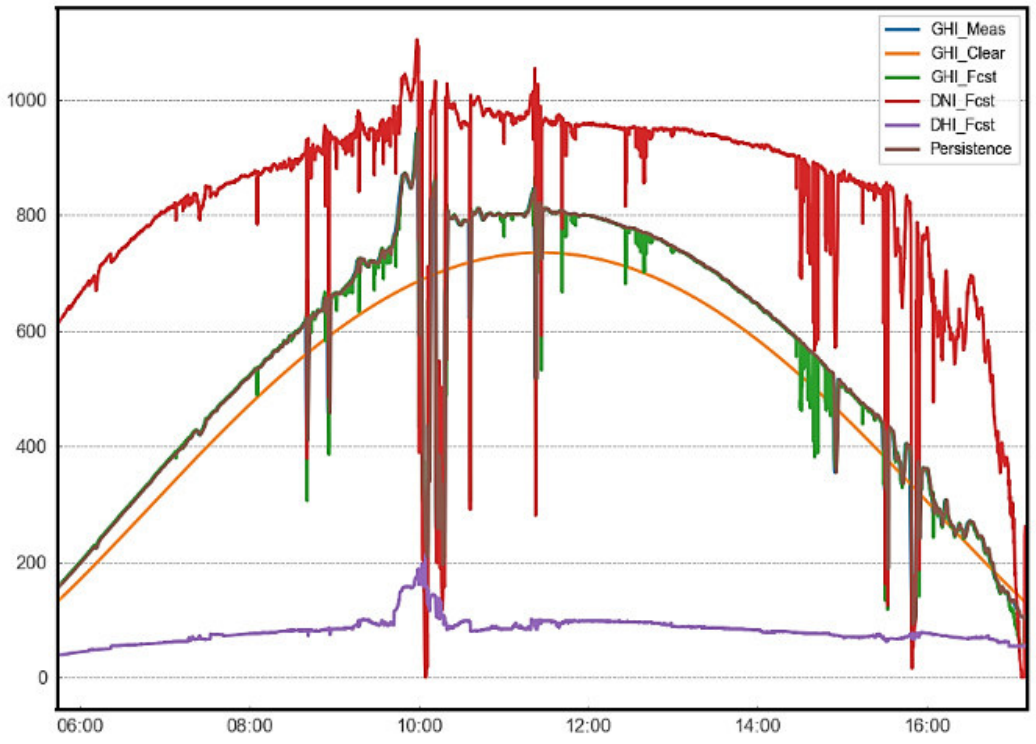

6 June

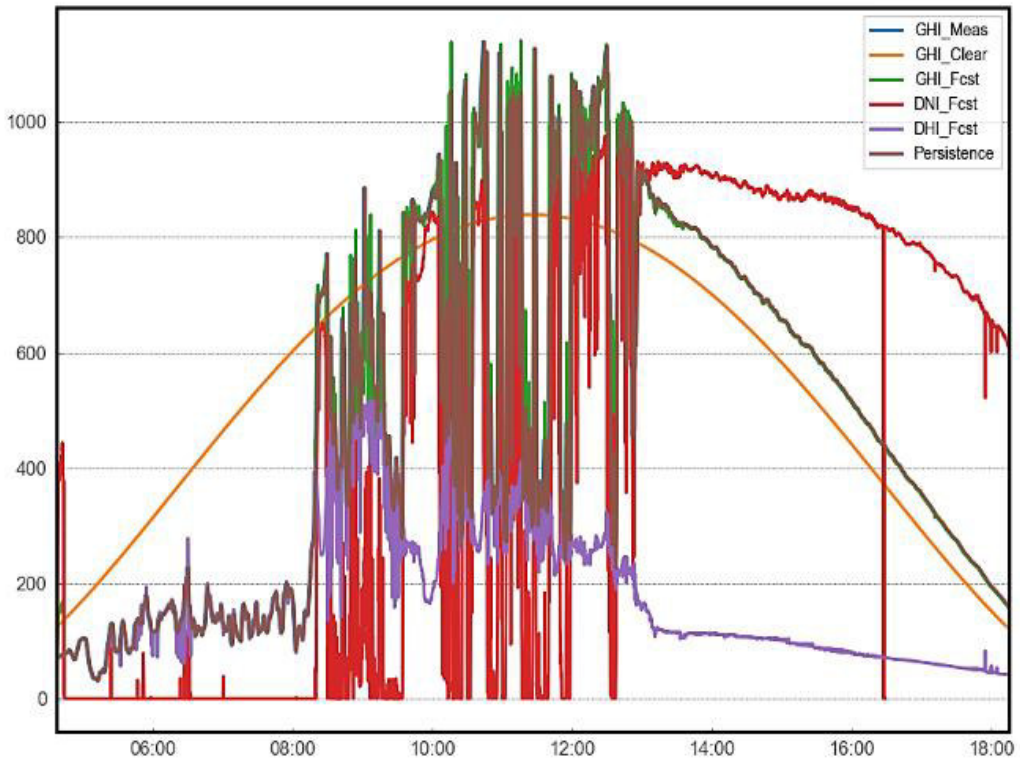

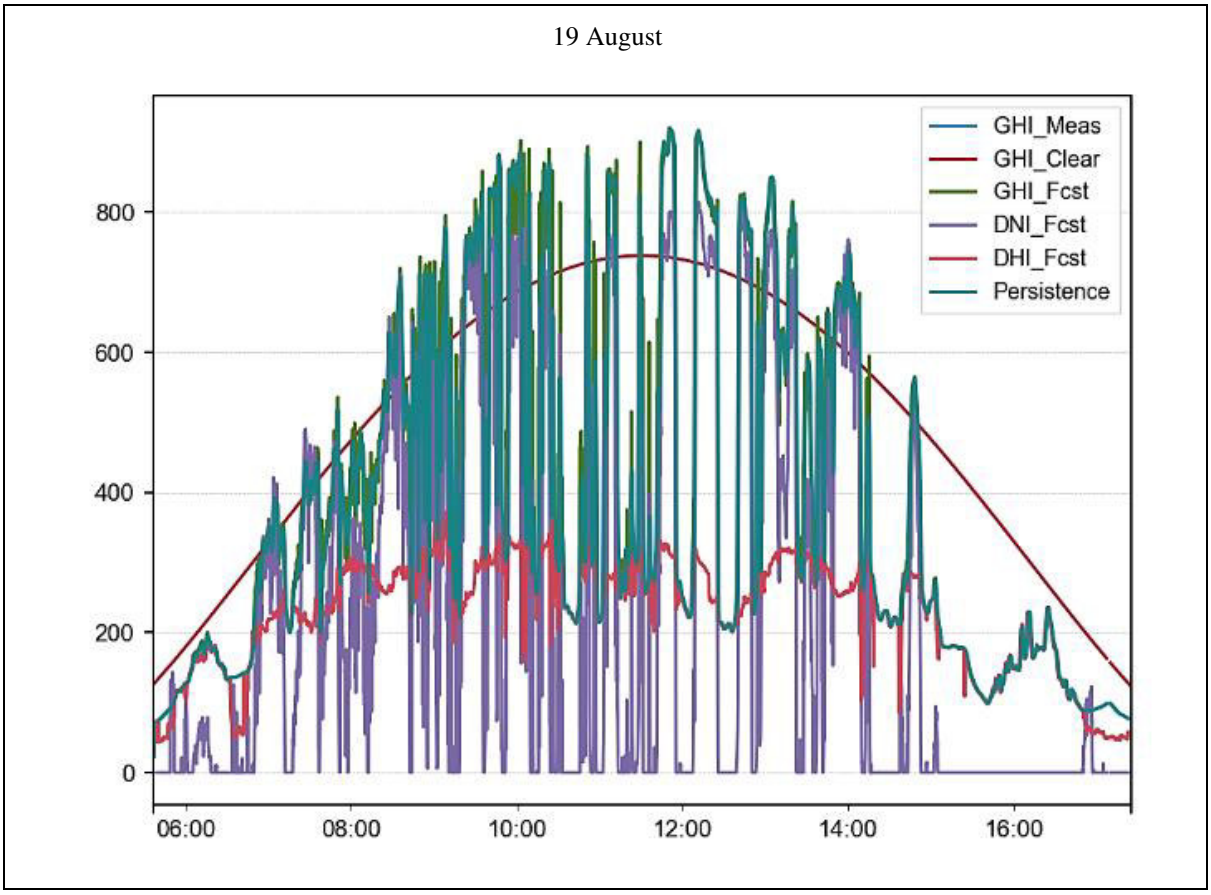

Figure 12: GHI, DHI and DNI and persistence GHI profile of 1-minute ahead GHI forecast for the five selected days

5.3 Results and Discussion

The model assesses the maximum allowable PV hosting capacity and consequent fuel consumption and PV penetration level for the five selected days, using the system configurations mentioned earlier. According to the load profile, the daily gross energy demand is 8823.06 kWh. Six 140kW DGs are available to supply the load. To meet the demand, diesel consumption is estimated to be 2186.72 litres per day for the DG only system. For the DG only configuration, the daily average number of DGs online is computed as 4.44.

For the DG-PV configuration (Case 2), the system performance is assessed after the introduction of PV forecasting strategy (table 2). The PV output power variability has a strong influence on the operation of DGs. This is very evident from the results presented in table 4, 5 and 6 and Appendix A. When PV forecasting is not employed, the injection of a relatively small amount of fluctuating PV generation into the electricity network is permitted so that it does not pose any significant technical issue to the system. This leads to the computation of the maximum allowed PV capacity that will not trigger an event leading to

the operating reserve falling below a certain amount, selected by the system operator. This study allows up to 50% of the OR to be used to cover any sudden reduction in PV power. This arbitrary level of OR inclusion has been selected for comparative purposes and is in line with what has been used in some SOPS systems by Horizon Power, a utility that supplies electricity to almost all the remote towns in Western Australia [43]. This approach is followed in this study to determine the allowed PV hosting capacity of the SOPS system.

The annual seasonal cycle strongly impacts on the annual solar irradiance pattern, and therefore the PV power output throughout the year. It follows that the PV hosting capacity for the system should be set to a safe amount which, regardless of the season, does not cause DG overload with the onset of cloud cover. Table 4 shows the PV hosting capacity determined for individual days and the final selection of PV hosting capacity for the SOPS system. Detailed results for the PV hosting capacity determined on specific days are given in appendix A. This approach establishes the PV hosting capacity to be 297kW for the DG-PV configuration (case 2) and 279kW for the DG-PV-BB configuration (case 3). These are the lowest values computed. When the batteries (BB) are integrated according to the algorithm presented, BB-RR takes part in daily energy charge/discharge activities and BB-ER provides the minimum operating reserve required. Hence, the arithmetic calculation of PV hosting capacity may vary from day to day depending on load profile, PV power fluctuation, DG scheduling and battery energy profile. A similar methodological analysis for 365 days, taking into consideration the dynamic load profile, would lead to the determination of the actual allowed PV hosting capacity for the SOPS system. This is recommended for future work.

Table 4: PV Hosting capacity determination for the SOPS system

#	System Configuration	Days	PV Hosting Capacity (kW)	Finalised PV Hosting Capacity (kW)
1	DG-only (base case scenario)	N/A	N/A	N/A
2	DG-PV	26 January	600	**297**
		25 February	299	
		18 April	454	
		6 June	**297**	
		19 August	323	
3	DG-PV-BB BB = 100kWh	26 January	600	**279**
		25 February	507	

#	System Configuration	Days	PV Hosting Capacity (kW)	Finalised PV Hosting Capacity (kW)
		18 April	432	
		6 June	**279**	
		19 August	286	
	DG-PV-BB BB = 50kWh	26 January	600	**279**
		25 February	507	
		18 April	432	
		6 June	**279**	
		19 August	286	

The application of 1-minute ahead PV forecasting informs the PSMS about the expected next minute's level of PV generation. In light of this, the PSMS dispatches the DGs in the current minute, in preparation for the next minute's instances. This strategy mitigates the technical challenges that could have arisen otherwise, by virtue of the uncertainty of the level of PV generation. This reduces the risk of a deficit in operating reserve for any future time instant, thereby allowing more PV capacity to be installed by prosumers. In this study, a high PV hosting capacity (600kW), which is higher than the maximum load of the system for the forecasting application cases (cases: 2.2-2.3, 3.2-3.3 and 3.5-3.6), is deliberately considered. It enables the BB-RR to be charged from the excess energy available during the sunshine hours. The study finds that this high PV capacity can be well integrated into the system, if 1-minute ahead PV forecasting is employed.

For simplicity, Tables 5, 6 and 7 present the analysis results of three different days, which are exposed to three different types of cloud coverage:

- 26 January (overcast day) in table 5
- 18 April (sunny day with clear sky) in table 6
- 19 August (random cloud movement throughout the day) in table 7

The tables present the values of the following parameters for each configuration cases: fuel consumption; energy supplied by both DG and PV; energy used from PV; the PV penetration level; the number of DG starts; and the average number of online DGs. The PV penetration level is calculated as the ratio between the amount of energy that is not served by the DGs and the total amount of daily energy demand. The "energy served by DGs" is the energy

served by the DGs to meet net load combined with the energy served to charge the BB at night, taking into account the energy losses in the BB system. Results for 25 February and 6 June are attached in Appendix A.

26 January (overcast day):

With the allowed PV hosting capacity being 297kW for case2 and 279kW for case 3 for the continuous overcast day (26 January) there are no unforecasted drops in PV power that lead to a reduction of operating reserve below 70 kW. This results in a PV penetration level of only 0.49% and 0.46% for cases 2.1, 3.1 and 3.4. When the maximum amount of 600kW of PV capacity is considered, the PV penetration level is found to be only 0.98% for both cases 2 and 3. As batteries are charged during the night from DGs, and the charging/discharging considers BB/inverter roundtrip efficiency, the energy served by the DGs for the higher capacity battery case is slightly higher than for the lower capacity battery case. However, the higher capacity battery case results in a lower average number of DGs online.

Table 5: Assessment of short-term PV forecasting for the overcast day of 26 January

Sl no	System configuration	Forecast strategy	Gross load demand kWh	PV hosting capacity kW	Fuel consumption L/day	Energy served by DG kWh	Energy available from PV kWh	PV energy used kWh	PV penetration level %	No. of DG starts	Average no. of DG online
1	DG-only	N/A	8823.66	N/A	2186.72	8823.66	N/A	N/A	N/A	6	4.44
2.1	DG-PV	No forecast	8823.66	297.00	2163.70	8780.63	43.02	43.02	0.49%	6	4.41
2.2		1-minute ahead forecast		600.00	2163.67	8736.74	86.91	86.91	0.98%	6	4.37
2.3		Perfect forecast		600.00	2163.84	8736.74	86.91	86.91	0.98%	5	4.37
3.1	DG-PV-100kWhBB	No forecast	8823.66	279.00	2109.16	8791.99	40.41	40.41	0.46%	5	3.26
3.2		1-minute ahead forecast		600.00	2108.85	8745.49	86.91	86.91	0.98%	6	3.25
3.3		Perfect forecast		600.00	2109.10	8745.49	86.91	86.91	0.98%	6	3.25
3.4	DG-PV-50kWhBB	No forecast	8823.66	279.00	2118.75	8787.62	40.41	40.41	0.46%	5	3.28
3.5		1-minute ahead forecast		600.00	2118.44	8741.12	86.91	86.91	0.98%	6	3.26
3.6		Perfect forecast		600.00	2118.68	8741.12	86.91	86.91	0.98%	6	3.26

18 April (sunny day with clear sky):

On 18 April, a clear sky day, the PV penetration level for case 2.1 is 19.64% (297kW). For cases 3.1 and 3.4 it is 18.45% (279kW). When the BB is not integrated, a comparison of case 1 with case 2.2 shows that, on average, one less DG is on operation throughout the day. When batteries are integrated, the PV hosting capacity is improved, as can be seen by comparing cases 2.2, 3.2 and 3.5. The inclusion of batteries and forecasting results in lowering the average number of DGs online, lowering fuel consumption, and improving PV penetration. Doubling the battery capacity from 50kWh to 100kWh does not show significant improvement in the system performance. However, it must be noted that the inclusion of battery and PV forecasting doubles the level of PV penetration from 19.64% (case 2.1) to 39.29% (cases 3.2, 3.5). In general, this doubles the fuel and cost savings.

Table 6: Assessment of short-term PV forecasting for the sunny clear sky day of 18 April

Sl no	System configuration	Forecast strategy	Gross load demand kWh	PV hosting capacity kW	Fuel consumption L/day	Energy served by DG kWh	Energy available from PV kWh	PV energy used kWh	PV penetration level %	No. of DG starts	Average no. of DG online
1	DG-only	N/A	8823.66	N/A	2186.72	8823.66	N/A	N/A	N/A	6	4.44
2.1	DG-PV	No forecast	8823.66	297.00	1772.85	7090.37	1733.29	1733.29	19.64%	10	3.88
2.2		1-minute ahead forecast		600.00	1395.69	5519.21	3501.60	3447.85	39.08%	15	3.33
2.3		Perfect forecast		600.00	1402.11	5545.70	3501.60	3376.40	38.27%	15	3.34
3.1	DG-PV-100kWhBB	No forecast	8823.66	279.00	1752.89	7205.33	1628.24	1628.24	18.45%	11	2.80
3.2		1-minute ahead forecast		600.00	1313.40	5411.98	3501.60	3466.75	39.29%	11	2.24
3.3		Perfect forecast		600.00	1320.71	5495.80	3501.60	3407.90	38.62%	12	2.26
3.4	DG-PV-50kWhBB	No forecast	8823.66	279.00	1743.62	7200.96	1628.24	1628.24	18.45%	12	2.80
3.5		1-minute ahead forecast		600.00	1324.11	5399.69	3501.60	3466.75	39.29%	12	2.27
3.6		Perfect forecast		600.00	1333.84	5469.37	3501.60	3407.90	38.62%	12	2.29

19 August (intermittent cloud cover throughout the day):

On this day, there are frequent cloud cover events (Figure 12), causing sharp net load fluctuations. Therefore, PV forecasting plays a significant role in enabling high PV

penetration levels on these intermittent cloudy days without causing any shortage in operating reserve. When 1-minute ahead PV forecasting is applied to the DG-PV-BB (100kWh) configuration (case 3.2), the average PV penetration level is 25.84%. This is almost double the amount of PV penetration for the DG-PV configuration without PV forecasting (case 2.1). Compared to the base case scenario, the DG-PV-BB (100kWh) configuration sees a reduction in average numbers of DGs online from 4.44 to 2.73. The reduced scheduling and loading of DGs results in diesel fuel savings of 27.12% for that day (comparing case 3.2 and 1). On a similar day, 6 June, the same outcome is observed (see Appendix A). The application of 1-minute ahead PV forecasting and 100kWh battery together increase the PV penetration level from 19.20% (case 2.1) to 35.79% (case 3.2). This results in a 38% fuel savings when compared to the base case configuration (case 1).

Table 7: Assessment of short-term PV forecasting for the intermittent cloud cover day of 19 August

Sl no	System configuration	Forecast strategy	Gross load demand kWh	PV hosting capacity kW	Fuel consumption L/day	Energy served by DG kWh	Energy available from PV kWh	PV energy used kWh	PV penetration level %	No. of DG starts	Average no. of DG online
1	DG-only	N/A	8823.66	N/A	2186.72	8823.66	N/A	N/A	N/A	6	4.44
2.1	DG-PV	No forecast	8823.66	297.00	1908.85	7650.68	1172.97	1172.97	13.29%	18	4.11
2.2		1-minute ahead forecast		600.00	1665.33	6622.70	2369.65	2252.63	25.53%	32	3.81
2.3		Perfect forecast		600.00	1662.24	6608.83	2369.65	2295.05	26.01%	33	3.81
3.1	DG-PV-100kWhBB	No forecast	8823.66	279.00	1871.18	7730.52	1101.89	1101.89	12.49%	20	3.01
3.2		1-minute ahead forecast		600.00	1593.69	6574.74	2369.65	2279.93	25.84%	30	2.73
3.3		Perfect forecast		600.00	1585.75	6575.72	2369.65	2310.45	26.18%	27	2.75
3.4	DG-PV-50kWhBB	No forecast	8823.66	279.00	1880.94	7726.14	1101.89	1101.89	12.49%	19	3.03
3.5		1-minute ahead forecast		600.00	1602.64	6569.88	2369.65	2279.93	25.84%	29	2.73
3.6		Perfect forecast		600.00	1596.20	6570.84	2369.65	2310.45	26.18%	26	2.75

Integration of PV-BB systems with the existing DGs, together with the application of 1-minute ahead PV forecasting delivers an improved level of PV penetration to the SOPS system, and significantly reduces the number of DGs required to be online for the whole day.

The reduced scheduling and loading of DGs save a significant amount of fuel, reducing operating and maintenance costs and benefiting the environment. On both 18 April and 6 June, it is observed that up to two less DGs are required to supply the load when the 1-minute ahead PV forecasting and BB are integrated in the configuration (case 3.2 in Figure 12). On these days, the estimated daily fuel savings are 873 litres (39.9%) and 831 litres (38%) of diesel, respectively (for case 3.2). This results in a reduction of around 2.28-2.34 tonnes of CO_2 emitted into the environment (burning 1-litre diesel = 2.68 kg of CO_2 emission). Figure 13 shows how the PV penetration level, fuel consumption and average numbers of DGs online are influenced by the BB systems and 1-minute ahead PV forecasting. From a comparative analysis, it is observed that the PV systems supplied 39.3% of the daily energy on 18 April. This amount is 35.8% and 25.8% for 6 June and 19 August, respectively. From figure 13 (a) it can be seen that the addition of 1-minute ahead PV-forecasting doubles the PV penetration level. This is the main mechanism by which PV forecasting saves diesel fuel.

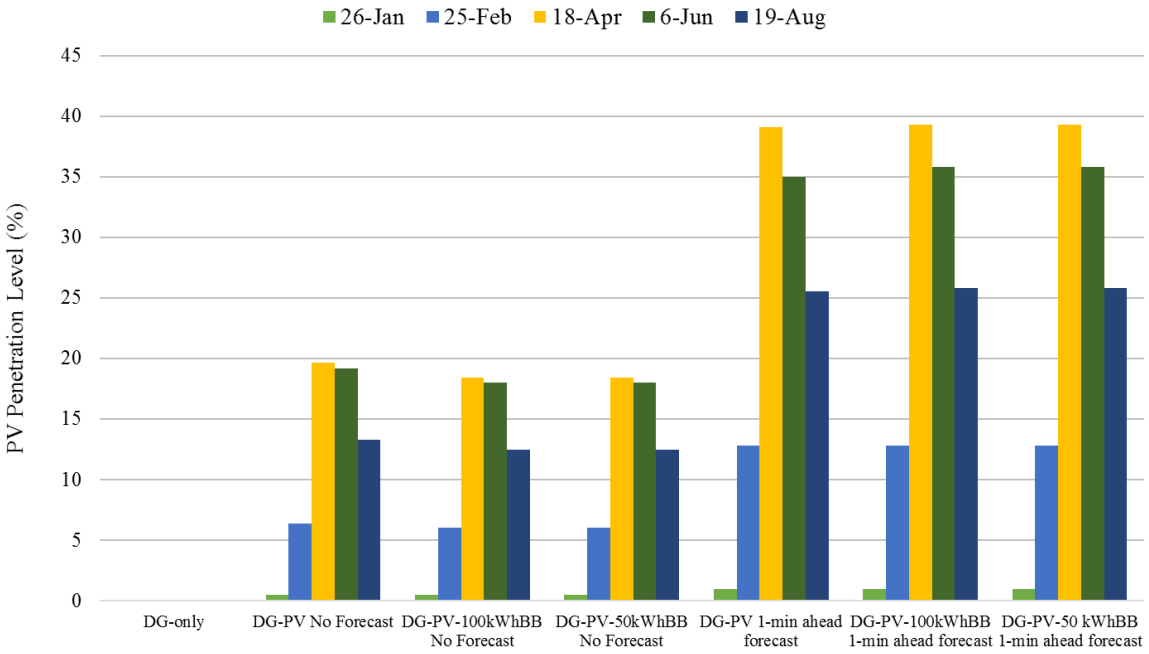

(a)

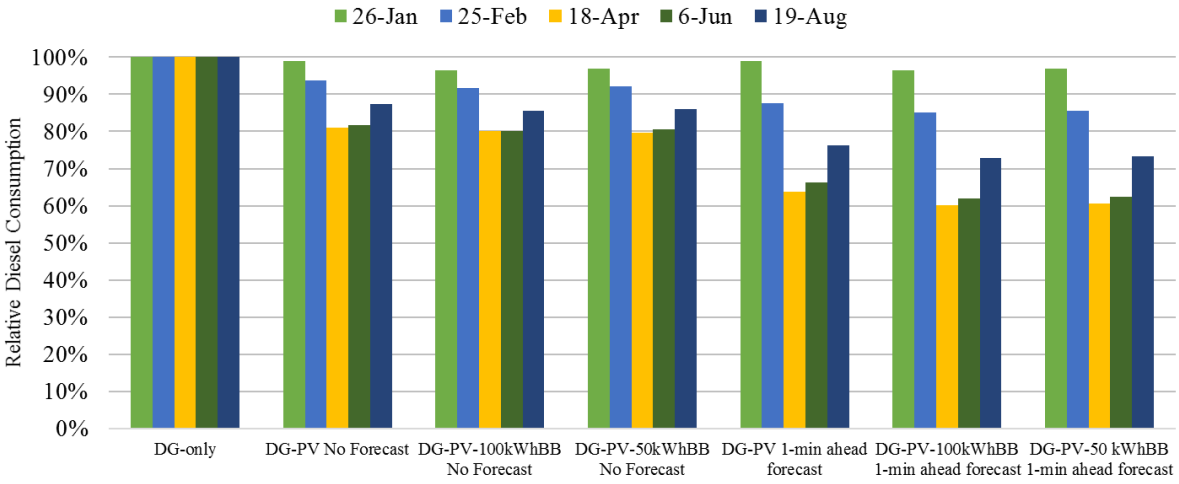

(b)

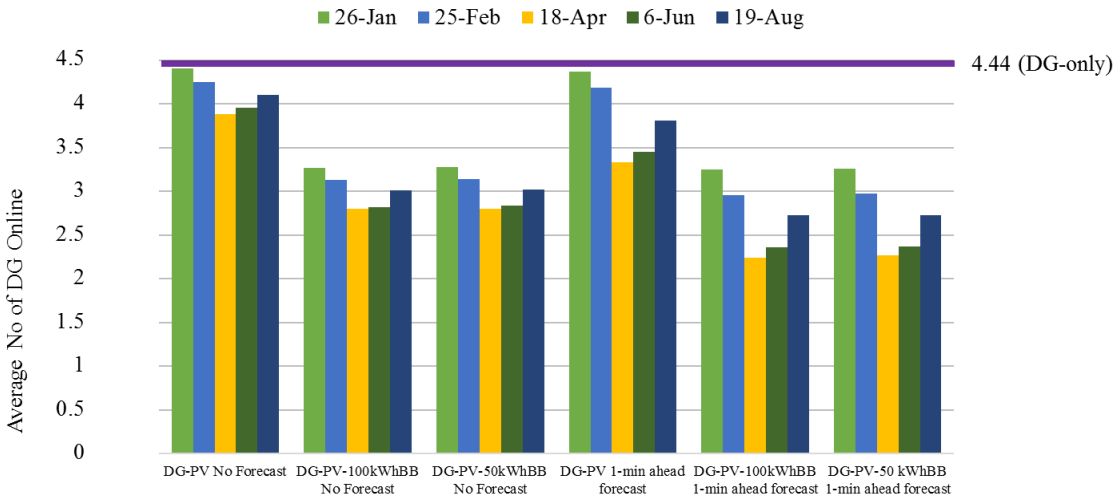

(c)

Figure 13: Influence of BB and 1-minute ahead PV forecasting on (a) PV penetration level, (b) fuel savings for various configuration cases and (c) average numbers of DGs online

The outcomes of the analysis indicate that different days exhibit differing PV penetration level and thus differing fuel savings potential. The addition of short-term PV forecasting improves the system performance by allowing much more prosumer PV capacity to be installed leading to much higher PV generation. The results can be summarised as follows:

- The tool demonstrates the benefits of having 1-minute ahead PV forecasting, compared to no forecasting. When clouds cause a sharp drop in PV power, 1-minute

ahead PV forecasting allows far more uncontrolled prosumer PV capacity to be installed without running short of operating reserve.

- Based on the five days of 1-minute ahead forecasting results analysed, the sky camera-based PV forecasting enables at least 600kW of PV capacity to be installed, whereas, with DG-PV-no forecasting, the allowed installed PV capacity is only 279kW.
- This additional 321kW of installed PV capacity saves 540.36 litres (average) of diesel fuel per day and reduces the average number of DGs online for the DG-PV-BB (100kWh, with 1-minute ahead forecast) configuration over the five days analysed.
- The addition of battery storage achieves additional fuel savings. The dual battery system increases the amount of available PV energy that can be utilised by storing excess PV energy for later use. It also reduces the required average number of online (30% minimum loaded) DGs, needed to maintain an adequate operating reserve.
- The 50kWh battery (with 1-minute ahead forecast) saves on average 530.74 litres of diesel fuel per day and also reduces the average number of DGs online over the five days analysed.
- Upsizing the battery energy capacity from 50kWh to 100kWh saves an additional 9.62 litres of diesel fuel per day (average).

The results demonstrate that the larger BB may not save sufficient fuel to justify the extra capital cost. However, the BB dispatch strategy does have a significant impact on fuel savings and there may exist more optimal battery sizing strategies to achieve fuel savings than those used in this study. To optimise the BB size (energy capacity), a thorough investigation is required, using one-minute data for the entire year for a SOPS system. It will also determine whether a dual or single battery/inverter system that provides the operating reserve (emergency backup until another DG can be started) and perhaps some additional energy storage capacity is required or not. The results in tables 5-7 and figure 13 show that application of PV forecasting and the integration of batteries benefit from one other. The literature reports many different percentage amounts of fuel-saving potential for different load and weather scenarios when the high share of PV is considered [17, 37]. However, fuel savings potential depends strongly on the available energy resource dispatch and the control strategies used to operate the system.

The results obtained in this study indicate that increasing the distributed PV to a higher penetration level could be safely managed if the design of the system is carefully chosen. It is

recommended that a high share of PV generation should be backed up with at least some BB capacity having immediate capability to take up the excess load. Care should be taken to accommodate PV forecast error as the error range varies from day to day, depending on weather conditions.

From the above discussion, it can be stated that short-term PV forecasting is a promising mechanism to allow high prosumer uncontrolled PV generation levels and reduce DG scheduling and fuel consumption. It is well demonstrated in this study that 1-minute ahead PV forecasting, using the cost-effective sky imagery-based system, offers an effective solution to address the technical challenges of high PV penetration as well as environmental issues of diesel-only systems.

6 Conclusion

This study incorporates a model that has been used to analyse the benefits of short-term PV forecasting and battery storage for different system configurations. The energy flow simulation tool developed in the study incorporates a 1-minute resolution energy flow data for a standalone off-grid power supply (SOPS) system in a remote area. The tool can assess the benefits of as short as 1-minute ahead PV forecasting using sky imager techniques to determine PV penetration level and consequential fuel savings potential for high PV integration into the system. This is a novel contribution of this study as currently, there is no other study available in the literature on the optimal temporal resolution of PV forecasting and no well-known commercially available energy flow modelling tool simulate power system operation with a resolution as high as 1-minute. The developed tool in this study is applied to three different system configurations: DG-only, DG-PV, and DG-PV-Battery for three different forecasting strategies: *no forecast*, *1-minute ahead forecast* and *perfect forecast*.

SOPS system configurations with and without battery storage system and 1-minute ahead PV forecasting have been studied to determine the potential PV hosting capacity and the consequent fuel savings. The application strategy is applied in a way that accommodates forecast errors by scheduling DGs one minute ahead of the time. However, the better the irradiance forecast performance is, the better the DG scheduling and fuel savings are. The analysis has been performed for selected days of the year in Oldenburg, Germany, where quantification of PV hosting capacity and PV penetration level, fuel-saving potential have

been estimated, and subsequent recommendations are made. For the days when random cloud movement occurs, the application of 1-minute ahead PV forecasting presents very similar results compared to the perfect forecasting (no forecast error).

Larger systems can benefit from a higher share of distributed PV, with battery and forecasting mechanisms each contributing to the maintenance of system stability with high PV penetration. It is expected that the benefits of forecast based approaches will be further enhanced by designing innovative application strategies and by utilising seasonal and cloud condition-oriented strategies within the control system. Overcoming the mentioned limitations in the development of the tool will achieve an even more precise outcome. The dispatch algorithm used in this study can be customised for each case by incorporating detailed analysis of the SOPS system size, daily load dynamics, seasonal impact on weather, and dynamic cloud movement components.

Based on the results obtained in this study, it can be seen that the integration of PV forecasting and batteries improves the system performance, where a decision has to be made to optimise the power and energy capacity of the dual battery bank system. Although the performance of the system is highly dependent on the particular geographic location, system configuration and load behaviour, the results confirm an advantage in incorporating 1-minute ahead PV forecasting. Even though the quantitative trends found in this analysis can significantly differ under other specific conditions, a general conclusion can be drawn that incorporating the 1-minute ahead forecasting can enable a significant increase in prosumer PV capacity, that reduces fuel consumption without compromising the reliability of the system.

The tool offers features appropriate to system planners or stakeholders who are keen to comprehensively understand the potential reliability of short-term PV forecasting, together with the diesel fuel savings and other potential benefits (e.g., reduced diesel generator operational costs) from short-term PV forecasting – with and without battery storage. Future work will entail refining the tool for PV-diesel-battery academic research, improving the dispatch algorithm by introducing dynamic behaviours of the modelling tool components, conducting further analysis using a location-specific one-minute data set for an entire year and then an experimental application on a real-life setup. This will provide more confidence in the reliability of the sky imagery-based PV forecasting mechanism and more accurately determine the system PV hosting capacity to be installed in a remote area SOPS system.

Acknowledgements

The authors would like to convey their gratitude to Ms. Dorothee Peters, from DLR Institute of Networked Energy Systems, Oldenburg, Germany for her constructive comments and suggestions on developing the energy flow modelling tool. A special gratitude for the "*Universities Australia/DAAD travel grant*" that supported the project "*Control strategies to maximize the Photovoltaic hosting capacity in remote diesel networks using sky camera based short-term solar forecasting techniques*" associated travel costs. A very special appreciation to the DLR Institute of Networked Energy Systems in Oldenburg, Germany for their substantial support to conduct this research.

References

[1] Jamal T, Urmee T, Calais M, Shafiullah GM, Carter C. Technical challenges of PV deployment into remote Australian electricity networks: A review. Renewable and Sustainable Energy Reviews. 2017;77:1309-25.
[2] Jamal T, Shafiullah GM, Carter C, Urmee T. A comprehensive techno-economic and power quality analysis of a remote PV-diesel system in Australia. Renew Energy Environ Sustain. 2017;2:24.
[3] Bekele G, Tadesse G. Feasibility study of small Hydro/PV/Wind hybrid system for off-grid rural electrification in Ethiopia. Applied Energy. 2012;97:5-15.
[4] Cader C, Bertheau P, Blechinger P, Huyskens H, Breyer C. Global cost advantages of autonomous solar–battery–diesel systems compared to diesel-only systems. Energy for Sustainable Development. 2016;31:14-23.
[5] Tao C, Shanxu D, Changsong C. Forecasting power output for grid-connected photovoltaic power system without using solar radiation measurement. The 2nd International Symposium on Power Electronics for Distributed Generation Systems2010. p. 773-7.
[6] Blechinger P, Cader C, Bertheau P, Huyskens H, Seguin R, Breyer C. Global analysis of the techno-economic potential of renewable energy hybrid systems on small islands. Energy Policy. 2016;98:674-87.
[7] Schmidt T, Calais M, Roy E, Burton A, Heinemann D, Kilper T, et al. Short-term solar forecasting based on sky images to enable higher PV generation in remote electricity networks. Renew Energy Environ Sustain. 2017;2:23.
[8] Schmidt T. High resolution solar irradiance forecasts based on sky images. Oldenburg, Germany: Carl von Ossietzky Universität Oldenburg; 2017.
[9] Parkinson G. What the Tesla big battery can and cannot do. 2017.
[10] Chenni R, Makhlouf M, Kerbache T, Bouzid A. A detailed modeling method for photovoltaic cells. Energy. 2007;32:1724-30.
[11] Jamal T, Shafiullah GM, Carter C, Ferdous S, Rahman MM. Benefits of Short-term PV Forecasting in a Remote Area Standalone Off-grid Power Supply System. IEEE PES General Meeting 2018. Portland, OR, USA2018.

[12] Anagnostos D, Schmidt T, Cavadias S, Soudris D, Poortmans J, Catthoor F. A method for detailed, short-term energy yield forecasting of photovoltaic installations. Renewable Energy. 2019;130:122-9.
[13] Liu L, Zhao Y, Chang D, Xie J, Ma Z, Sun Q, et al. Prediction of short-term PV power output and uncertainty analysis. Applied Energy. 2018;228:700-11.
[14] West SR, Rowe D, Sayeef S, Berry A. Short-term irradiance forecasting using skycams: Motivation and development. Solar Energy. 2014;110:188-207.
[15] Sayeef S, West S. Very short-term solar forecasting using inexpensive fisheye camera sky-imagery. In: Proceedings of the 52nd Annual Conference ASES, editor. Solar2014: The 52nd Annual Conference of the Australian Solar Council. Melbourne, Australia: Proceedings of the 52nd Annual Conference, Australian Solar Energy Society (Australian Solar Council); 2014.
[16] Schmidt T, Kalisch J, Lorenz E, Heinemann D. Evaluating the spatio-temporal performance of sky-imager-based solar irradiance analysis and forecasts. Atmos Chem Phys. 2016;16:3399-412.
[17] Olivier Liandrat, Antonin Braun, Etienne Buessler, Marion Lafuma, Sylvain Cros, Andre Gomez, et al. Sky-Imager Forecasting for Improved Management of a Hybrid Photovoltaic-Diesel System. 3rd International Hybrid Power Systems Workshop. Tenerife, Spain2018.
[18] Stefferud K, Kleissl J, Schoene J. Solar forecasting and variability analyses using sky camera cloud detection & motion vectors. Power and Energy Society General Meeting, 2012 IEEE2012. p. 1-6.
[19] Chow CW, Urquhart B, Lave M, Dominguez A, Kleissl J, Shields J, et al. Intra-hour forecasting with a total sky imager at the UC San Diego solar energy testbed. Solar Energy. 2011;85:2881-93.
[20] HOMER Energy. HOMER Pro. 2019.
[21] Natural Resources Canada. RETScreen. 2019.
[22] National Renewable Energy Laboratory. System Advisor Model (SAM) General Description (Version 2017.9.5). 2019.
[23] Reilly C. Off the grid: How renewable energy is helping remote towns take back the power. Australia2018.
[24] AECOM. Australia's Off-Grid Clean Energy Market Research Paper, Prepared for Australian Renewable Energy Agency. 2014.
[25] ARENA. Keynote address by ARENA CEO Ivor Frischknecht – Increasing renewables in remote, off-grid areas at the Remote Area Power Supply conference. 2014.
[26] Jamal T, Urmee T, Shafiullah G, Shahnia F. Using Experts' Opinions and Multi-Criteria Decision Analysis to Determine the Weighing of Criteria Employed in Planning Remote Area Microgrids. International Conference and Utility Exhibition on Green Energy for Sustainable Development. Thailand: IEEE; 2018.
[27] Bass RB, Carr J, Aguilar J, Whitener K. Determining the Power and Energy Capacities of a Battery Energy Storage System to Accommodate High Photovoltaic Penetration on a Distribution Feeder. IEEE Power and Energy Technology Systems Journal. 2016;3:119-27.
[28] McConnell D. Hornsdale Power Reserve, SA's battery is massive, but it can do much more than store energy. Australia2017.
[29] Tazvinga H, Xia X, Zhang J. Minimum cost solution of photovoltaic–diesel–battery hybrid power systems for remote consumers. Solar Energy. 2013;96:292-9.
[30] Rodríguez-Gallegos CD, Gandhi O, Bieri M, Reindl T, Panda SK. A diesel replacement strategy for off-grid systems based on progressive introduction of PV and batteries: An Indonesian case study. Applied Energy. 2018;229:1218-32.
[31] Salas V, Suponthana W, Salas RA. Overview of the off-grid photovoltaic diesel batteries systems with AC loads. Applied Energy. 2015;157:195-216.

[32] Elsinga B, van Sark WGJHM. Short-term peer-to-peer solar forecasting in a network of photovoltaic systems. Applied Energy. 2017;206:1464-83.
[33] Chaudhary P, Rizwan M. Energy management supporting high penetration of solar photovoltaic generation for smart grid using solar forecasts and pumped hydro storage system. Renewable Energy. 2018;118:928-46.
[34] Litjens GBMA, Worrell E, van Sark WGJHM. Assessment of forecasting methods on performance of photovoltaic-battery systems. Applied Energy. 2018;221:358-73.
[35] Moshövel J, Kairies K-P, Magnor D, Leuthold M, Bost M, Gährs S, et al. Analysis of the maximal possible grid relief from PV-peak-power impacts by using storage systems for increased self-consumption. Applied Energy. 2015;137:567-75.
[36] Angenendt G, Zurmühlen S, Axelsen H, Sauer DU. Comparison of different operation strategies for PV battery home storage systems including forecast-based operation strategies. Applied Energy. 2018;229:884-99.
[37] Peters D, Kilper T, Calais M, Jamal T, von Maydell K. Solar Short-Term Forecasts for Predictive Control of Battery Storage Capacities in Remote PV Diesel Networks. Transition Towards 100% Renewable Energy: Selected Papers from the World Renewable Energy Congress WREC 2017. Cham: Springer International Publishing; 2018. p. 325-33.
[38] Mazzola S, Vergara C, Astolfi M, Li V, Perez-Arriaga I, Macchi E. Assessing the value of forecast-based dispatch in the operation of off-grid rural microgrids. Renewable Energy. 2017;108:116-25.
[39] Saleh M, Meek L, Masoum MAS, Abshar M. Battery-Less Short-Term Smoothing of Photovoltaic Generation Using Sky Camera. IEEE Transactions on Industrial Informatics. 2018;14:403-14.
[40] Jamal T, Shoeb MA, Shafiullah GM, Carter CE, Urmee T. A design consideration for solar PV-diesel remote electricity network: Australia perspective. 2016 IEEE Innovative Smart Grid Technologies - Asia (ISGT-Asia)2016. p. 821-6.
[41] Erbs D, Klein S, Duffie J. Estimation of the diffuse radiation fraction for hourly, daily, and monthly-average global radiation. Solar Energy. 1982;28.
[42] Rohani G, Nour M. Techno-economical analysis of stand-alone hybrid renewable power system for Ras Musherib in United Arab Emirates. Energy. 2014;64:828-41.
[43] Jamal T. Verbal communication with Mr.Craig Carter (Adjunct Professor at Murdoch University, Australia and Industry Expert). 2018.

APPENDIX A

Individual Daily Results:

26 January:

Sl no	System configuration	Forecast strategy	Gross load demand	PV hosting capacity	Fuel consumption	Energy served by DG	Energy available from PV	PV energy used	PV penetration level	No. of DG starts	Average no. of DG online
			kWh	kW	L/day	kWh	kWh	kWh	%		
1	DG-only	N/A	8823.66	N/A	2186.72	8823.66	N/A	N/A	N/A	6	4.44
2	DG-PV	No forecast	8823.66	600.00	2163.70	8736.72	86.91	86.91	0.99%	6	4.41
		1-minute ahead		600.00	2163.67	8736.74	86.91	86.91	0.99%	6	4.37
		Perfect forecast		600.00	2163.84	8736.74	86.91	86.91	0.99%	5	4.37
3	DG-PV-100kWhBB	No forecast	8823.66	600.00	2109.16	8745.49	86.91	86.91	0.99%	5	3.26
		1-minute ahead		600.00	2108.85	8745.49	86.91	86.91	0.98%	6	3.25
		Perfect forecast		600.00	2109.10	8745.49	86.91	86.91	0.98%	6	3.25
	DG-PV-50kWhBB	No forecast	8823.66	600.00	2118.75	8745.49	86.91	86.91	0.99%	5	3.28
		1-minute ahead		600.00	2118.44	8741.12	86.91	86.91	0.98%	6	3.26
		Perfect forecast		600.00	2118.68	8741.12	86.91	86.91	0.98%	6	3.26

25 February:

Sl no	System configuration	Forecast strategy	Gross load demand	PV hosting capacity	Fuel consumption	Energy served by DG	Energy available from PV	PV energy used	PV penetration level	No. of DG starts	Average no. of DG online
			kWh	kW	L/day	kWh	kWh	kWh	%		
1	DG-only	N/A	8823.66	N/A	2186.72	8823.66	N/A	N/A	N/A	6	4.44
2	DG-PV	No forecast	8823.66	299.00	2050.77	8255.36	568.27	568.27	6.44%	14	4.25
		1-minute ahead		600.00	1916.19	7685.61	1140.33	1131.20	12.82%	18	4.19
		Perfect forecast		600.00	1917.62	7685.70	1140.33	1140.33	12.92%	19	4.13
3	DG-PV-100kWhBB	No forecast	8823.66	507.00	1903.58	7777.32	963.58	963.58	10.92%	15	3.05
		1-minute ahead		600.00	1860.13	7692.07	1140.33	1131.20	12.82%	19	2.96
		Perfect forecast		600.00	1860.66	7692.07	1140.33	1140.33	12.92%	19	2.97
	DG-PV-50kWhBB	No forecast	8823.66	507.00	1913.09	7819.62	963.58	963.58	10.92%	15	3.05
		1-minute ahead		600.00	1869.72	7679.79	1140.33	1131.20	12.82%	19	2.97
		Perfect forecast		600.00	1870.24	7687.70	1140.33	1140.33	12.92%	19	2.98

18 April:

Sl no	System configuration	Forecast strategy	Gross load demand	PV hosting capacity	Fuel consumption	Energy served by DG	Energy available from PV	PV energy used	PV penetration level	No. of DG starts	Average no. of DG online
			kWh	kW	L/day	kWh	kWh	kWh	%		
1	DG-only	N/A	8823.66	N/A	2186.72	8823.66	N/A	N/A	N/A	6	4.44
2	DG-PV	No forecast	8823.66	454.00	1555.50	6177.28	2649.54	2649.54	30.03%	9	3.60
		1-minute ahead		600.00	1395.69	5519.21	3501.60	3447.85	39.08%	15	3.33
		Perfect forecast		600.00	1402.11	5545.70	3501.60	3376.40	38.27%	15	3.34
3	DG-PV-100kWhBB	No forecast	8823.66	432.00	1534.66	6233.89	2521.15	2521.15	28.57%	10	2.54
		1-minute ahead		600.00	1313.40	5411.98	3501.60	3466.75	39.29%	11	2.24
		Perfect forecast		600.00	1320.71	5495.80	3501.60	3407.90	38.62%	12	2.26
	DG-PV-50kWhBB	No forecast	8823.66	432.00	1543.81	6272.66	2521.15	2521.15	28.57%	9	2.55
		1-minute ahead		600.00	1324.11	5399.69	3501.60	3466.75	39.29%	12	2.27
		Perfect forecast		600.00	1333.84	5469.37	3501.60	3407.90	38.62%	12	2.29

6 June:

Sl no	System configuration	Forecast strategy	Gross load demand	PV hosting capacity	Fuel consumption	Energy served by DG	Energy available from PV	PV energy used	PV penetration level	No. of DG starts	Average no. of DG online
			kWh	kW	L/day	kWh	kWh	kWh	%		
1	DG-only	N/A	8823.66	N/A	2186.72	8823.66	N/A	N/A	N/A	6	4.44
2	DG-PV	No forecast	8823.66	297.00	1785.30	7129.29	1694.37	1694.37	19.20%	19	3.95
		1-minute ahead		600.00	1449.69	5733.62	3422.97	3096.78	35.10%	22	3.45
		Perfect forecast		600.00	1475.19	5754.35	3422.97	3126.88	35.44%	23	3.47
3	DG-PV-100kWhBB	No forecast	8823.66	279.00	1752.82	7240.72	1591.68	1591.68	18.04%	17	2.82
		1-minute ahead		600.00	1355.71	5678.72	3422.97	3158.36	35.79%	15	2.36
		Perfect forecast		600.00	1358.97	5690.97	3422.97	3197.70	36.24%	16	2.38
	DG-PV-50kWhBB	No forecast	8823.66	279.00	1762.55	7236.35	1591.68	1591.68	18.04%	17	2.84
		1-minute ahead		600.00	1365.33	5674.34	3422.97	3158.36	35.79%	16	2.37
		Perfect forecast		600.00	1368.46	5686.59	3422.97	3197.70	36.24%	17	2.38

19 August:

Sl no	System configuration	Forecast strategy	Gross load demand	PV hosting capacity	Fuel consumption	Energy served by DG	Energy available from PV	PV energy used	PV penetration level	No. of DG starts	Average no. of DG online
			kWh	kW	L/day	kWh	kWh	kWh	%		
1	DG-only	N/A	8823.66	N/A	2186.72	8823.66	N/A	N/A	N/A	6	4.44
2	DG-PV	No forecast	8823.66	323.00	1885.18	7548.00	1275.66	1275.66	14.46%	22	4.09
		1-minute ahead		600.00	1665.33	6622.70	2369.65	2252.63	25.53%	32	3.81
		Perfect forecast		600.00	1662.24	6608.83	2369.65	2295.05	26.01%	33	3.81
3	DG-PV-100kWhBB	No forecast	8823.66	286.00	1864.14	7613.25	1129.53	1129.53	12.80%	17	2.99
		1-minute ahead		600.00	1593.69	6574.74	2369.65	2279.93	25.84%	30	2.73
		Perfect forecast		600.00	1585.75	6575.72	2369.65	2310.45	26.18%	27	2.75
	DG-PV-50kWhBB	No forecast	8823.66	286.00	1873.87	7653.67	1129.53	1129.53	12.80%	16	3.01
		1-minute ahead		600.00	1602.64	6569.88	2369.65	2279.93	25.84%	29	2.73
		Perfect forecast		600.00	1596.20	6570.84	2369.65	2310.45	26.18%	26	2.75

After finalising the PV hosting capacity, the following tables represent the days for 25 February and 6 June:

25-Feb

Sl no	System configuration	Forecast strategy	Gross load demand	PV hosting capacity	Fuel consumption	Energy served by DG	Energy available from PV	PV energy used	PV penetration level	No. of DG starts	Average no. of DG online
			kWh	kW	L/day	kWh	kWh	kWh	%		
1	DG-only	N/A	8823.66	N/A	2186.72	8823.66	N/A	N/A	N/A	6	4.44
2	DG-PV	No forecast	8823.66	297.00	2051.63	8259.19	564.46	564.46	6.40%	14	4.25
		1-minute ahead forecast		600.00	1916.19	7685.61	1140.33	1131.20	12.82%	18	4.19
		Perfect forecast		600.00	1917.62	7685.70	1140.33	1140.33	12.92%	19	4.13
3	DG-PV-100kWhBB	No forecast	8823.66	279.00	2004.34	8302.15	530.25	530.25	6.01%	11	3.13
		1-minute ahead forecast		600.00	1860.13	7692.07	1140.33	1131.20	12.82%	19	2.96
		Perfect forecast		600.00	1860.66	7692.07	1140.33	1140.33	12.92%	19	2.97
	DG-PV-50kWhBB	No forecast	8823.66	279.00	2013.97	8297.78	530.25	530.25	6.01%	11	3.14
		1-minute ahead forecast		600.00	1869.72	7679.79	1140.33	1131.20	12.82%	19	2.97
		Perfect forecast		600.00	1870.24	7687.70	1140.33	1140.33	12.92%	19	2.98

6-Jun

Sl no	System configuration	Forecast strategy	Gross load demand	PV hosting capacity	Fuel consumption	Energy served by DG	Energy available from PV	PV energy used	PV penetration level	No. of DG starts	Average no. of DG online
			kWh	kW	L/day	kWh	kWh	kWh	%		
1	DG-only	N/A	8823.66	N/A	2186.72	8823.66	N/A	N/A	N/A	6	4.44
2	DG-PV	No forecast	8823.66	297.00	1785.30	7129.29	1694.37	1694.37	19.20%	19	3.95
		1-minute ahead forecast		600.00	1449.69	5733.62	3422.97	3096.78	35.10%	22	3.45
		Perfect forecast		600.00	1475.19	5754.35	3422.97	3126.88	35.44%	23	3.47
3	DG-PV-100kWhBB	No forecast	8823.66	279.00	1752.82	7240.72	1591.68	1591.68	18.04%	17	2.82
		1-minute ahead forecast		600.00	1355.71	5678.72	3422.97	3158.36	35.79%	15	2.36
		Perfect forecast		600.00	1358.97	5690.97	3422.97	3197.70	36.24%	16	2.38
	DG-PV-50kWhBB	No forecast	8823.66	279.00	1762.55	7236.35	1591.68	1591.68	18.04%	17	2.84
		1-minute ahead forecast		600.00	1365.33	5674.34	3422.97	3158.36	35.79%	16	2.37
		Perfect forecast		600.00	1368.46	5686.59	3422.97	3197.70	36.24%	17	2.38

An Energy Flow Simulation Tool for Incorporating Short-Term PV Forecasting in a Diesel-PV-Battery Off-Grid Power Supply System

Taskin Jamal[*], Craig Carter[*], Thomas Schmidt[#], GM Shafiullah[*], Martina Calais[*], Tania Urmee[*]

*College of Science, Health, Engineering and Education, Murdoch University, WA 6150, Australia

[#]DLR Institute of Networked Energy Systems, Energy Systems Analysis, 26122 Oldenburg, Germany

Abstract

One of the primary technical challenges of integrating high levels of PV generation into standalone off-grid power supply systems is their variable power output characteristics. In dealing with this issue, the integration of reliable PV forecasting techniques and preferably energy storage, are highly effective. Applying a short-term PV forecasting method, together with a compensatory controllable resource, can help in the management of system operation. This study incorporates the development of an energy flow modelling tool that has been used to analyse the benefits of 1-minute ahead PV forecasting and battery storage for different system configurations. Based on the five days of 1-minute ahead forecasting results analysed, it is found that PV forecasting enables the prosumer to install more than double the PV capacity, compared to the allowed installed PV capacity when no forecasting is employed. This additional PV capacity saves around 24-25% (on average) of diesel fuel per day for the diesel-PV-battery configuration. The outcomes evidently indicate that incorporating 1-minute ahead PV forecasting enables a significant increase of PV hosting capacity of the system, without compromising the reliability of the system.

Keywords: Energy flow modelling tool, Short-term PV forecasting, PV hosting capacity, PV penetration level, Standalone off-grid power supply system, remote area electricity

1. Introduction

Across the world, electricity access in remote and rural areas has always been economically and technically challenging due to the long distances between the load centres and their nearest power grid line and substation, low load densities and challenging topography [1]. Predominantly, diesel generators (DG) are used to meet the load demands for these areas due to their convenience and economic advantages [2, 3]. Nevertheless, solar PV systems are the most widely used and the fastest growing off-grid renewable energy technology (RET) deployed in these off-grid type power supply systems. This is due to the abundance of solar irradiance available in most parts of the world, and the rapidly decreasing cost of PV technologies [4].

One of the primary technical challenges of integrating PV systems into power supply systems is their variable power output characteristics. This variability is due to diurnal and seasonal impacts together with random cloud movements [1]. As it might be perceived as an inconsistent resource, PV power raises a grid integration concern, in particular, due to the difficulty of dispatching that energy [5]. Therefore, in dealing with this variable nature of PV output power, the integration of energy storage technologies and reliable forecasting techniques are essential.

The integration of distributed PV systems with centralised battery energy storage systems is gaining importance in remote area standalone off-grid power supply (SOPS) systems. A comprehensive study conducted by Blechinger et al. has revealed that PV-battery based systems along with DG based systems could be economically operated for almost 1,800 small islands worldwide with populations below 100,000 per island [6]. Cader et al. have remarked that in many regions around the world, the introduction of DG-PV-battery systems achieves significant reductions in the levelised cost of energy, compared to diesel-only systems [4].

Generally, a low spatial diversity of PV systems in a small area leads to very high PV power variability compared to dispersed PV systems. An isolated or island community can be fully or partially shaded or unshaded by fast-moving clouds in a time span ranging from a few seconds to minutes [7, 8]. Hence, to accommodate this variable nature of power output, there is a need to ensure power supply quality and network stability. Therefore, either DGs must offer sufficient flexibility or battery storage must be introduced to provide an adequate buffer against short-term PV power fluctuations. DG flexibility includes spinning reserve (SR, a

subset of operating reserve) and step load capability. If the DGs and storage systems do not offer enough flexibility, network operators have to limit the maximum PV penetration to certain levels, which adversely affects the uptake of PV systems [1]. Depending on the system control mechanism, batteries can also provide grid-forming and black start capability. They can be seen by the system as a synchronous generator and can provide frequency support by acting as a "virtual generator". They can also detect and clear faults across the entire network, as well as providing synthetic inertia to the system [9].

Proper control of PV power output can facilitate stable, reliable and effective operation of the system. The motion of clouds affects the performance of PV systems and therefore must be forecast to avoid undesired technical issues and costs [10]. To manage the PV power output variability, system operators need knowledge of cloud movement prediction. Power utilities are always concerned with meeting the minimum requirement of operating reserve (OR) at every instant, to ensure high reliability of operation at a minimal cost. Applying a short-term PV forecasting method, together with an alternative compensatory controllable resource, can help in the management of system operation in maintaining the system stability while increasing PV penetration level [11-15]. This is discussed in detail in later sections. However, the benefit of short-term PV forecasting varies with the network's specific design and control mechanism.

Solar irradiance and PV output forecasting is not a new concept in power systems operation. Different methods are used for solar PV forecasting depending on application level, forecast horizon and cloud conditions [8, 16]. The forecast accuracy depends on the area of the site, and whether forecasting is performed for a single, small location or a large area. Short-term PV forecasting using ground-based sky imagery mechanisms demonstrates clear advantages over other well-known, conventional methods. These include numerical weather prediction (NWP), satellite imaging and statistical-based methods [8, 17]. Complex configurations of clouds and the associated small scale dynamics limit the application of modern-day NWP models. These models also lack the necessary temporal and spatial resolution to predict small scale atmospheric phenomena precisely. Hence, very high-resolution sensors are required.

Ground-based sensors, i.e. sky imagery mechanisms, provide useful and continuously updated information on current sky conditions. A depiction of the future sky can be achieved through observing and analysing subsequent images captured by the sky-facing camera. This technique fills the forecasting gap mentioned above by providing sub-kilometre resolution of

cloud coverage. This can be combined with measures of solar irradiance, cloud height above ground and basic geometrical considerations, with further support from machine learning and maps of the local surface, yielding a sufficiently accurate irradiance prediction [8, 12, 14-19].

To improve the PV penetration levels in a remote area DG-PV-battery based SOPS system, it is essential to offset the uncertainties of the PV output variability as much as possible using high-resolution data computation. In these types of systems smaller sized DGs of a few hundred kilowatts capacity usually take roughly around a minute to go to full load from a cold start. Hence, this calls for an assessment of 1-minute-level DG scheduling to ensure adequate system operating reserve. On the other hand, the PV forecast period should be adapted to the system size. Smaller sized power systems have similar array areas and therefore have higher fluctuation probabilities and need higher resolution forecasting. Currently, there is no study available in the literature on the optimal temporal resolution of PV forecasting. The effect of various temporal resolutions cannot be quantified. Thus, the data computation resolution of a 1-minute window for PV forecasting and DG-battery dispatch represents a sensible approach and hence, this study investigates the benefit of 1-minute–level PV forecasting to enable high PV penetration into a diesel-PV-battery based SOPS system. The study considers PV irradiance forecast resolutions as high as 1-second but averaged to 1-minute for better computing performance.

Most well-known and commercially available microgrid and renewable energy-based system simulation software tools used for energy flow modelling do not accurately simulate minute-level system operation. For example, HOMER Pro by HOMER Energy [20], RETScreen Expert by Natural Resources Canada [21], and the System Advisor Model (SAM) by the US National Renewable Energy Laboratory (NREL) [22] can perform system simulations at an hourly resolution. Therefore, to incorporate 1-minute ahead PV forecasting into the energy flow of a system, a Microsoft Excel-based energy flow simulation tool is developed in this study to assess the performance of a test SOPS system. The core novelty offered in this study can thus be summarised as follows:

- Development of an energy flow simulation tool that simulates 1-minute resolution real power flow, using a customizable generation dispatch strategy to meet the system reliability objectives
- Development of an algorithm for the application of sky camera-based 1-minute ahead PV forecasting data and

- Assessment of short-term (1-minute) PV forecasting benefits in relation to system performance

The remainder of the article comprises: Section 2, which provides key background information; Section 3, which describes the methodology; Section 4, which sets out the development of the tool; Section 5, which describes the application of the tool to assess PV forecasting benefits; and finally Section 6, which presents the conclusions reached by the study.

2. Issues and opportunities of PV forecasting into diesel-PV-battery SOPS systems

The integration of PV generators and batteries into SOPS systems is gaining popularity among stakeholders. In many remote, rural and off-grid communities around the world, there are now ample numbers of DG-PV-battery-based SOPS systems being used for electricity supply [23, 24]. For example, the former Chief Executive Officer (CEO) of Australian Renewable Energy Agency (ARENA) mentioned in a speech that, "*In off-grid locations, renewable energy has unique advantages over the incumbent fossil fuels. Many remote Australian communities rely on diesel generators that are expensive to run and which create energy uncertainty due to the volatility of fuel prices ... So unpredictable diesel costs, falling renewable generation costs and increased energy security can all provide motivators for the adoption of renewables … Regional Australia's Renewables – Industry (I-RAR) has a fairly wide remit, focussing on developing renewable energy solutions for remote areas where fossil fuels are currently or would otherwise be used to generate electricity*" [25]. This illustrates the significant interest remote utilities have to improve system components so as to facilitate the use of more renewables in power systems.

Battery storage systems, along with other smart control mechanisms, are offering better solutions to many of the technical challenges posed by variable PV generators. A recent study has found that academics, industry experts and consultants now agree that DG-PV-battery systems are superior to DG-PV or DG-only systems for remote off-grid communities, considering the economic and technical issues involved [26]. Cader et al. have used a novel research framework to form an overview of the overall potential of DG-PV-battery based systems worldwide [4]. According to that study, where there were higher shares of PV, a centralised battery bank (BB) was used for load shifting and reduced diesel consumption.

This required substantial initial capital investment but operation and maintenance costs were decreased compared to the DG-only scenario.

Where batteries are incorporated into SOPS system, the response time and sizing are critical. Bass et al. [27] have determined the power and energy capacity of the centralised battery bank for a rural type feeder in Portland, OR, USA. The centralised BB control mechanism enabled the feeder to integrate a higher share of PV output (30-55% of the average maximum feeder load) [27]. The Hornsdale Power Reserve in South Australia owns a substantial capacity 100MW and 129MWh Li-ion battery. The power output of the BB can rise from zero to 30 MW, or drop from 30 MW to zero, within a few milliseconds [28].

A well-developed DG-PV-battery SOPS system model incorporating robust generation dispatch strategies provides a more reasonable estimate of fuel and cost savings. Employing a load-following DG dispatch strategy showed that the DG-PV-battery model could achieve 73-77% fuel savings in winter and 80.5-82% fuel savings in summer, compared to the DG only scenario [29]. A study based on an Indonesian island has shown that the gradual reduction of the number of online DGs by employing more PV-battery systems still results in low initial capital expenditure [30]. A review by Salas et al. of current techniques used in off-grid DG-PV-battery systems has demonstrated that for low PV penetration (<20%) no extra control or energy storage is required [31]. However, it has also shown that for medium (20-65%) and high PV penetration (65-100%) systems, support from energy storage and a robust control management system is required [31].

In order to incorporate more PV systems into electricity supply systems, detailed PV power output information and knowledge of power fluctuation patterns are very important. Elsinga et al. [32] commented that solar irradiance forecasting is an essential component in economic realisation for high levels of PV penetration. Their study utilised a short-term, intra-hour solar forecasting method and found that during the highly variable days, this method had superior performance to the persistence method [32]. In [33], the researchers successfully demonstrated the management of system with a high penetration of PV generation in a smart grid using 15-minutes ahead PV power forecasting. Litjens et al. [34] developed and assessed forecasting methods using 5-minute resolution data to predict PV yield in order to improve self-consumption of PV power, decrease curtailment losses and improve revenues. Another study has shown that integration of batteries and solar irradiance forecasting into the system has higher potential to relieve the network than a system which only maximises self-

consumption [35]. Analysis of a German residential demand profile has shown that 26% more PV capacity can be added to the grid using PV-battery systems with persistence forecast algorithms [35]. Angenendt et al. [36] looked into forecast-based operation strategies to increase BB lifetime and reduce PV curtailment. Liu et al. [13] incorporated solar prediction interval and deterministic point predictions into their algorithm, resulting in a better performance than conventional forecast methods.

PV forecasting yields benefits to the power system in various ways by addressing the technical challenges of high levels of PV penetration. A short-term PV forecasting mechanism using "Sky Camera" (sky imager) images has been used to forecast the solar irradiance levels in these several research works [15, 16, 18, 37]. The authors' previous research has revealed that the application of sky imagery-based short-term PV forecasting enables the system to integrate high levels of PV penetration without adversely affecting system stability. It offers favourable outcomes during high net load fluctuations caused by abrupt PV and load variations. Schmidt et al. [7] investigated the possibility of reducing spinning reserve requirements under constant clear sky conditions with high levels of PV penetration in the network. This study mentioned that "*the accurate prediction of changes in solar irradiance in the 2-5 min time window is of importance rather than the accurate prediction of irradiance at a specific point in time and space*".

Mazzola et al. assessed the potential benefit of PV forecasting and revealed that cost savings could vary from 2-7% depending on the forecast quality and the composition of the microgrid [38]. Liandrat et al. [17] utilised a thermal-infrared sky imager for PV forecasting to optimise the hybrid DG-PV system. Their study considered a relatively high PV penetration level of 30% and 10-minutes ahead irradiance forecasting for an island in France. However, the study case was limited to considerations of a constant load throughout the analysis period. Also, the efficiencies of PV and DG were 100%, and all DGs were always operating at their nominal output. The results revealed that compared to the 'no forecast' scenario, the inclusion of forecasting in the system control reduces the overall fuel consumption, helps to inject more PV into the network and reduces the potential number of blackout events. The estimated cost reduction was around US$97,000 per year [17]. However, the consideration of load dynamics, realistic efficiency curves for PV and DGs and dynamic control of DG output would result in a different cost estimation.

A recent study [39] concentrated on the use of a binary prediction model for PV forecast to eliminate the use of batteries in the network. The study showed that the elimination of battery storage is the most economical option only when the annual percentage of an average number of cloudy days does not exceed the percentage share of battery costs within the overall operation & maintenance costs of a DG-PV system. This is not always the case for the majority of remote and rural areas.

In light of the discussion above, it is apparent that to facilitate high levels of PV penetration in a SOPS system, the following issues need to be considered:

- BB dispatch and control mechanism to address stability issues
- DG dispatch strategies to reduce fuel consumption
- Real-time irradiance measurement to improve performance of PV forecasting
- Selection of a time window to accurately predict changes in solar irradiance

To address the above issues, sky camera-based 1-minute ahead PV forecasting is applied in this study, enabling the system to integrate a high level of PV penetration without adversely affecting system stability. The dispatch strategy followed in this study provides the potential for higher reductions of CO_2 emissions from fossil fuel-based power generation, as self-consumption of PV energy by the prosumers is maximised.

3. Methodology

The overall methodology of this study is displayed as a flowchart in Figure 1. The work is carried out in three steps. Step 1 describes the design and specification of the SOPS system. Step 2 explains the development of the energy flow simulation tool and step 3 discusses the application of the tool to assess the PV forecasting benefits for SOPS systems in remote areas.

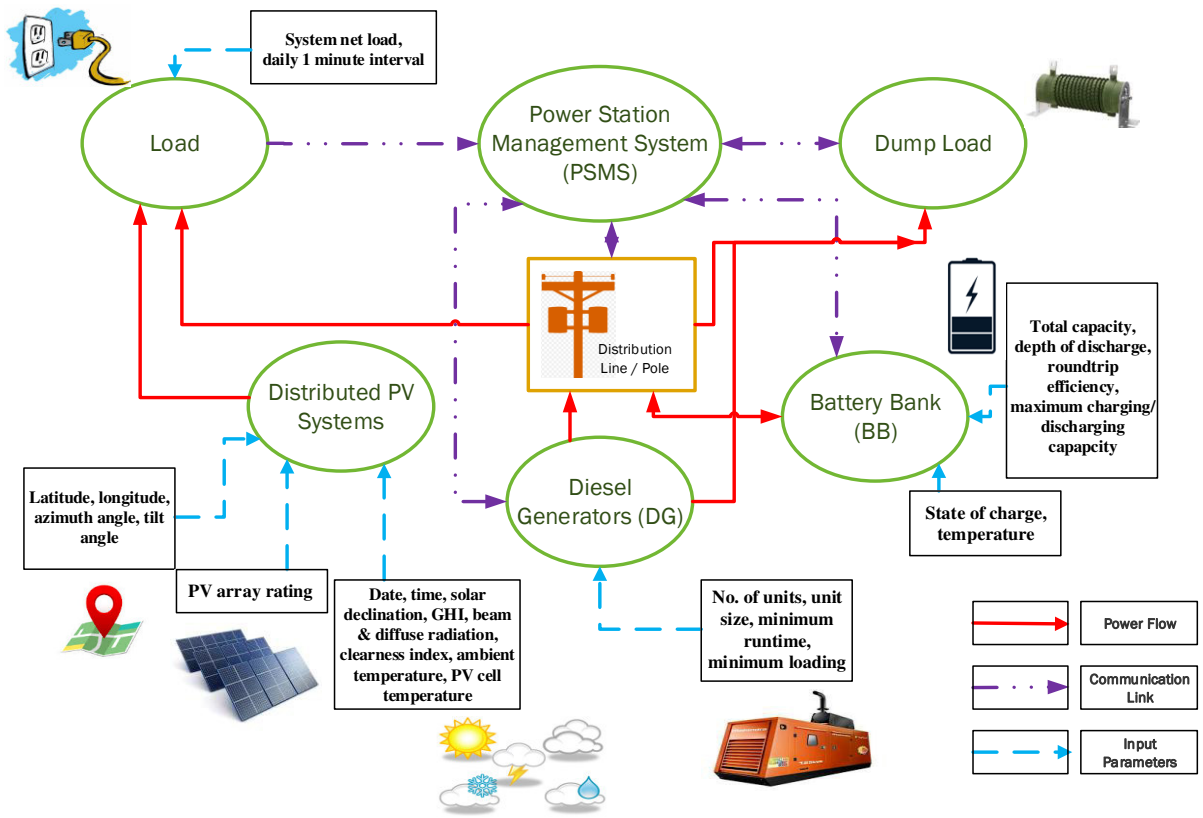

Figure 1: The infrastructure of the SOPS system and the system components used in the tool

3.1 *Step 1: Design of the SOPS System*

A meaningful operational strategy must be grounded in a reasonable estimate of how the SOPS system would operate in reality. System design, operational strategies and selection of load profiles are discussed in some of our previous studies [2, 40]. For this study, the SOPS system is assumed to be located in a remote town where central grid expansion is not feasible, and where the community is keen to install distributed PV systems and centralised battery systems, alongside the currently operating DGs. The model takes weather information from the city of Oldenburg in the state of Lower Saxony, Germany. The study considers the integration of a high PV share into the SOPS system which is distributed throughout the town and is assumed to comprise rooftop installations on residential and commercial settlements. However, to avoid technical and social complexities, it is assumed that the battery systems are not distributed, but rather that there is a battery bank (BB) at the power station. The system considers a generic load profile of a standard remote community. The SOPS system has six DGs, the maximum available. Each has a capacity of 170kVA to meet the daily total electricity demand of 8823.06 kWh. The PV systems are distributed along the three

distribution feeders in the town. Figure 2 presents the 24-h load profile that is employed in the tool for simulation. Table 1 shows the important system parameter values considered for DGs, PV and battery.

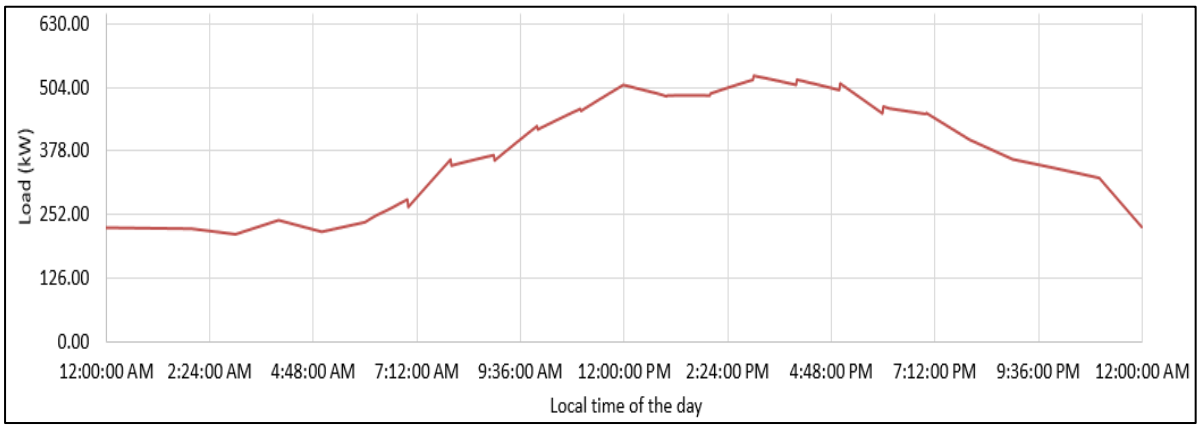

Figure 2: Daily load profile

Table 1: System component parameter values

Item	Parameter	Unit	Value
Gross load	Maximum	kW	527
	Minimum	kW	266
	Average	kW	368
DG	Unit capacity	kW	140
	Maximum allowable loading	%	90
	Minimum loading	%	30
	Minimum runtime	minute	30
PV	Slope of surface (Tilt)	degree	53
	PV derating factor	%	95
	Max power point efficiency under standard test conditions (STC)	%	13.5
Battery	Technology		Lithium Ion
	Battery charge efficiency	%	95
	Battery discharge efficiency	%	95
	Power rating	kW	140

3.2 *Step 2: Development of the Energy Flow Simulation Tool*

As stated earlier, 1-minute-level resolution profile of the generator scheduling and OR is essential to assess the benefits of the 1-minute-level short-term PV forecasting feature. To

address this issue, the tool has been developed utilising a 1-minute simulation time step, as it enables adequate representation of the energy flow and generator dispatch. Other commercially available pre-feasibility analysis software tools do not provide in concise form the 1-minute-level resolution simulation outcome needed by the significant number of stakeholders who lack technical understanding and related knowledge. This causes a slow and delayed uptake of PV systems in remote and rural areas all around the world [26]. Considering these issues, a tool is required which is handy and useful for this group of stakeholders. The study has fulfilled this gap by developing the tool using Microsoft Excel. The uniqueness of the tool lies in the fact that all the worksheets are observable and each of the steps is transparent during the execution of the logical algorithm. The algorithm addresses the objective functions of the problem using simple linear programming techniques. The tool offers two types of outcomes: (i) the generation of 1-minute resolution power generation and operational reserve profiles of the SOPS system using the user-defined operational algorithm, and (ii) the use of the PV forecast data to determine the DG operational profile and consequent fuel savings. Figure 3 presents an overview of the tool, showing the parameters required as input and the expected output from the tool. Figure 4 shows the schematic representation and the single line diagram of the SOPS system.

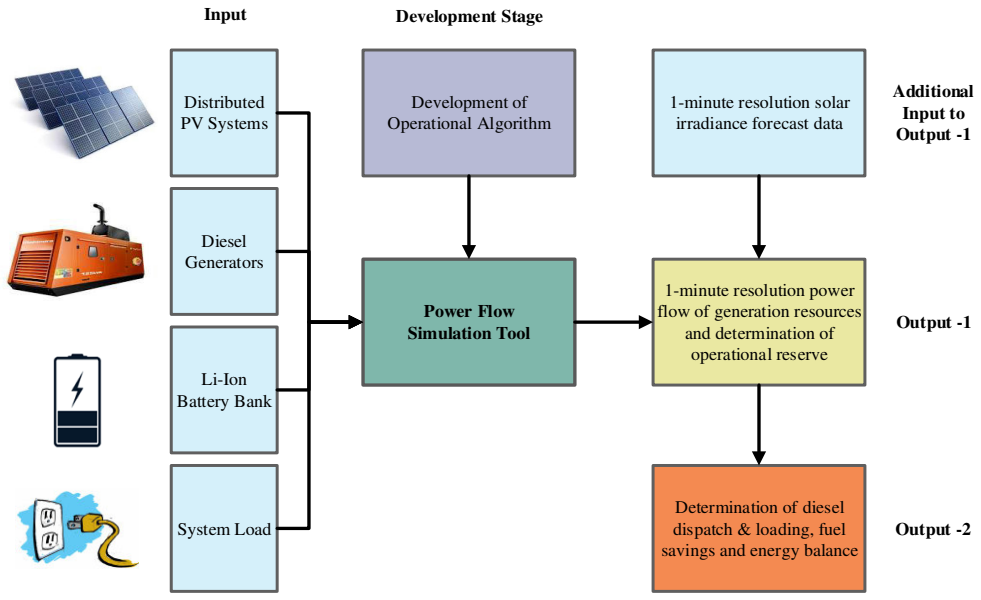

Figure 3: Flowchart showing the inputs and outputs of the energy flow simulation tool

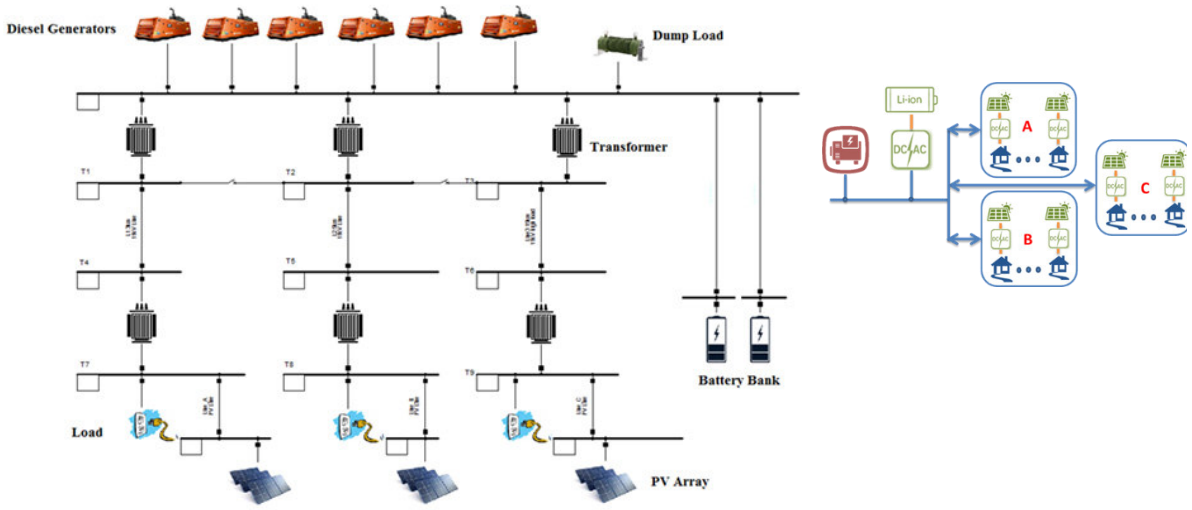

Figure 4: Block Diagram of a sample SOPS system for three rural type feeders: A, B and C

3.3 *Step 3: Assess PV Forecasting Benefits using the tool*

The tool can be used to assess the benefits of 1-minute resolution short-term PV forecasting for the specified SOPS system. Figure 5 shows the logical sequence followed for this application. The 1-minute ahead irradiance forecast data acquired from the image and irradiance processing software is applied to the energy flow simulation. A discussion based on several case studies is presented in section 5 and includes details of image acquisition and processing for the software.

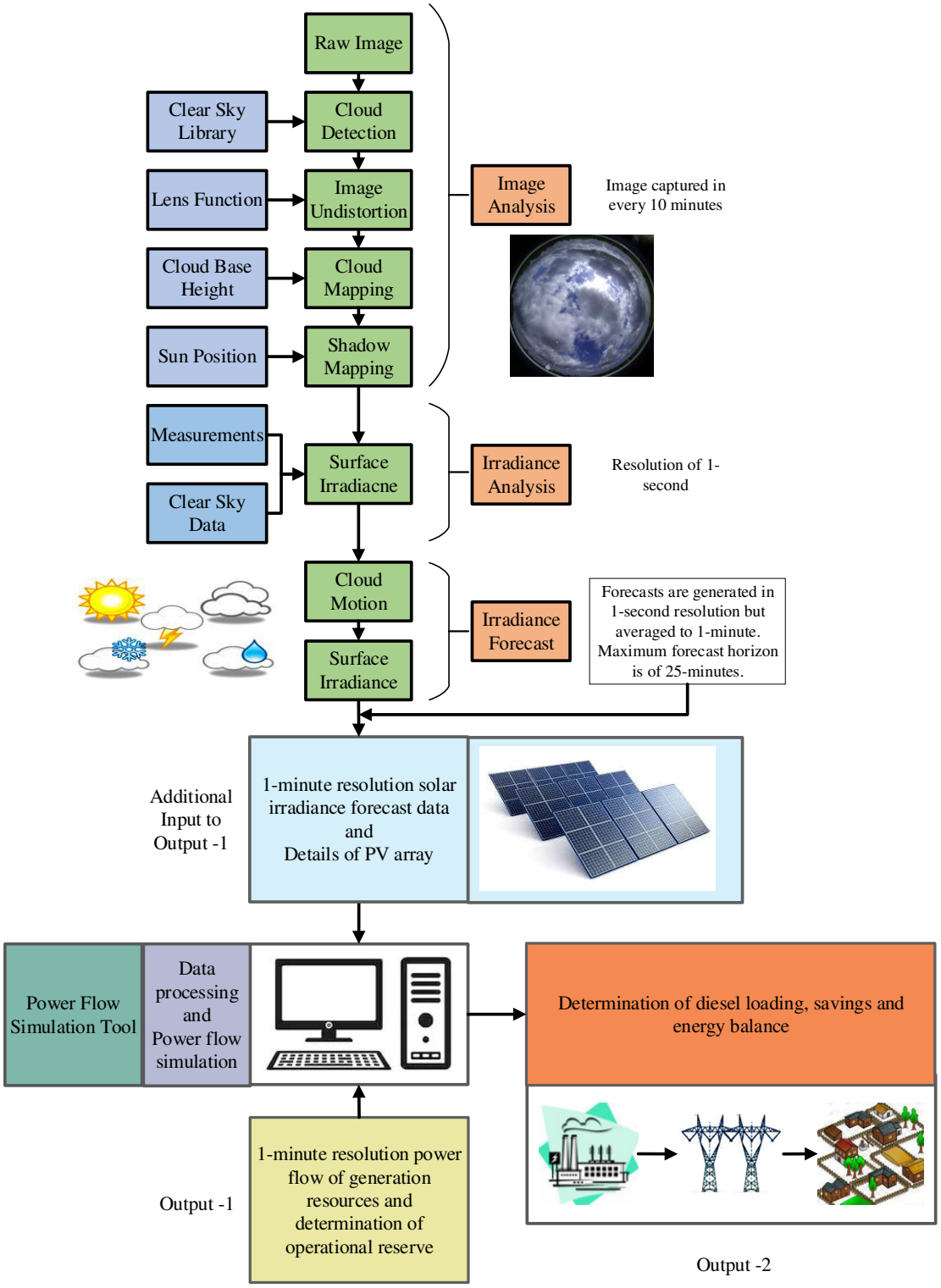

Figure 5: Stages and strategies of the approach leading to tool development

4. Description of the Energy Flow Simulation Tool

A distinguishing feature of the tool is that it takes 1-minute data as inputs to simulate 1-minute output. The specific inputs are: system load profile of 1-minute resolution, PV array information, DG capacity, battery capacity and location-specific information. The DGs and the BB are operated in automated control mode. PV systems are assumed to be distributed on the rooftops of the community buildings and households. An automatic 'Power Station Management System' (PSMS) communicates with 'Generator Supervisory Systems' on each of the DGs and the BB controller, and schedules them to supply the consumer loads. The whole battery bank is divided into two individual systems – the BB regular response (BB-RR) system and the BB emergency response (BB-ER) system. There is no advisory control imposed on the distributed PV systems. This section discusses the mathematical modelling of the components and the logical algorithms used to develop the energy flow simulation tool.

4.1 PV Array Modelling

The essential inputs required to calculate the PV array output include day of the year, location-specific information (e.g. latitude, longitude), weather information (e.g. solar irradiance), ambient temperature, clearness index and PV systems related information (e.g. the orientation of the array and array size). Some performance-related characteristics are also required, such as the PV inverter's manufacturer specifications. The total (global) irradiance incident on the horizontal surface of a PV array (plane of array) is the arithmetic sum of the direct (beam) and diffuse irradiance components incident on a horizontal surface, as shown in Eq. (1):

$$E_{POA} = E_b + E_d \quad (1)$$

Where, E_{POA} is the total irradiance incident on the plane of array (kW/m^2), E_b is the direct irradiance incident on a horizontal surface (kW/m^2) and E_d is the diffuse irradiance incident on a horizontal surface (kW/m^2)

To determine the irradiance incident on the array for each time step, the global horizontal irradiance is calculated from the beam and diffuse components. The diffuse component can be determined from the clearness index using Eq. (2) and Eq. (3) [41]. Clearness index is the ratio of the irradiance on the plane of the array to the extraterrestrial irradiance, as shown in Eq. (2):

$$kt = {}^{E_{POA}}/_{E_O} \tag{2}$$

$$\frac{E_d}{E_{POA}} = \begin{cases} 1.0 - 0.09kt, & kt \leq 0.22 \\ 0.9511 - 0.1604kt + 4.388kt^2 - 16.638kt^3 + 12.336kt^4, & 0.22 < kt \leq 0.80 \\ 0.165, & kt > 0.80 \end{cases} \tag{3}$$

Where kt is the clearness index and E_O is the extraterrestrial irradiance on a horizontal surface (kW/m^2)

The ideal performance of a PV module is achieved when the connected solar inverter is operating at the maximum power point (MPP). The model assumes that solar inverters have maximum power point tracking (MPPT) capability. MPPT is a performance characteristic which inverters and charge controllers use to harness the maximum power from the PV array at a particular time. They do this by operating at the point when the output power (i.e. the product of the output current and output voltage) is maximised for a given irradiance or cell temperature [42]. The global irradiance incident on the PV array (E_t) is dependent on the beam irradiance, diffuse irradiance, anisotropic index, slope of the array surface (tilt angle), zenith angle and global horizontal irradiance on the earth's surface. The total power generation from a PV array is determined using Eq. (4):

$$P_{PV} = P_{PVRated} \times DF_{PV} \left(\frac{E_t}{E_{t,STC}}\right) \times \left[1 + \alpha_{temp}\left(T_{cell} - T_{cell,STC}\right)\right] \tag{4}$$

Where, P_{PV} is the output power of the PV array (kW), $P_{PVRated}$ is the rated capacity of the PV array at STC (kW), DF_{PV} is the PV derating factor (%), E_t is the total global irradiance incident on the PV array (kW/m^2), $E_{t,STC}$ is the solar irradiation incident at STC (1 kW/m^2), α_{temp} is the temperature coefficient of power (%/°C), T_{cell} is the PV cell temperature at the current time step (°C) and $T_{cell,STC}$ is the PV cell temperature at STC (25°C)

PV cell temperature depends on factors, such as air temperature, irradiance, wind speed, and module materials. In each time step, Eq. (5) is used to calculate the PV cell temperature:

$$T_{cell} = \frac{T_{amb} + \left(T_{cell,NOCT} - T_{amb,NOCT}\right)\left(\frac{E_t}{E_{t,NOCT}}\right)\left[1 - \frac{\eta_{mp,STC}\left(1 - \alpha_{temp}T_{cell,STC}\right)}{\tau\alpha}\right]}{1 + \left(T_{cell,NOCT} - T_{amb,NOCT}\right)\left(\frac{E_t}{E_{t,NOCT}}\right)\left(\frac{\alpha_{temp}\eta_{mp,STC}}{\tau\alpha}\right)} \tag{5}$$

Where, T_{cell} is PV cell temperature (°C), T_{amb} is ambient temperature (°C), $T_{cell,NOCT}$ is the PV cell temperature at Nominal Operating Cell Temperature (NOCT) (°C), $T_{amb,NOCT}$ is the ambient temperature at NOCT (°C), E_t is the total global irradiance incident on the PV array (kW/m^2), $E_{t,NOCT}$ is the total global irradiance incident on the PV array at NOCT (kW/m^2), $\eta_{mp,STC}$ is the maximum power point efficiency under STC (%), α = solar absorptance of the array (%), α_{temp} is the temperature coefficient of power (%/°C) and $T_{cell,STC}$ is the PV cell temperature at STC (25°C)

4.2 Diesel Generator (DG) Modelling

Generators are usually of two types: engine-generator and electric generator. Diesel generators are classified as engine-generators. Diesel engines running below a recommended minimum loading level for an extended period result in low efficiency and cylinder bore glazing. This reduces engine operating life, therefore increasing the annual operational and maintenance costs. It should also be noted that the specified minimum loading for diesel generators varies from manufacturer to manufacturer [1]. Generator power output is given by Eq. (6). Generator fuel curve defines the required amount of fuel consumed to meet the demand. Eq. (7) gives the generator's fuel consumption in litres/h.

$$P_{DG^{min}} \geq P_{DG}(i) \geq P_{DG^{rated}} \tag{6}$$

$$F = F_0 + F_1 P_{DG} \tag{7}$$

Where, P_{DG} represents instantaneous power from the DG unit, $P_{DG^{min}}$ and $P_{DG^{rated}}$ represents minimum allowable power output from the DG unit and the rated power of the DG unit, respectively, F is total fuel consumption (L/h), F_0 is fuel curve intercept coefficient in L/h/kW, and F_1 is fuel curve slope in L/h/kW

4.3 Battery Bank (BB) Modelling

A battery model based on Li-ion technology is used in this tool. It takes as inputs the battery string size (Wh), the initial and minimum state of charge (SOC) of the battery bank and specified roundtrip efficiency. The current energy capacity of the BB is calculated using Eq. (8) and Eq. (9). During charging/discharging, the SOC limit is always checked for both the battery systems using Eq. (10).

$$E_{BB-RR}(i+1) = E_{BB-RR}(i-1) + E_{BB-RR}(i) \quad (8)$$

$$E_{BB-ER}(i+1) = E_{BB-ER}(i-1) + E_{BB-ER}(i) \quad (9)$$

$$BB_{SOC}{}^{min} \geq BB_{SOC}(i) \geq BB_{SOC}{}^{max} \quad (10)$$

Where, $E_{BB-RR}(i)$ represents the BB-RR energy at time instant 'i', $E_{BB-RR}(i+1)$ represents the BB-RR energy at the next time instant, $E_{BB-RR}(i-1)$ represents the BB-RR energy at the previous time instant 'i-1', $E_{BB-ER}(i)$ represents the BB-ER energy at the current time instant 'i', $E_{BB-ER}(i+1)$ represents the BB-ER energy at the next time instant, BB_{SOC} is the SOC at any time instant, $BB_{SOC}{}^{min}$ is the minimum level of SOC allowed and $BB_{SOC}{}^{max}$ is the maximum level of SOC allowed when battery gets charged

4.4 Inverter Modelling

It is assumed in the modelling that all the inverters are integrated with the individual system components. The inverters dedicated to the battery banks are bi-directional grid-tied inverters, and the dedicated inverters that are coupled to the PV arrays are grid-tied PV inverters. Eq. (11) and Eq. (12) show the basic mathematical expressions used for measuring an inverter's uni-directional input and output power.

$$P_{inv-BB}(i) = P_{BB}\,(i) \times \eta_{inv} \quad (11)$$

$$P_{inv-PV}(i) = P_{PV}\,(i) \times \eta_{inv} \quad (12)$$

Where, P_{PV} is the output power of the PV array (kW), P_{BB} is the output power of the BB (kW), P_{inv-BB} is the input/output power of the battery inverter, P_{inv-PV} is the input/output power from the solar inverter and η_{inv} is the inverter efficiency

4.5 Operation of the PV systems and the Battery Bank

It is assumed that the daytime gross load demand will be offset by the electricity generated by the PV systems, and that any excess of generation will be used to charge the battery in order to prevent the DGs from under-loading. In all cases, at least one DG will remain connected for grid forming and supplying electricity to the grid (system). The net system load seen by the PSMS is the estimated net load (based on historical statistics) and the forecasted net load, measured using Eq. (13) and Eq. (14). Eq. (15) and Eq. (16) represent the calculation of gross

load when the DGs are in regular operation, in cases where one source is not generating power. The algorithm used in this tool assumes the maximum loading (δ) and the minimum loading (∂) of each DG unit to be 90% and 15%, respectively. The PSMS continuously sends the BB a power set point limit, ensuring that preselected minimum loadings of all online DGs are maintained. The PV systems' short-term power fluctuations are smoothed out by BB-RR which acts as an energy buffer, absorbing excess PV energy and topping up during periods of cloud cover. BB-ER is dedicated to responding only in emergencies. It corresponds to the immediate action required to provide grid stability and take up the load in cases of sudden failure of an online DG. The algorithm used in this tool regards 85% of the whole BB capacity as dedicated to BB-RR and the remaining 15% capacity as BB-ER (see Eq. (17), where $\boldsymbol{\rho} = 0.85$ and $\boldsymbol{\sigma} = 0.15$).

$$Net\ Load\ (i) = Gross\ load\ (i) - P_{PV}(i) \tag{13}$$

$$Net\ Load\ (i) = \sum_{DG=1}^{n} P_{DG}\ (i) + P_{BB-RR}(i) \tag{14}$$

$$\partial * P_{DG^{rated}} \leq P_{DG}(i) \leq \delta * P_{DG^{rated}} \tag{15}$$

$$Gross\ Load\ (i) = \begin{cases} P_{PV}(i) + \sum_{DG=1}^{n} P_{DG}\ (i)\ ; when\ P_{BB-RR}(i) = 0 \\ \sum_{DG=1}^{n} P_{DG}\ (i) + P_{BB-RR}(i)\ ; when\ P_{PV}(i) = 0 \\ \sum_{DG=1}^{n} P_{DG}\ (i)\ ; when\ P_{PV}(i) = P_{BB-RR}(i) = 0 \end{cases} \tag{16}$$

$$E_{BB-RR} = \rho\ \times E_{BB}\ and\ E_{BB-ER} = \sigma \times E_{BB} \tag{17}$$

Where P_{PV} represents instantaneous power from PV array, P_{DG} represents instantaneous power from DG, P_{BB-RR} represents instantaneous power from BB-RR, $P_{DG^{min}}$ means minimum DG loading capability, $P_{DG^{rated}}$ represents the rated power of a DG unit

The PSMS maintains the BB's power flow (negative when importing, positive when exporting) at a determined power set point. To do this, it also takes into account the net load fluctuation and minimum diesel loading. Figure 6 shows the logical sequences followed by the PSMS for generation dispatch to meet the load demand. This follows Eq. (16).

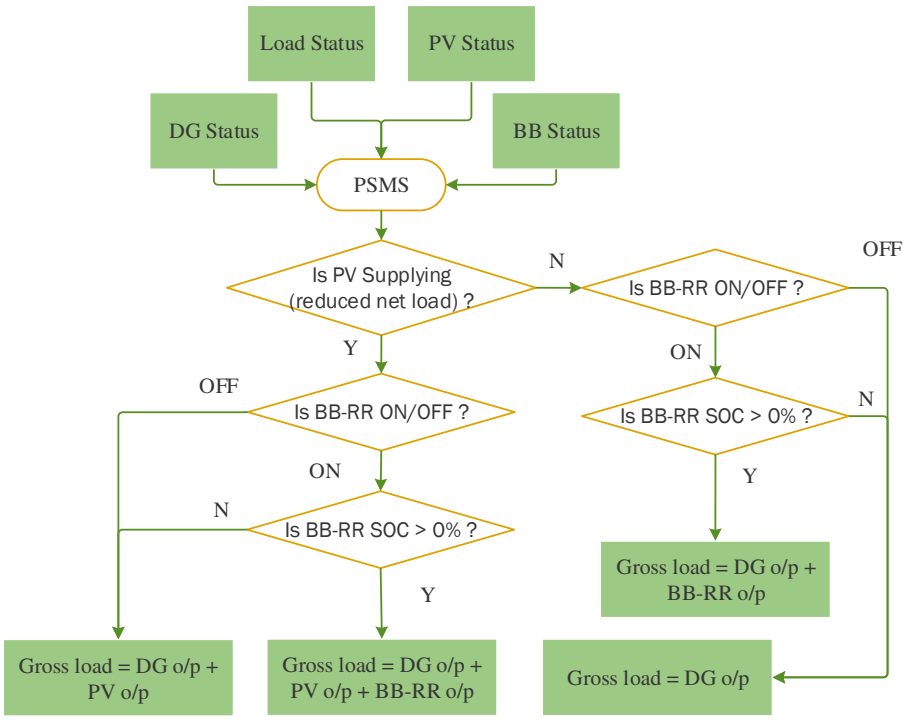

Figure 6: Generation dispatch method to meet the load demand

4.6 DG Plant Schedule and Operating Reserve

The system has enough DG capacity to provide an operating reserve sufficient to cover the net system load at every time step for specified contingency events such as sudden cloud cover, sudden load increase or loss of generation capacity. The DG units' dispatch priority depends on user preference. An additional DG is scheduled ON when an increasing net system load plus a specified margin covering the loss of a DG equals the sum of the de-rated power ratings of on-line DGs. The BB-ER system always keeps a pre-determined energy reserve. If this reserve is capable of discharging the same power that the biggest de-rated DG unit can supply, then BB-ER capacity is considered to be the operating reserve equivalent to the biggest de-rated DG, see Eq. (18). If the BB-ER system does not take part in providing an operating reserve, then the PSMS brings on one or more additional DGs to provide the minimum operating reserve. This is equal to the capacity of the biggest DG unit, see Eq. (19). The overall operating reserve at any instant also covers a certain range of load and PV output fluctuations, neither of which should exceed the capacity of one DG unit. The BB-ER system maintains a minimum stored energy of 5kWh to cover the loss of a DG unit for at least two minutes. The minimum runtime for a DG unit is assumed to be thirty minutes, see Eq. (20). When the supervisory system of any DG unit receives a signal to turn it off, it checks for the minimum runtime constraint before responding to the command. A DG unit is scheduled OFF

when a reducing total net load plus the required minimum operating reserve margin drops below the sum of the de-rated power ratings of those DGs that are to remain in service. The DG to be scheduled OFF is first changed by the PSMS from operating in isochronous frequency to frequency droop control. The PSMS then lowers the DG's power set point to near zero, disconnects it from the generator busbar, and runs it for a further few seconds to cool the unit. Figure 7 shows the diesel generator dispatch algorithm which follows Eq. (18) – Eq. (20).

$$P_{BB-ER}{}^{max}(i) = P_{DG}{}^{rated}(i) \tag{18}$$

$$OR\ (i) = \begin{cases} OR_{BB-ER}(i)\ ; when\ E_{BB-ER}(i)\ \geq 5kWh \\ SR_{DG}(i)\ ; when\ \ E_{BB-ER}(i)\ < 5kWh \end{cases} \tag{19}$$

$$t_{P_{DG}}^{min} = 30\ minute \tag{20}$$

Where $P_{BB-ER}{}^{max}$ represents the maximum deliverable power from BB-ER, OR means operating reserve of the system, OR_{BB-ER} represents the operating reserve contribution from BB-ER, SR_{DG} represents spinning reserve contribution from DG units and E_{BB-ER} represents the energy capacity of BB-ER

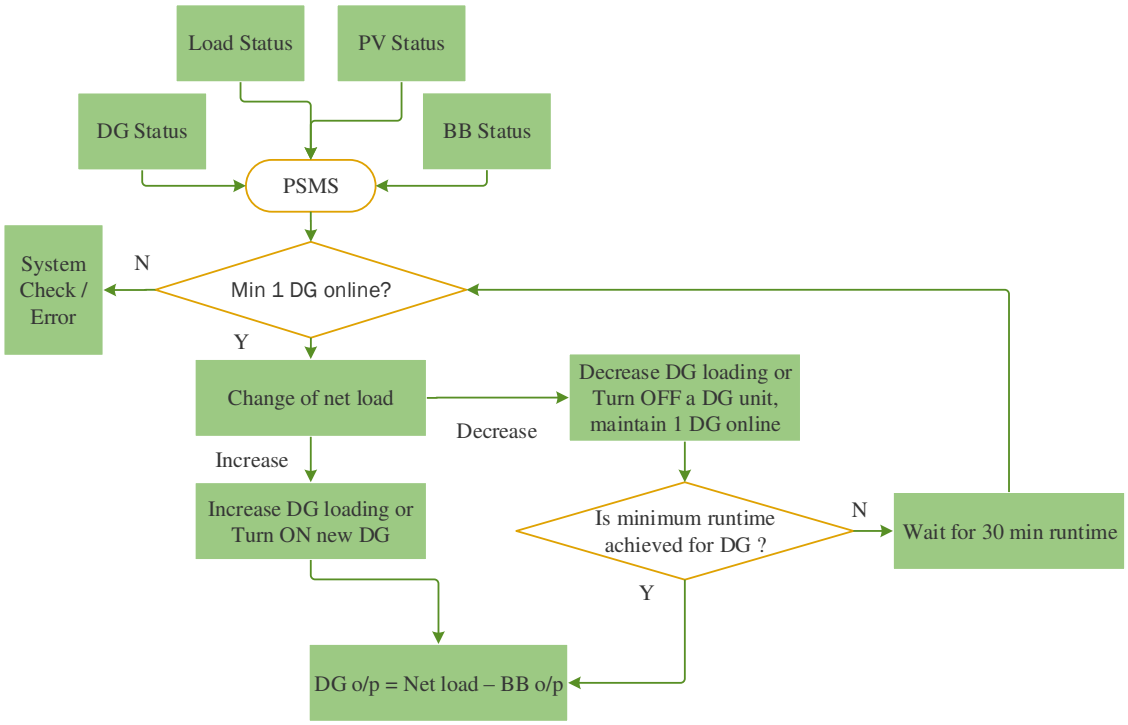

Figure 7: Diesel generator dispatch algorithm

4.7 Operational Steps

The system net load increases when the load demand increases and (or) the total PV output from prosumers decreases for every time step, and vice versa. With rising PV output, DGs may face an under-loading situation or even a reverse power condition. During these periods of excess energy arising from high PV penetration or under-loading of DGs, the PSMS sends a power setpoint signal to the BB-RR to stop discharging immediately and to start charging and boosting the state of charge (SOC), see Eq. (21) – Eq. (23). As soon as the excess electrical power becomes zero, according to Eq. (21), the BB-RR resumes its normal discharging function in accordance with the regular instructions from the PSMS. If the BB-RR hits the maximum SOC level, then to prevent the DGs from going to an under-loading condition to meet the energy balance scenario, a short-term dump load is activated. The dump load has to be employed to maintain system stability and energy balance by avoiding the DGs going to a reverse power condition. The PSMS monitors the SOC levels of the BB-RR and BB-ER, according to Eq. (22). Between these levels, PSMS sends a signal to the BB-RR in an effort to sustain diesel loading at the specified minimum loading and, at the very least, to keep DGs out of overload (for example, after a DG trip). It corrects for overcharging (excess

PV power) by adjusting the power set point of the dump load and it corrects for undercharging by stopping BB-RR from discharging any further. It also controls the BB-RR system such that it does not discharge during the off-PV generation period. Battery discharge is allowed only during the sunshine hours, up to 19:00, see Eq. (24) – Eq. (25). Simultaneous charging and discharging processes of the BB are avoided using a binary decision variable, β_{BB}, see Eq. (26). Figure 8-9 shows the battery bank charging and discharge algorithms, respectively.

$$Excess\ Power\ (i) = \begin{cases} 0\ ; when\ Gross\ load\ (i)\ \geq\ P_{PV}(i) + P_{DG}(i) + P_{BB}(i) \\ P_{PV}(i) + P_{DG^{min}}(i) - \ Gross\ load\ (i)\ ; when\ P_{PV}(i) + P_{DG^{min}}(i) >\ Gross\ load\ (i) \end{cases} \quad (21)$$

$$BB - RR_{SOC^{min}} \leq BB - RR_{SOC}(i) \leq BB - RR_{SOC^{max}} \quad (22)$$

$$P_{BB-RR^{max}}\ (i) = P_{DG^{rated}} \quad (23)$$

$$P_{BB-RR}\ (i) = \begin{cases} P_{BB-RR^{-}}\ (i);\ charging\ \ when\ Excess\ Energy\ (i) > 0\ \ and\ also\ 00{:}00 < i < 06{:}00 \\ P_{BB-RR^{+}}\ (i); discharging\ when\ BB - RR_{SOC}(i)\ >\ BB - RR_{SOC^{min}}\ and\ i = sunshine\ hrs, upto\ 1 \end{cases} \quad (24)$$

$$P_{BB-ER}(i) = \begin{cases} P_{BB-ER^{-}}\ (i);\ charging\ \ when\ E_{BB-ER}(i)\ < 5kWh\ \ and\ Emergency\ Situation = OFF \\ P_{BB-ER^{+}}\ (i); discharging\ when\ Emergency\ Situation = ON \end{cases} \quad (25)$$

$$0\ \leq\ P_{BB-RR^{+}}\ (i) \leq\ \beta_{BB} \times P_{BB-RR^{max}}\ (i) \quad (26)$$

$$0\ \leq\ P_{BB-RR^{-}}\ (i) \leq (1 - \beta_{BB}) \times P_{BB-RR^{max}}\ (i)$$

Where, $BB - RR_{SOC}$ represents the SOC of BB-RR, $P_{BB-RR^{max}}$ represents the maximum absorbed or deliverable power from BB-RR, $P_{BB-RR^{+}}$ represents discharging state and $P_{BB-RR^{-}}$ represents charging state

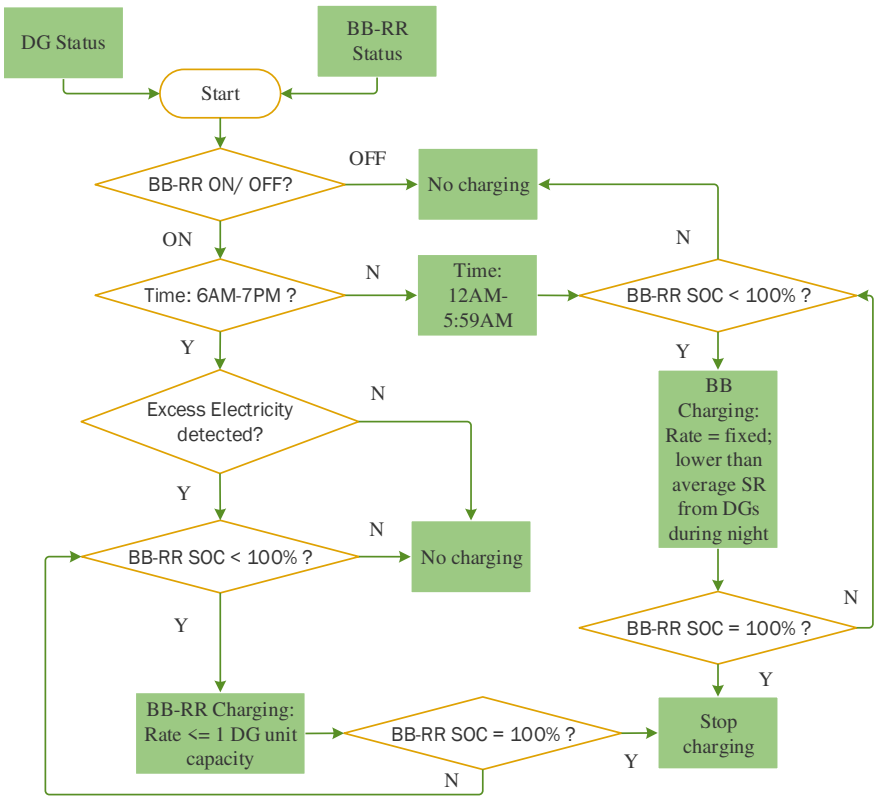

(a)

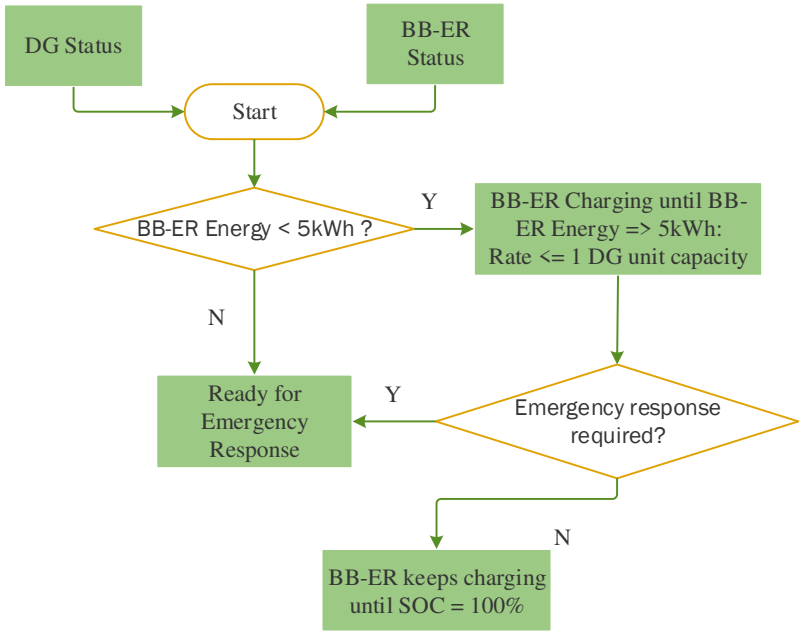

(b)

Figure 8: Battery bank charging algorithm: (a) for BB-RR and (b) for BB-ER

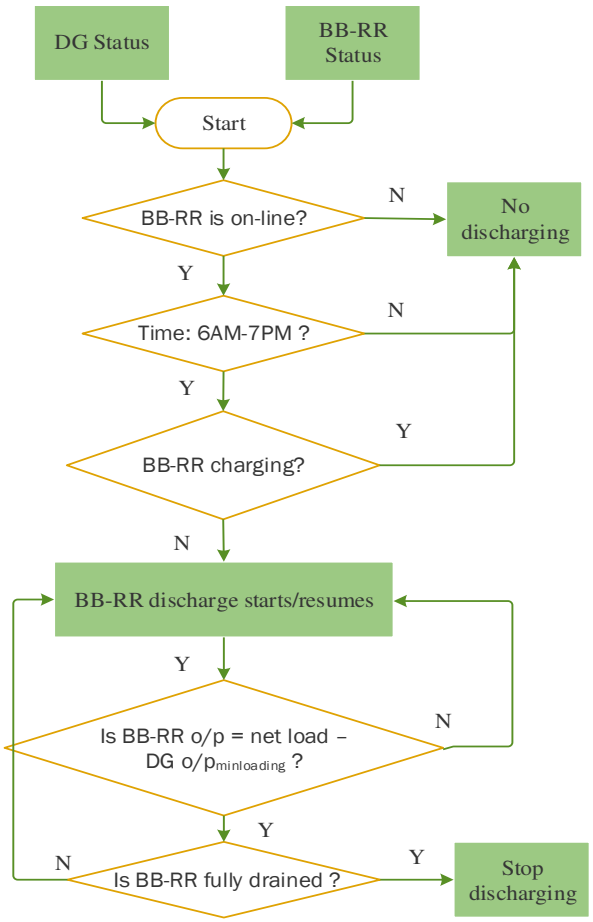

Figure 9: Battery bank discharge algorithm

4.8 Operating Reserve provided by the BB

As stated earlier, the capacity of the BB-ER is always kept at such a level that there remains sufficient reserve contribution to cover the loss of the biggest DG unit of the system. To illustrate the BB system division and minimum storage capacity determination of the BB-ER system, we can consider the example where the BB has a total capacity of 100kWh, according to Eq. (17), and BB-RR and BB-ER have capacities of 85kWh and 15kWh, respectively. This corresponds to a low power/high energy system for BB-RR and high power/low energy system to represent BB-ER's activity. The maximum charge and discharge rate are set equal to the largest DG capacity (e.g., 140kW) so that the BB is equivalent to, but not greater than, the largest DG capacity. When the BB-ER is required to respond, it can discharge at a maximum rate equal to the largest DG capacity of 140kW for enough time to allow DG to turn ON and maintain the N+1 redundancy criterion. The minimum capacity of the BB-ER is maintained according to the Eq. (19). Figure 10 shows the working principle of the BB-ER system as an operating reserve.

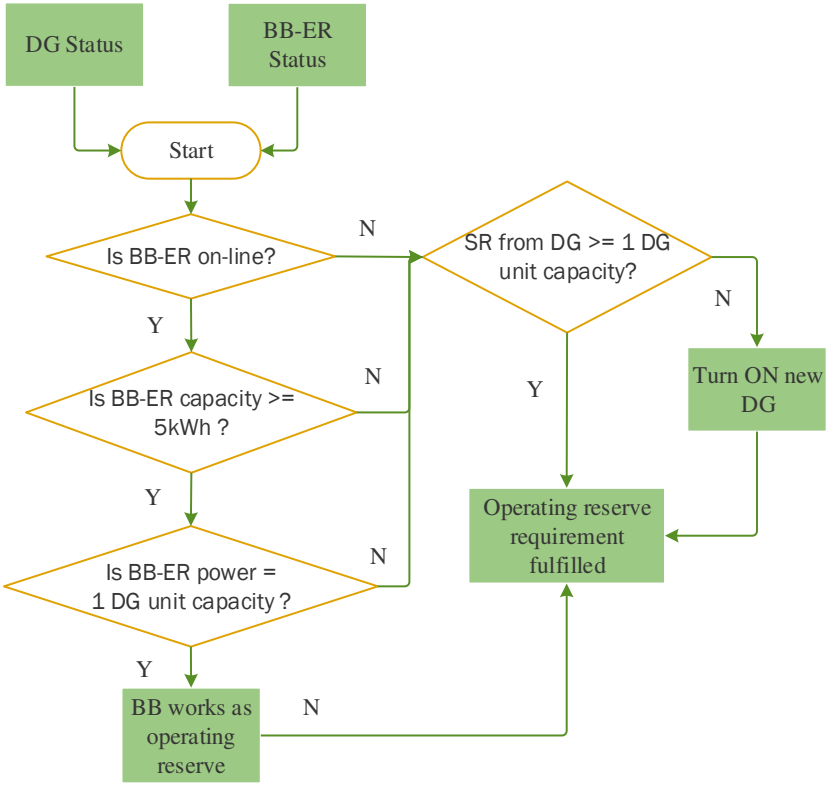

Figure 10: Operating reserve management from the BB-ER system

4.9 System Operation with Battery Bank Offline

When the BB (i.e. the BB-RR and BB-ER) is off-line, it does not contribute to any smoothing or the system operating reserve capacity. In this situation, all frequency and voltage controls are provided by the DGs. Because the net load fluctuations (assumed to be the same as the PV systems output variability) are not being managed by the BB, a dump load has to be employed.

4.10 Computation of Minimum Number of DGs Required Online

For different scenarios based on the available energy resources, the computation of the minimum number of DGs required to be online for every time instant follows Eq. (27)- Eq. (30).

Scenario 1: DG-PV system, no PV forecasting applied:

In this scenario, no BB is active. Therefore, DG provides support for the operating reserve, see Eq. (27).

$$N_{\min\_DG}(i) = Roundup\left\{\frac{\left(Gross\ load\ (i-1) - P_{PV}(i-1) + Min\_OR\ (i)\right)}{\delta * P_{DG^{rated}}}\right\} \quad (27)$$

Where, $N_{\min\_DG}$ represents the minimum number of DGs required online in the current time, $Min\_OR\ (i)$ represents the minimum amount of operating reserve required in kW in the current time which is equal to 140kW.

Scenario 2: DG-PV-BB system, no PV forecasting applied:

In this scenario, the BB is active and BB-ER provides support for the operating reserve, see Eq. (28).

$$N_{min\_DG} = Roundup\left\{\frac{\left(Gross\ load\ (i-1) - P_{PV}(i-1)\right)}{\delta * P_{DG^{rated}}}\right\};\ when\ Min_{OR}(i) = OR_{BB-ER}(i) \quad (28)$$

Scenario 3: DG-PV system, with 1-minute ahead PV forecasting applied:

In this scenario no BB is active. Hence, DG provides support for the operating reserve. In addition, in this step 1-minute ahead PV forecasting is applied, see Eq. (29).

$$N_{\min\_DG} = Roundup\left\{\frac{\left(Gross\ load\ (i) - P_{PV}(i+1) + Min\_OR\ (i)\right)}{\delta * P_{DG^{rated}}}\right\} \quad (29)$$

Scenario 4: DG-PV-BB system, with 1-minute ahead PV forecasting applied:

In this scenario, the BB is active and BB-ER provides support for the operating reserve. In addition, in this step 1-minute ahead PV forecasting is applied, see Eq. (29).

$$N_{min\_DG} = Roundup\left\{\frac{\left(Gross\ load\ (i) - P_{PV}(i+1)\right)}{\delta * P_{DG^{rated}}}\right\};\ when\ Min_{OR}(i) = OR_{BB-ER}(i) \quad (30)$$

The above formulae determine the minimum number of DGs required online for various scenarios. However, the current minute generation of the required online DGs added to the current minute BB generation (where the BB is included and online) equals the current minute gross load less the current minute PV power, see Eq. (13) and Eq. (14).

4.11 Advantages and Limitations of the Tool

In the next section, the tool will be applied to some case-based scenarios. This will demonstrate some significant advantages of the tool, specifically:

- It uses as input a minute-level resolution data from various available sources. The tool provides insight into the issues that need to be addressed on a minute by minute basis in order to apply them to the control mechanism of the power system to assess benefits.
- Short-term PV forecasting can forecast as little as 1-minute ahead solar irradiance levels. Therefore, this application requires a tool that can simulate minute-level resolution power flows. The tool achieves this and computes the overall fuel consumption, fuel savings and operational reserve requirements for any period considered.
- The dispatch algorithm can be customised, and every step is visible and transparent. This is an outstanding feature of the tool. A techno-economic analysis is recommended before using this tool, in order to learn about the economic configuration of any particular power supply system.

However, by their inherent nature, energy flow models have limitations. These are:

- They do not consider reactive power, frequency or voltage as technical parameters in making any decisions.
- The line loss calculation is omitted while dispatching power to the loads.
- They assume that the speed of completing a charging/discharging cycle has no negative impact on battery operation and lifetime.
- They do not consider cost functions as a decisive factor.

5. Assess PV forecasting benefits

This section assesses the benefits of short-term PV forecasting using the tool in order to allow higher shares of PV generation into the SOPS system. The current study focuses on the application of 1-minute ahead PV forecasting of irradiance data acquired by the “sky camera” (sky imager) device and image processing software.

A complex configuration of hardware is set up at the University of Oldenburg (53.15232 °N, 8.166022 °E) in Oldenburg, Germany. The sky imager used is a commercial network camera Vivotek FE8172V, equipped with a fisheye lens [8]. The essential specifications for this camera are a circular fisheye frame in a 1920*1920 pixels image plane and a full 180° view field. This takes images every 10 seconds from sunrise to sunset. A Python-based interface was developed to control most of the settings automatically. For this research, the maximum field of view for the camera has been set to 160° (±80° of the zenith angle). The experimental setup is presented in figure 11 [8]. The focus is on forecasts of global horizontal irradiance (GHI), measured at the location of the camera. Sky imagers take consecutive images of the sky and record the current cloud positions adjacent to and cover the camera location. An image processing mechanism is used to measure the cloud movement and determine the direction relative to the sun's position [8].

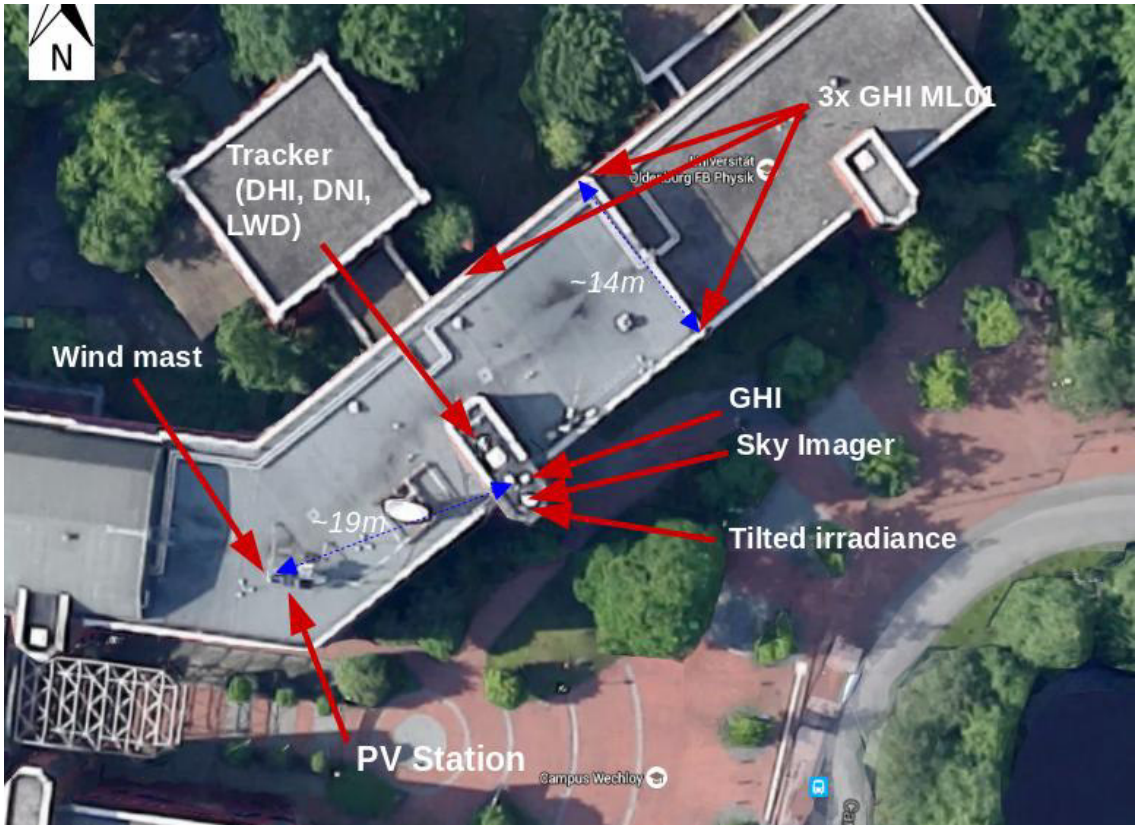

(a)

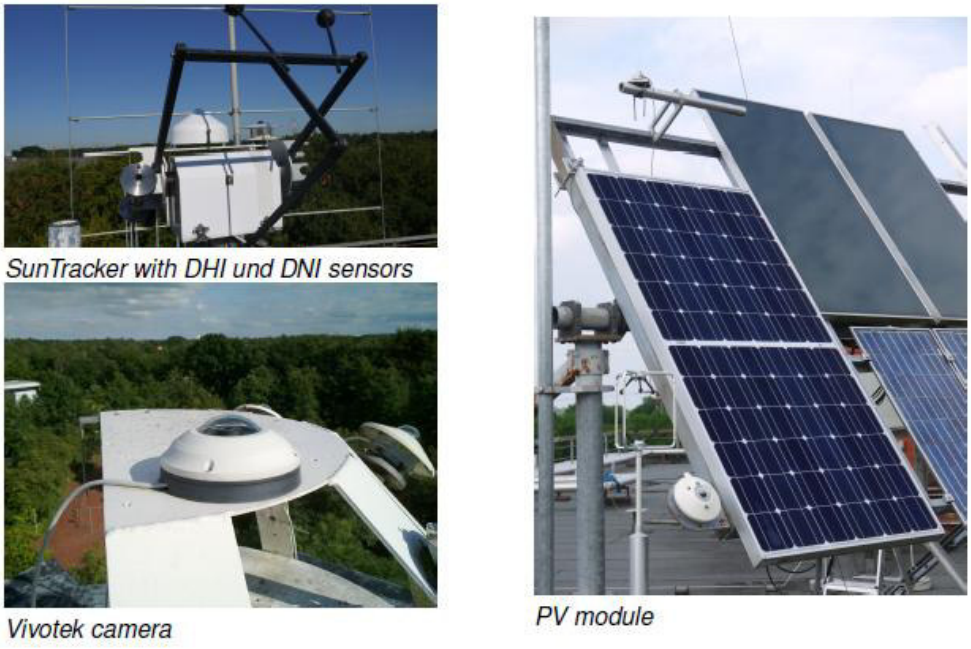

(b)

Figure 11 (a): Top view of energy meteorology station at the University of Oldenburg. Measuring equipment for three main horizontal irradiance components are located together with a sky imager above the staircase of the building. A PV station with wind measurements is located about 19 meters nearby. A triangle of GHI measurements with photodiodes for cloud motion estimation is also located on the rooftop. Background source: Google. (b): Shows the sensors, camera and the PV module used in the experimental setup [8].

These images are then processed to obtain 1-minute ahead PV forecasting. For comparative analysis, a GHI forecast using perfect forecast data is also obtained. The perfect forecast method is characterised by the assumption of zero error in the irradiance forecast for the next time step. In forecasting applications where timing can be neglected (for example, predicting 10-min averages of variability), the sky imager technique outperforms the persistence forecasts. The persistence forecast method assumes the forecast GHI to be the same as the current GHI measurement in the next time instant. In clear-sky or overcast homogeneous sky conditions, persistence forecasts typically show low forecast errors [8]. Even if there are forecast errors, the sky imager-based techniques, making use of visible sky information, can predict cloud events. In these situations, other statistical models based on time series analysis fail due to the non-periodic nature of cloud coverage. Here lies the novelty of the sky-imagery-based short-term PV forecasting mechanism.

Single point measurement of solar irradiance, together with single sky camera image recordings and processing of cloud events, mean that any geographic diversity of solar irradiance due to intermittent cloud cover is not taken into account. Consequently, the

'smoothed' net total of solar PV power coming from geographically dispersed prosumer PV systems during intermittent broken cloud cover is not taken into account. The sky camera will tend to predict a 1-minute ahead forecast drop in PV power that would only arise when the entire town is blanketed by a rapidly moving large cloud within one minute. Therefore, the sky camera forecast of a drop in PV power caused by cloud cover will generally be a worst-case forecast, unless the sky camera does not forecast a minute ahead cloud cover event.

5.1 Application of PV Forecasting

This section describes the strategies used to assess the system performance, using 1-minute ahead PV forecasting. The energy flow model developed in the study is used to analyse the strategies, given in Table 2. Three system configurations are each assessed in relation to three forecasting strategies when PV systems are integrated. The base case scenario has been chosen as the DG-only operation scenario for the SOPS system (see Table 2).

The application successfully addresses all the issues mentioned in section 2. All technical constraints are thoroughly checked and adhered to in every time instant, while the tool is running. This helps the system to reduce the potential number of events where the N+1 redundancy criterion is violated. In addition, this study proposes a strategy to calculate the maximum allowed PV hosting capacity, when the PV forecasting mechanism is not applied. It assesses the benefits of 1-minute ahead PV forecasting of increasing the allowed PV hosting capacity and therefore the PV energy injection and then assesses the system performance in terms of fuel savings and PV share in the overall generation requirements.

In order to maintain simplicity in the analysis, the seasonal variations in the load profile are ignored (Figure 2) for the days on which the analysis has been performed.

Table 2: System configuration for application of PV forecasting

Case No.	System Configuration	PV Forecast Strategy	Remarks
1	DG-only (base case scenario)	N/A	• DGs are employed to meet the net load and try to maintain adequate OR.
2	DG-PV	2.1 No forecasting 2.2 1-minute ahead PV forecasting 2.3 Perfect forecasting	• DGs are employed to meet the net load and try to maintain adequate OR. • PV system hosting capacity is affected by PV forecast strategy. • BB is not employed.

Case No.	System Configuration	PV Forecast Strategy	Remarks
3	DG-PV-BB BB = 100kWh	3.1 No forecasting 3.2 1-minute ahead PV forecasting 3.3 Perfect forecasting	• DGs are employed to meet the net load and try to maintain adequate OR. • PV system hosting capacity is affected by PV forecast strategy. • BB is employed which comprises BB-RR and BB-ER (dual battery system).
	DG-PV-BB BB = 50kWh	3.4 No forecasting 3.5 1-minute ahead PV forecasting 3.6 Perfect forecasting	

5.2 Selection of the days

Five days, covering the primary seasonal and solar irradiance variations, have been selected for the assessment. The choice of days is based on comparatively superior values for some essential metrics such as 'forecasting skill' score and root mean square error (RMSE) of the forecast irradiance compared to the measured irradiance according to the Eq. (31) and Eq. (32) [8, 12]. However, it is to be noted that the primary emphasis in this research is given on the development of an algorithm on how to use the PV irradiance forecasted data and the application of forecasting mechanism. Hence, the metrics values for different days throughout the year would have no impact on the methodological approach but DG scheduling and the consequential fuel savings.

$$RMSE_{\%}(FH) = \frac{\sqrt{\sum_{i}^{N} \left(M_i(FH) - F_i(FH)\right)^2 / N}}{\overline{M(FH)}} \tag{31}$$

$$FSS_{\%} = \left(1 - \frac{RMSE_{Forecast}}{RMSE_{Persistence}}\right) \tag{32}$$

Where, RMSE = Root-mean-square error, FSS = Forecast skill score, FH = Forecast horizon, M_i = Measurement at i-th instant, F_i = Forecast at i-th instant.

One of the selected days is a clear sky day, one is an overcast day, while the others are intermittent cloudy days, where random cloud movements have been observed. Table 3 sets out the values of the essential metrics and describes each day. The forecast root mean square error can be seen to be higher in summer than in winter, while the mean bias error represents the average deviation. The forecast skill is computed by comparing the one minute ahead

forecast with the persistence forecast. The cloud coverage represents the percentage of cloud presence in the sky, and the standard deviation indicates the variability. Figure 12 shows the measured GHI, clear sky GHI, forecast GHI, forecast DNI, forecast DHI, and persistence GHI value for all five days.

Table 3: Selection of days and weather description

Date	Root mean square error	Mean bias error	Forecast Skill	Cloud coverage (0-100)	Standard deviation of cloud coverage	Sky cloud condition	Season at Oldenburg
26 January	4.796	0.143	0.491	99.536	0.137	Overcast, cloudy	Winter, coolest month
25 February	138.503	66.706	-0.580	57.630	36.179	Mixed: overcast in the afternoon, clear in the morning	Winter, driest month
18 April	81.745	15.928	0.124	5.921	4.866	Clear sky with few irradiance drops	Spring
6 June	168.544	41.305	0.120	48.297	41.861	Mixed day with a high overcast part in the morning and clear in the afternoon	Spring, wet month
19 August	166.641	20.859	0.175	70.965	14.143	Mixed, irradiance drop throughout the day	Summer, warmest month

26 January

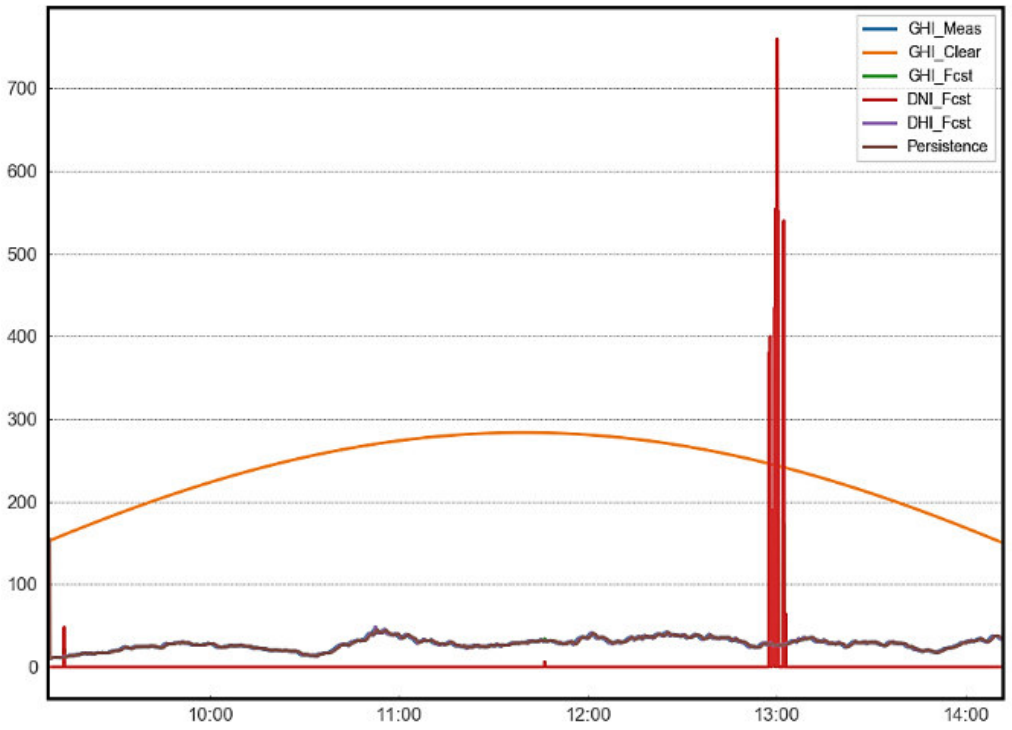

25 February

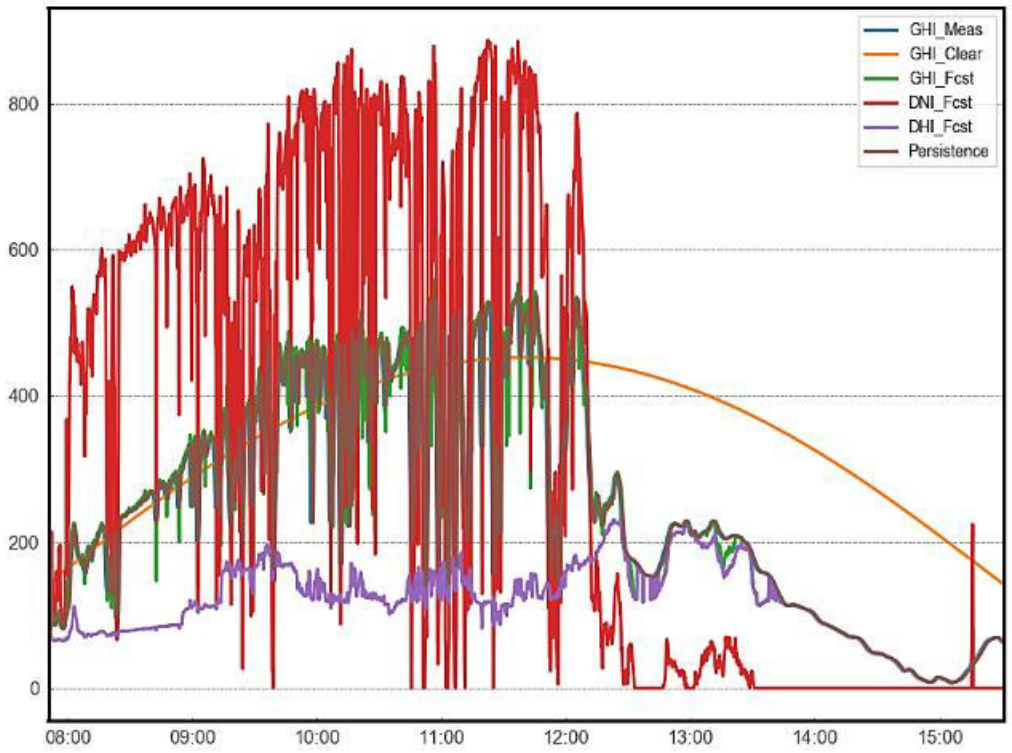

18 April

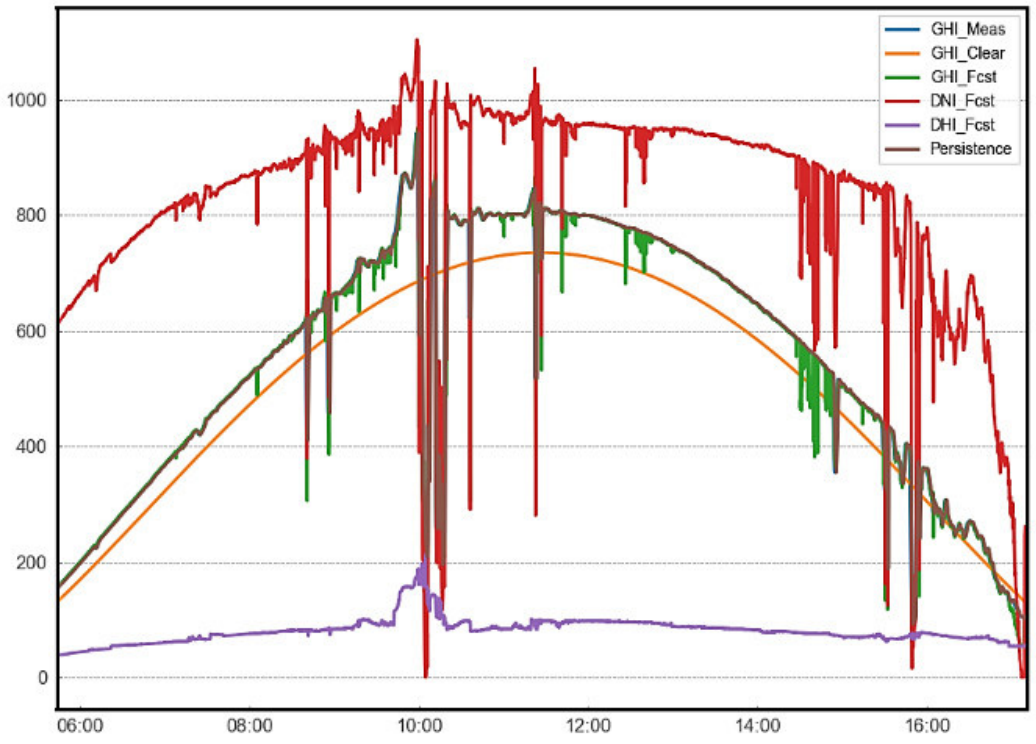

6 June

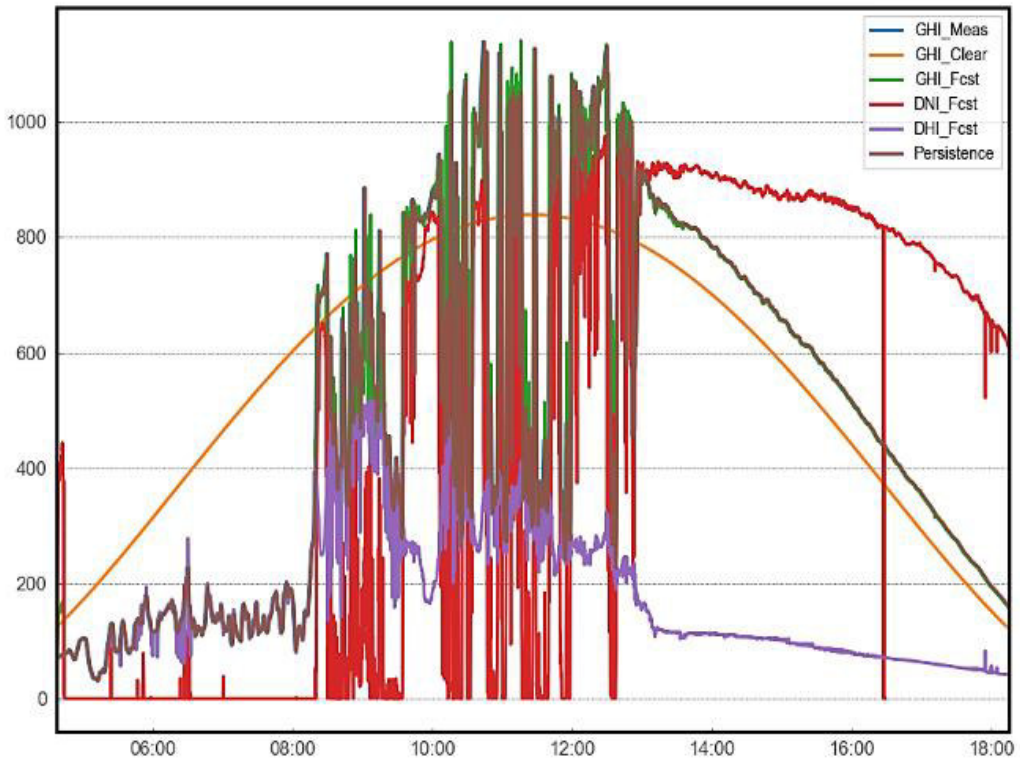

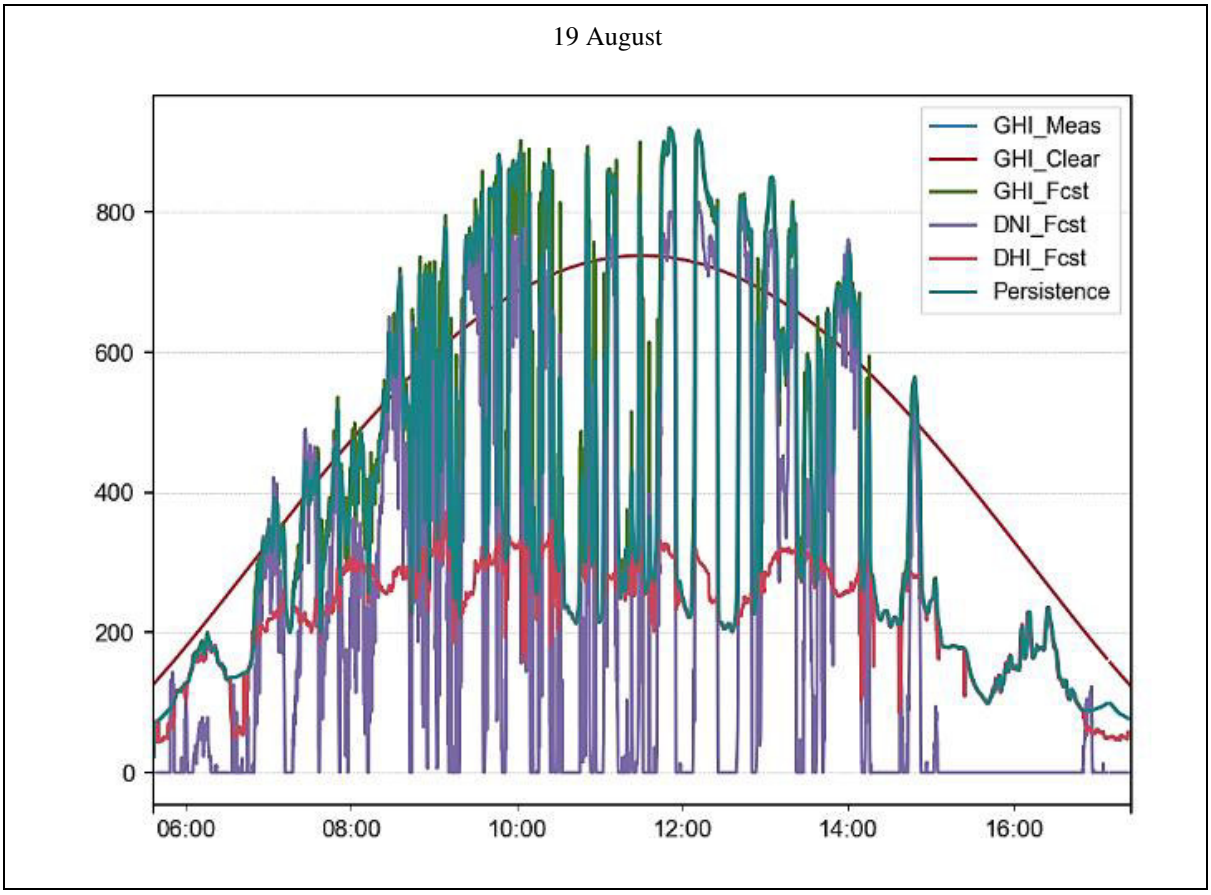

Figure 12: GHI, DHI and DNI and persistence GHI profile of 1-minute ahead GHI forecast for the five selected days

5.3 Results and Discussion

The model assesses the maximum allowable PV hosting capacity and consequent fuel consumption and PV penetration level for the five selected days, using the system configurations mentioned earlier. According to the load profile, the daily gross energy demand is 8823.06 kWh. Six 140kW DGs are available to supply the load. To meet the demand, diesel consumption is estimated to be 2186.72 litres per day for the DG only system. For the DG only configuration, the daily average number of DGs online is computed as 4.44.

For the DG-PV configuration (Case 2), the system performance is assessed after the introduction of PV forecasting strategy (table 2). The PV output power variability has a strong influence on the operation of DGs. This is very evident from the results presented in table 4, 5 and 6 and Appendix A. When PV forecasting is not employed, the injection of a relatively small amount of fluctuating PV generation into the electricity network is permitted so that it does not pose any significant technical issue to the system. This leads to the computation of the maximum allowed PV capacity that will not trigger an event leading to

the operating reserve falling below a certain amount, selected by the system operator. This study allows up to 50% of the OR to be used to cover any sudden reduction in PV power. This arbitrary level of OR inclusion has been selected for comparative purposes and is in line with what has been used in some SOPS systems by Horizon Power, a utility that supplies electricity to almost all the remote towns in Western Australia [43]. This approach is followed in this study to determine the allowed PV hosting capacity of the SOPS system.

The annual seasonal cycle strongly impacts on the annual solar irradiance pattern, and therefore the PV power output throughout the year. It follows that the PV hosting capacity for the system should be set to a safe amount which, regardless of the season, does not cause DG overload with the onset of cloud cover. Table 4 shows the PV hosting capacity determined for individual days and the final selection of PV hosting capacity for the SOPS system. Detailed results for the PV hosting capacity determined on specific days are given in appendix A. This approach establishes the PV hosting capacity to be 297kW for the DG-PV configuration (case 2) and 279kW for the DG-PV-BB configuration (case 3). These are the lowest values computed. When the batteries (BB) are integrated according to the algorithm presented, BB-RR takes part in daily energy charge/discharge activities and BB-ER provides the minimum operating reserve required. Hence, the arithmetic calculation of PV hosting capacity may vary from day to day depending on load profile, PV power fluctuation, DG scheduling and battery energy profile. A similar methodological analysis for 365 days, taking into consideration the dynamic load profile, would lead to the determination of the actual allowed PV hosting capacity for the SOPS system. This is recommended for future work.

Table 4: PV Hosting capacity determination for the SOPS system

#	System Configuration	Days	PV Hosting Capacity (kW)	Finalised PV Hosting Capacity (kW)
1	DG-only (base case scenario)	N/A	N/A	N/A
2	DG-PV	26 January	600	**297**
		25 February	299	
		18 April	454	
		6 June	**297**	
		19 August	323	
3	DG-PV-BB BB = 100kWh	26 January	600	**279**
		25 February	507	

#	System Configuration	Days	PV Hosting Capacity (kW)	Finalised PV Hosting Capacity (kW)
		18 April	432	
		6 June	**279**	
		19 August	286	
	DG-PV-BB BB = 50kWh	26 January	600	**279**
		25 February	507	
		18 April	432	
		6 June	**279**	
		19 August	286	

The application of 1-minute ahead PV forecasting informs the PSMS about the expected next minute's level of PV generation. In light of this, the PSMS dispatches the DGs in the current minute, in preparation for the next minute's instances. This strategy mitigates the technical challenges that could have arisen otherwise, by virtue of the uncertainty of the level of PV generation. This reduces the risk of a deficit in operating reserve for any future time instant, thereby allowing more PV capacity to be installed by prosumers. In this study, a high PV hosting capacity (600kW), which is higher than the maximum load of the system for the forecasting application cases (cases: 2.2-2.3, 3.2-3.3 and 3.5-3.6), is deliberately considered. It enables the BB-RR to be charged from the excess energy available during the sunshine hours. The study finds that this high PV capacity can be well integrated into the system, if 1-minute ahead PV forecasting is employed.

For simplicity, Tables 5, 6 and 7 present the analysis results of three different days, which are exposed to three different types of cloud coverage:

- 26 January (overcast day) in table 5
- 18 April (sunny day with clear sky) in table 6
- 19 August (random cloud movement throughout the day) in table 7

The tables present the values of the following parameters for each configuration cases: fuel consumption; energy supplied by both DG and PV; energy used from PV; the PV penetration level; the number of DG starts; and the average number of online DGs. The PV penetration level is calculated as the ratio between the amount of energy that is not served by the DGs and the total amount of daily energy demand. The "energy served by DGs" is the energy

served by the DGs to meet net load combined with the energy served to charge the BB at night, taking into account the energy losses in the BB system. Results for 25 February and 6 June are attached in Appendix A.

26 January (overcast day):

With the allowed PV hosting capacity being 297kW for case2 and 279kW for case 3 for the continuous overcast day (26 January) there are no unforecasted drops in PV power that lead to a reduction of operating reserve below 70 kW. This results in a PV penetration level of only 0.49% and 0.46% for cases 2.1, 3.1 and 3.4. When the maximum amount of 600kW of PV capacity is considered, the PV penetration level is found to be only 0.98% for both cases 2 and 3. As batteries are charged during the night from DGs, and the charging/discharging considers BB/inverter roundtrip efficiency, the energy served by the DGs for the higher capacity battery case is slightly higher than for the lower capacity battery case. However, the higher capacity battery case results in a lower average number of DGs online.

Table 5: Assessment of short-term PV forecasting for the overcast day of 26 January

Sl no	System configuration	Forecast strategy	Gross load demand kWh	PV hosting capacity kW	Fuel consumption L/day	Energy served by DG kWh	Energy available from PV kWh	PV energy used kWh	PV penetration level %	No. of DG starts	Average no. of DG online
1	DG-only	N/A	8823.66	N/A	2186.72	8823.66	N/A	N/A	N/A	6	4.44
2.1	DG-PV	No forecast	8823.66	297.00	2163.70	8780.63	43.02	43.02	0.49%	6	4.41
2.2		1-minute ahead forecast		600.00	2163.67	8736.74	86.91	86.91	0.98%	6	4.37
2.3		Perfect forecast		600.00	2163.84	8736.74	86.91	86.91	0.98%	5	4.37
3.1	DG-PV-100kWhBB	No forecast	8823.66	279.00	2109.16	8791.99	40.41	40.41	0.46%	5	3.26
3.2		1-minute ahead forecast		600.00	2108.85	8745.49	86.91	86.91	0.98%	6	3.25
3.3		Perfect forecast		600.00	2109.10	8745.49	86.91	86.91	0.98%	6	3.25
3.4	DG-PV-50kWhBB	No forecast	8823.66	279.00	2118.75	8787.62	40.41	40.41	0.46%	5	3.28
3.5		1-minute ahead forecast		600.00	2118.44	8741.12	86.91	86.91	0.98%	6	3.26
3.6		Perfect forecast		600.00	2118.68	8741.12	86.91	86.91	0.98%	6	3.26

18 April (sunny day with clear sky):

On 18 April, a clear sky day, the PV penetration level for case 2.1 is 19.64% (297kW). For cases 3.1 and 3.4 it is 18.45% (279kW). When the BB is not integrated, a comparison of case 1 with case 2.2 shows that, on average, one less DG is on operation throughout the day. When batteries are integrated, the PV hosting capacity is improved, as can be seen by comparing cases 2.2, 3.2 and 3.5. The inclusion of batteries and forecasting results in lowering the average number of DGs online, lowering fuel consumption, and improving PV penetration. Doubling the battery capacity from 50kWh to 100kWh does not show significant improvement in the system performance. However, it must be noted that the inclusion of battery and PV forecasting doubles the level of PV penetration from 19.64% (case 2.1) to 39.29% (cases 3.2, 3.5). In general, this doubles the fuel and cost savings.

Table 6: Assessment of short-term PV forecasting for the sunny clear sky day of 18 April

Sl no	System configuration	Forecast strategy	Gross load demand kWh	PV hosting capacity kW	Fuel consumption L/day	Energy served by DG kWh	Energy available from PV kWh	PV energy used kWh	PV penetration level %	No. of DG starts	Average no. of DG online
1	DG-only	N/A	8823.66	N/A	2186.72	8823.66	N/A	N/A	N/A	6	4.44
2.1	DG-PV	No forecast	8823.66	297.00	1772.85	7090.37	1733.29	1733.29	19.64%	10	3.88
2.2		1-minute ahead forecast		600.00	1395.69	5519.21	3501.60	3447.85	39.08%	15	3.33
2.3		Perfect forecast		600.00	1402.11	5545.70	3501.60	3376.40	38.27%	15	3.34
3.1	DG-PV-100kWhBB	No forecast	8823.66	279.00	1752.89	7205.33	1628.24	1628.24	18.45%	11	2.80
3.2		1-minute ahead forecast		600.00	1313.40	5411.98	3501.60	3466.75	39.29%	11	2.24
3.3		Perfect forecast		600.00	1320.71	5495.80	3501.60	3407.90	38.62%	12	2.26
3.4	DG-PV-50kWhBB	No forecast	8823.66	279.00	1743.62	7200.96	1628.24	1628.24	18.45%	12	2.80
3.5		1-minute ahead forecast		600.00	1324.11	5399.69	3501.60	3466.75	39.29%	12	2.27
3.6		Perfect forecast		600.00	1333.84	5469.37	3501.60	3407.90	38.62%	12	2.29

19 August (intermittent cloud cover throughout the day):

On this day, there are frequent cloud cover events (Figure 12), causing sharp net load fluctuations. Therefore, PV forecasting plays a significant role in enabling high PV

penetration levels on these intermittent cloudy days without causing any shortage in operating reserve. When 1-minute ahead PV forecasting is applied to the DG-PV-BB (100kWh) configuration (case 3.2), the average PV penetration level is 25.84%. This is almost double the amount of PV penetration for the DG-PV configuration without PV forecasting (case 2.1). Compared to the base case scenario, the DG-PV-BB (100kWh) configuration sees a reduction in average numbers of DGs online from 4.44 to 2.73. The reduced scheduling and loading of DGs results in diesel fuel savings of 27.12% for that day (comparing case 3.2 and 1). On a similar day, 6 June, the same outcome is observed (see Appendix A). The application of 1-minute ahead PV forecasting and 100kWh battery together increase the PV penetration level from 19.20% (case 2.1) to 35.79% (case 3.2). This results in a 38% fuel savings when compared to the base case configuration (case 1).

Table 7: Assessment of short-term PV forecasting for the intermittent cloud cover day of 19 August

Sl no	System configuration	Forecast strategy	Gross load demand kWh	PV hosting capacity kW	Fuel consumption L/day	Energy served by DG kWh	Energy available from PV kWh	PV energy used kWh	PV penetration level %	No. of DG starts	Average no. of DG online
1	DG-only	N/A	8823.66	N/A	2186.72	8823.66	N/A	N/A	N/A	6	4.44
2.1	DG-PV	No forecast	8823.66	297.00	1908.85	7650.68	1172.97	1172.97	13.29%	18	4.11
2.2		1-minute ahead forecast		600.00	1665.33	6622.70	2369.65	2252.63	25.53%	32	3.81
2.3		Perfect forecast		600.00	1662.24	6608.83	2369.65	2295.05	26.01%	33	3.81
3.1	DG-PV-100kWhBB	No forecast	8823.66	279.00	1871.18	7730.52	1101.89	1101.89	12.49%	20	3.01
3.2		1-minute ahead forecast		600.00	1593.69	6574.74	2369.65	2279.93	25.84%	30	2.73
3.3		Perfect forecast		600.00	1585.75	6575.72	2369.65	2310.45	26.18%	27	2.75
3.4	DG-PV-50kWhBB	No forecast	8823.66	279.00	1880.94	7726.14	1101.89	1101.89	12.49%	19	3.03
3.5		1-minute ahead forecast		600.00	1602.64	6569.88	2369.65	2279.93	25.84%	29	2.73
3.6		Perfect forecast		600.00	1596.20	6570.84	2369.65	2310.45	26.18%	26	2.75

Integration of PV-BB systems with the existing DGs, together with the application of 1-minute ahead PV forecasting delivers an improved level of PV penetration to the SOPS system, and significantly reduces the number of DGs required to be online for the whole day.

The reduced scheduling and loading of DGs save a significant amount of fuel, reducing operating and maintenance costs and benefiting the environment. On both 18 April and 6 June, it is observed that up to two less DGs are required to supply the load when the 1-minute ahead PV forecasting and BB are integrated in the configuration (case 3.2 in Figure 12). On these days, the estimated daily fuel savings are 873 litres (39.9%) and 831 litres (38%) of diesel, respectively (for case 3.2). This results in a reduction of around 2.28-2.34 tonnes of CO_2 emitted into the environment (burning 1-litre diesel = 2.68 kg of CO_2 emission). Figure 13 shows how the PV penetration level, fuel consumption and average numbers of DGs online are influenced by the BB systems and 1-minute ahead PV forecasting. From a comparative analysis, it is observed that the PV systems supplied 39.3% of the daily energy on 18 April. This amount is 35.8% and 25.8% for 6 June and 19 August, respectively. From figure 13 (a) it can be seen that the addition of 1-minute ahead PV-forecasting doubles the PV penetration level. This is the main mechanism by which PV forecasting saves diesel fuel.

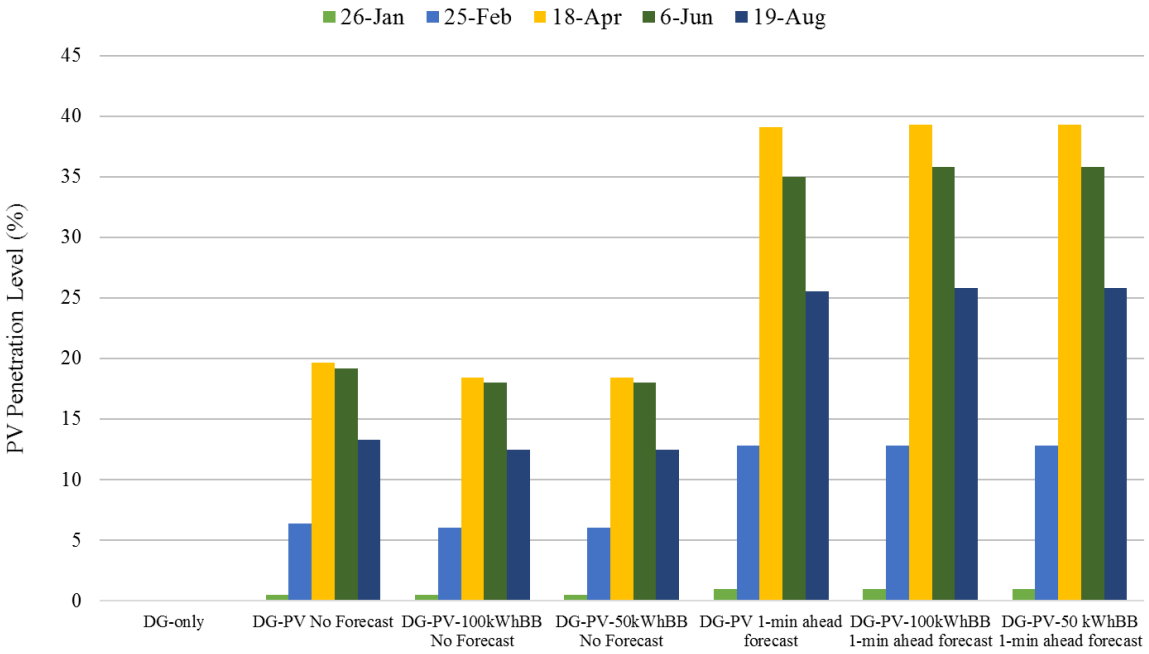

(a)

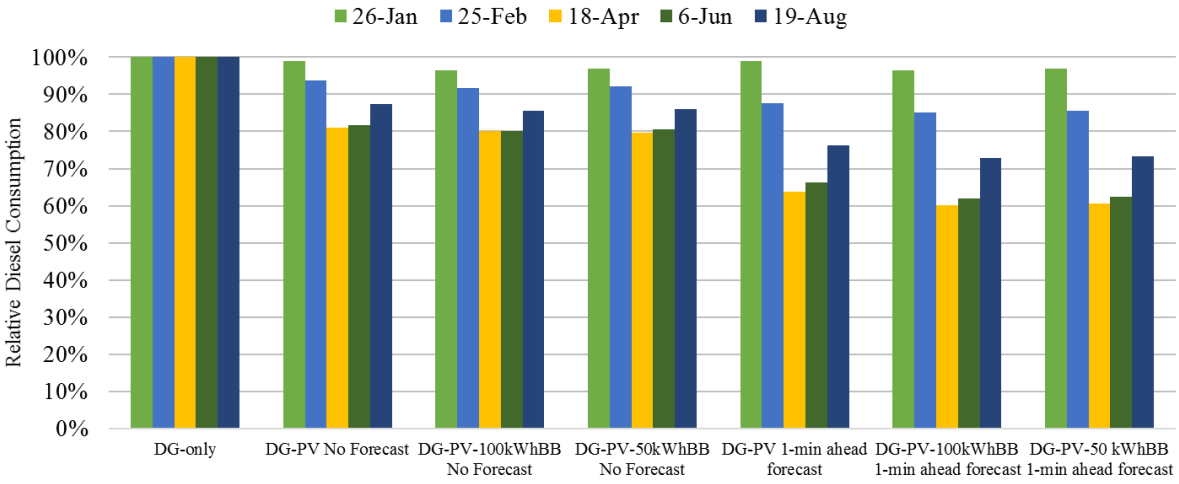

(b)

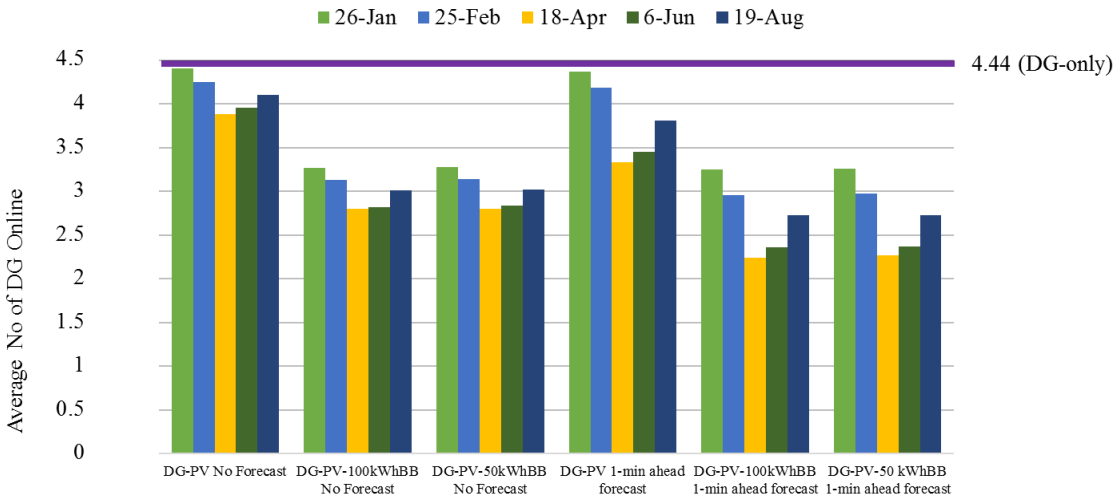

(c)

Figure 13: Influence of BB and 1-minute ahead PV forecasting on (a) PV penetration level, (b) fuel savings for various configuration cases and (c) average numbers of DGs online

The outcomes of the analysis indicate that different days exhibit differing PV penetration level and thus differing fuel savings potential. The addition of short-term PV forecasting improves the system performance by allowing much more prosumer PV capacity to be installed leading to much higher PV generation. The results can be summarised as follows:

- The tool demonstrates the benefits of having 1-minute ahead PV forecasting, compared to no forecasting. When clouds cause a sharp drop in PV power, 1-minute

ahead PV forecasting allows far more uncontrolled prosumer PV capacity to be installed without running short of operating reserve.

- Based on the five days of 1-minute ahead forecasting results analysed, the sky camera-based PV forecasting enables at least 600kW of PV capacity to be installed, whereas, with DG-PV-no forecasting, the allowed installed PV capacity is only 279kW.
- This additional 321kW of installed PV capacity saves 540.36 litres (average) of diesel fuel per day and reduces the average number of DGs online for the DG-PV-BB (100kWh, with 1-minute ahead forecast) configuration over the five days analysed.
- The addition of battery storage achieves additional fuel savings. The dual battery system increases the amount of available PV energy that can be utilised by storing excess PV energy for later use. It also reduces the required average number of online (30% minimum loaded) DGs, needed to maintain an adequate operating reserve.
- The 50kWh battery (with 1-minute ahead forecast) saves on average 530.74 litres of diesel fuel per day and also reduces the average number of DGs online over the five days analysed.
- Upsizing the battery energy capacity from 50kWh to 100kWh saves an additional 9.62 litres of diesel fuel per day (average).

The results demonstrate that the larger BB may not save sufficient fuel to justify the extra capital cost. However, the BB dispatch strategy does have a significant impact on fuel savings and there may exist more optimal battery sizing strategies to achieve fuel savings than those used in this study. To optimise the BB size (energy capacity), a thorough investigation is required, using one-minute data for the entire year for a SOPS system. It will also determine whether a dual or single battery/inverter system that provides the operating reserve (emergency backup until another DG can be started) and perhaps some additional energy storage capacity is required or not. The results in tables 5-7 and figure 13 show that application of PV forecasting and the integration of batteries benefit from one other. The literature reports many different percentage amounts of fuel-saving potential for different load and weather scenarios when the high share of PV is considered [17, 37]. However, fuel savings potential depends strongly on the available energy resource dispatch and the control strategies used to operate the system.

The results obtained in this study indicate that increasing the distributed PV to a higher penetration level could be safely managed if the design of the system is carefully chosen. It is

recommended that a high share of PV generation should be backed up with at least some BB capacity having immediate capability to take up the excess load. Care should be taken to accommodate PV forecast error as the error range varies from day to day, depending on weather conditions.

From the above discussion, it can be stated that short-term PV forecasting is a promising mechanism to allow high prosumer uncontrolled PV generation levels and reduce DG scheduling and fuel consumption. It is well demonstrated in this study that 1-minute ahead PV forecasting, using the cost-effective sky imagery-based system, offers an effective solution to address the technical challenges of high PV penetration as well as environmental issues of diesel-only systems.

6 Conclusion

This study incorporates a model that has been used to analyse the benefits of short-term PV forecasting and battery storage for different system configurations. The energy flow simulation tool developed in the study incorporates a 1-minute resolution energy flow data for a standalone off-grid power supply (SOPS) system in a remote area. The tool can assess the benefits of as short as 1-minute ahead PV forecasting using sky imager techniques to determine PV penetration level and consequential fuel savings potential for high PV integration into the system. This is a novel contribution of this study as currently, there is no other study available in the literature on the optimal temporal resolution of PV forecasting and no well-known commercially available energy flow modelling tool simulate power system operation with a resolution as high as 1-minute. The developed tool in this study is applied to three different system configurations: DG-only, DG-PV, and DG-PV-Battery for three different forecasting strategies: *no forecast*, *1-minute ahead forecast* and *perfect forecast*.

SOPS system configurations with and without battery storage system and 1-minute ahead PV forecasting have been studied to determine the potential PV hosting capacity and the consequent fuel savings. The application strategy is applied in a way that accommodates forecast errors by scheduling DGs one minute ahead of the time. However, the better the irradiance forecast performance is, the better the DG scheduling and fuel savings are. The analysis has been performed for selected days of the year in Oldenburg, Germany, where quantification of PV hosting capacity and PV penetration level, fuel-saving potential have

been estimated, and subsequent recommendations are made. For the days when random cloud movement occurs, the application of 1-minute ahead PV forecasting presents very similar results compared to the perfect forecasting (no forecast error).

Larger systems can benefit from a higher share of distributed PV, with battery and forecasting mechanisms each contributing to the maintenance of system stability with high PV penetration. It is expected that the benefits of forecast based approaches will be further enhanced by designing innovative application strategies and by utilising seasonal and cloud condition-oriented strategies within the control system. Overcoming the mentioned limitations in the development of the tool will achieve an even more precise outcome. The dispatch algorithm used in this study can be customised for each case by incorporating detailed analysis of the SOPS system size, daily load dynamics, seasonal impact on weather, and dynamic cloud movement components.

Based on the results obtained in this study, it can be seen that the integration of PV forecasting and batteries improves the system performance, where a decision has to be made to optimise the power and energy capacity of the dual battery bank system. Although the performance of the system is highly dependent on the particular geographic location, system configuration and load behaviour, the results confirm an advantage in incorporating 1-minute ahead PV forecasting. Even though the quantitative trends found in this analysis can significantly differ under other specific conditions, a general conclusion can be drawn that incorporating the 1-minute ahead forecasting can enable a significant increase in prosumer PV capacity, that reduces fuel consumption without compromising the reliability of the system.

The tool offers features appropriate to system planners or stakeholders who are keen to comprehensively understand the potential reliability of short-term PV forecasting, together with the diesel fuel savings and other potential benefits (e.g., reduced diesel generator operational costs) from short-term PV forecasting – with and without battery storage. Future work will entail refining the tool for PV-diesel-battery academic research, improving the dispatch algorithm by introducing dynamic behaviours of the modelling tool components, conducting further analysis using a location-specific one-minute data set for an entire year and then an experimental application on a real-life setup. This will provide more confidence in the reliability of the sky imagery-based PV forecasting mechanism and more accurately determine the system PV hosting capacity to be installed in a remote area SOPS system.

Acknowledgements

The authors would like to convey their gratitude to Ms. Dorothee Peters, from DLR Institute of Networked Energy Systems, Oldenburg, Germany for her constructive comments and suggestions on developing the energy flow modelling tool. A special gratitude for the "*Universities Australia/DAAD travel grant*" that supported the project "*Control strategies to maximize the Photovoltaic hosting capacity in remote diesel networks using sky camera based short-term solar forecasting techniques*" associated travel costs. A very special appreciation to the DLR Institute of Networked Energy Systems in Oldenburg, Germany for their substantial support to conduct this research.

References

[1] Jamal T, Urmee T, Calais M, Shafiullah GM, Carter C. Technical challenges of PV deployment into remote Australian electricity networks: A review. Renewable and Sustainable Energy Reviews. 2017;77:1309-25.
[2] Jamal T, Shafiullah GM, Carter C, Urmee T. A comprehensive techno-economic and power quality analysis of a remote PV-diesel system in Australia. Renew Energy Environ Sustain. 2017;2:24.
[3] Bekele G, Tadesse G. Feasibility study of small Hydro/PV/Wind hybrid system for off-grid rural electrification in Ethiopia. Applied Energy. 2012;97:5-15.
[4] Cader C, Bertheau P, Blechinger P, Huyskens H, Breyer C. Global cost advantages of autonomous solar–battery–diesel systems compared to diesel-only systems. Energy for Sustainable Development. 2016;31:14-23.
[5] Tao C, Shanxu D, Changsong C. Forecasting power output for grid-connected photovoltaic power system without using solar radiation measurement. The 2nd International Symposium on Power Electronics for Distributed Generation Systems2010. p. 773-7.
[6] Blechinger P, Cader C, Bertheau P, Huyskens H, Seguin R, Breyer C. Global analysis of the techno-economic potential of renewable energy hybrid systems on small islands. Energy Policy. 2016;98:674-87.
[7] Schmidt T, Calais M, Roy E, Burton A, Heinemann D, Kilper T, et al. Short-term solar forecasting based on sky images to enable higher PV generation in remote electricity networks. Renew Energy Environ Sustain. 2017;2:23.
[8] Schmidt T. High resolution solar irradiance forecasts based on sky images. Oldenburg, Germany: Carl von Ossietzky Universität Oldenburg; 2017.
[9] Parkinson G. What the Tesla big battery can and cannot do. 2017.
[10] Chenni R, Makhlouf M, Kerbache T, Bouzid A. A detailed modeling method for photovoltaic cells. Energy. 2007;32:1724-30.
[11] Jamal T, Shafiullah GM, Carter C, Ferdous S, Rahman MM. Benefits of Short-term PV Forecasting in a Remote Area Standalone Off-grid Power Supply System. IEEE PES General Meeting 2018. Portland, OR, USA2018.

[12] Anagnostos D, Schmidt T, Cavadias S, Soudris D, Poortmans J, Catthoor F. A method for detailed, short-term energy yield forecasting of photovoltaic installations. Renewable Energy. 2019;130:122-9.
[13] Liu L, Zhao Y, Chang D, Xie J, Ma Z, Sun Q, et al. Prediction of short-term PV power output and uncertainty analysis. Applied Energy. 2018;228:700-11.
[14] West SR, Rowe D, Sayeef S, Berry A. Short-term irradiance forecasting using skycams: Motivation and development. Solar Energy. 2014;110:188-207.
[15] Sayeef S, West S. Very short-term solar forecasting using inexpensive fisheye camera sky-imagery. In: Proceedings of the 52nd Annual Conference ASES, editor. Solar2014: The 52nd Annual Conference of the Australian Solar Council. Melbourne, Australia: Proceedings of the 52nd Annual Conference, Australian Solar Energy Society (Australian Solar Council); 2014.
[16] Schmidt T, Kalisch J, Lorenz E, Heinemann D. Evaluating the spatio-temporal performance of sky-imager-based solar irradiance analysis and forecasts. Atmos Chem Phys. 2016;16:3399-412.
[17] Olivier Liandrat, Antonin Braun, Etienne Buessler, Marion Lafuma, Sylvain Cros, Andre Gomez, et al. Sky-Imager Forecasting for Improved Management of a Hybrid Photovoltaic-Diesel System. 3rd International Hybrid Power Systems Workshop. Tenerife, Spain2018.
[18] Stefferud K, Kleissl J, Schoene J. Solar forecasting and variability analyses using sky camera cloud detection & motion vectors. Power and Energy Society General Meeting, 2012 IEEE2012. p. 1-6.
[19] Chow CW, Urquhart B, Lave M, Dominguez A, Kleissl J, Shields J, et al. Intra-hour forecasting with a total sky imager at the UC San Diego solar energy testbed. Solar Energy. 2011;85:2881-93.
[20] HOMER Energy. HOMER Pro. 2019.
[21] Natural Resources Canada. RETScreen. 2019.
[22] National Renewable Energy Laboratory. System Advisor Model (SAM) General Description (Version 2017.9.5). 2019.
[23] Reilly C. Off the grid: How renewable energy is helping remote towns take back the power. Australia2018.
[24] AECOM. Australia's Off-Grid Clean Energy Market Research Paper, Prepared for Australian Renewable Energy Agency. 2014.
[25] ARENA. Keynote address by ARENA CEO Ivor Frischknecht – Increasing renewables in remote, off-grid areas at the Remote Area Power Supply conference. 2014.
[26] Jamal T, Urmee T, Shafiullah G, Shahnia F. Using Experts' Opinions and Multi-Criteria Decision Analysis to Determine the Weighing of Criteria Employed in Planning Remote Area Microgrids. International Conference and Utility Exhibition on Green Energy for Sustainable Development. Thailand: IEEE; 2018.
[27] Bass RB, Carr J, Aguilar J, Whitener K. Determining the Power and Energy Capacities of a Battery Energy Storage System to Accommodate High Photovoltaic Penetration on a Distribution Feeder. IEEE Power and Energy Technology Systems Journal. 2016;3:119-27.
[28] McConnell D. Hornsdale Power Reserve, SA's battery is massive, but it can do much more than store energy. Australia2017.
[29] Tazvinga H, Xia X, Zhang J. Minimum cost solution of photovoltaic–diesel–battery hybrid power systems for remote consumers. Solar Energy. 2013;96:292-9.
[30] Rodríguez-Gallegos CD, Gandhi O, Bieri M, Reindl T, Panda SK. A diesel replacement strategy for off-grid systems based on progressive introduction of PV and batteries: An Indonesian case study. Applied Energy. 2018;229:1218-32.
[31] Salas V, Suponthana W, Salas RA. Overview of the off-grid photovoltaic diesel batteries systems with AC loads. Applied Energy. 2015;157:195-216.

[32] Elsinga B, van Sark WGJHM. Short-term peer-to-peer solar forecasting in a network of photovoltaic systems. Applied Energy. 2017;206:1464-83.
[33] Chaudhary P, Rizwan M. Energy management supporting high penetration of solar photovoltaic generation for smart grid using solar forecasts and pumped hydro storage system. Renewable Energy. 2018;118:928-46.
[34] Litjens GBMA, Worrell E, van Sark WGJHM. Assessment of forecasting methods on performance of photovoltaic-battery systems. Applied Energy. 2018;221:358-73.
[35] Moshövel J, Kairies K-P, Magnor D, Leuthold M, Bost M, Gährs S, et al. Analysis of the maximal possible grid relief from PV-peak-power impacts by using storage systems for increased self-consumption. Applied Energy. 2015;137:567-75.
[36] Angenendt G, Zurmühlen S, Axelsen H, Sauer DU. Comparison of different operation strategies for PV battery home storage systems including forecast-based operation strategies. Applied Energy. 2018;229:884-99.
[37] Peters D, Kilper T, Calais M, Jamal T, von Maydell K. Solar Short-Term Forecasts for Predictive Control of Battery Storage Capacities in Remote PV Diesel Networks. Transition Towards 100% Renewable Energy: Selected Papers from the World Renewable Energy Congress WREC 2017. Cham: Springer International Publishing; 2018. p. 325-33.
[38] Mazzola S, Vergara C, Astolfi M, Li V, Perez-Arriaga I, Macchi E. Assessing the value of forecast-based dispatch in the operation of off-grid rural microgrids. Renewable Energy. 2017;108:116-25.
[39] Saleh M, Meek L, Masoum MAS, Abshar M. Battery-Less Short-Term Smoothing of Photovoltaic Generation Using Sky Camera. IEEE Transactions on Industrial Informatics. 2018;14:403-14.
[40] Jamal T, Shoeb MA, Shafiullah GM, Carter CE, Urmee T. A design consideration for solar PV-diesel remote electricity network: Australia perspective. 2016 IEEE Innovative Smart Grid Technologies - Asia (ISGT-Asia)2016. p. 821-6.
[41] Erbs D, Klein S, Duffie J. Estimation of the diffuse radiation fraction for hourly, daily, and monthly-average global radiation. Solar Energy. 1982;28.
[42] Rohani G, Nour M. Techno-economical analysis of stand-alone hybrid renewable power system for Ras Musherib in United Arab Emirates. Energy. 2014;64:828-41.
[43] Jamal T. Verbal communication with Mr.Craig Carter (Adjunct Professor at Murdoch University, Australia and Industry Expert). 2018.

APPENDIX A

Individual Daily Results:

26 January:

Sl no	System configuration	Forecast strategy	Gross load demand	PV hosting capacity	Fuel consumption	Energy served by DG	Energy available from PV	PV energy used	PV penetration level	No. of DG starts	Average no. of DG online
			kWh	kW	L/day	kWh	kWh	kWh	%		
1	DG-only	N/A	8823.66	N/A	2186.72	8823.66	N/A	N/A	N/A	6	4.44
2	DG-PV	No forecast	8823.66	600.00	2163.70	8736.72	86.91	86.91	0.99%	6	4.41
		1-minute ahead		600.00	2163.67	8736.74	86.91	86.91	0.99%	6	4.37
		Perfect forecast		600.00	2163.84	8736.74	86.91	86.91	0.99%	5	4.37
3	DG-PV-100kWhBB	No forecast	8823.66	600.00	2109.16	8745.49	86.91	86.91	0.99%	5	3.26
		1-minute ahead		600.00	2108.85	8745.49	86.91	86.91	0.98%	6	3.25
		Perfect forecast		600.00	2109.10	8745.49	86.91	86.91	0.98%	6	3.25
	DG-PV-50kWhBB	No forecast	8823.66	600.00	2118.75	8745.49	86.91	86.91	0.99%	5	3.28
		1-minute ahead		600.00	2118.44	8741.12	86.91	86.91	0.98%	6	3.26
		Perfect forecast		600.00	2118.68	8741.12	86.91	86.91	0.98%	6	3.26

25 February:

Sl no	System configuration	Forecast strategy	Gross load demand	PV hosting capacity	Fuel consumption	Energy served by DG	Energy available from PV	PV energy used	PV penetration level	No. of DG starts	Average no. of DG online
			kWh	kW	L/day	kWh	kWh	kWh	%		
1	DG-only	N/A	8823.66	N/A	2186.72	8823.66	N/A	N/A	N/A	6	4.44
2	DG-PV	No forecast	8823.66	299.00	2050.77	8255.36	568.27	568.27	6.44%	14	4.25
		1-minute ahead		600.00	1916.19	7685.61	1140.33	1131.20	12.82%	18	4.19
		Perfect forecast		600.00	1917.62	7685.70	1140.33	1140.33	12.92%	19	4.13
3	DG-PV-100kWhBB	No forecast	8823.66	507.00	1903.58	7777.32	963.58	963.58	10.92%	15	3.05
		1-minute ahead		600.00	1860.13	7692.07	1140.33	1131.20	12.82%	19	2.96
		Perfect forecast		600.00	1860.66	7692.07	1140.33	1140.33	12.92%	19	2.97
	DG-PV-50kWhBB	No forecast	8823.66	507.00	1913.09	7819.62	963.58	963.58	10.92%	15	3.05
		1-minute ahead		600.00	1869.72	7679.79	1140.33	1131.20	12.82%	19	2.97
		Perfect forecast		600.00	1870.24	7687.70	1140.33	1140.33	12.92%	19	2.98

18 April:

Sl no	System configuration	Forecast strategy	Gross load demand	PV hosting capacity	Fuel consumption	Energy served by DG	Energy available from PV	PV energy used	PV penetration level	No. of DG starts	Average no. of DG online
			kWh	kW	L/day	kWh	kWh	kWh	%		
1	DG-only	N/A	8823.66	N/A	2186.72	8823.66	N/A	N/A	N/A	6	4.44
2	DG-PV	No forecast	8823.66	454.00	1555.50	6177.28	2649.54	2649.54	30.03%	9	3.60
		1-minute ahead		600.00	1395.69	5519.21	3501.60	3447.85	39.08%	15	3.33
		Perfect forecast		600.00	1402.11	5545.70	3501.60	3376.40	38.27%	15	3.34
3	DG-PV-100kWhBB	No forecast	8823.66	432.00	1534.66	6233.89	2521.15	2521.15	28.57%	10	2.54
		1-minute ahead		600.00	1313.40	5411.98	3501.60	3466.75	39.29%	11	2.24
		Perfect forecast		600.00	1320.71	5495.80	3501.60	3407.90	38.62%	12	2.26
	DG-PV-50kWhBB	No forecast	8823.66	432.00	1543.81	6272.66	2521.15	2521.15	28.57%	9	2.55
		1-minute ahead		600.00	1324.11	5399.69	3501.60	3466.75	39.29%	12	2.27
		Perfect forecast		600.00	1333.84	5469.37	3501.60	3407.90	38.62%	12	2.29

6 June:

Sl no	System configuration	Forecast strategy	Gross load demand	PV hosting capacity	Fuel consumption	Energy served by DG	Energy available from PV	PV energy used	PV penetration level	No. of DG starts	Average no. of DG online
			kWh	kW	L/day	kWh	kWh	kWh	%		
1	DG-only	N/A	8823.66	N/A	2186.72	8823.66	N/A	N/A	N/A	6	4.44
2	DG-PV	No forecast	8823.66	297.00	1785.30	7129.29	1694.37	1694.37	19.20%	19	3.95
		1-minute ahead		600.00	1449.69	5733.62	3422.97	3096.78	35.10%	22	3.45
		Perfect forecast		600.00	1475.19	5754.35	3422.97	3126.88	35.44%	23	3.47
3	DG-PV-100kWhBB	No forecast	8823.66	279.00	1752.82	7240.72	1591.68	1591.68	18.04%	17	2.82
		1-minute ahead		600.00	1355.71	5678.72	3422.97	3158.36	35.79%	15	2.36
		Perfect forecast		600.00	1358.97	5690.97	3422.97	3197.70	36.24%	16	2.38
	DG-PV-50kWhBB	No forecast	8823.66	279.00	1762.55	7236.35	1591.68	1591.68	18.04%	17	2.84
		1-minute ahead		600.00	1365.33	5674.34	3422.97	3158.36	35.79%	16	2.37
		Perfect forecast		600.00	1368.46	5686.59	3422.97	3197.70	36.24%	17	2.38

19 August:

Sl no	System configuration	Forecast strategy	Gross load demand	PV hosting capacity	Fuel consumption	Energy served by DG	Energy available from PV	PV energy used	PV penetration level	No. of DG starts	Average no. of DG online
			kWh	kW	L/day	kWh	kWh	kWh	%		
1	DG-only	N/A	8823.66	N/A	2186.72	8823.66	N/A	N/A	N/A	6	4.44
2	DG-PV	No forecast	8823.66	323.00	1885.18	7548.00	1275.66	1275.66	14.46%	22	4.09
		1-minute ahead		600.00	1665.33	6622.70	2369.65	2252.63	25.53%	32	3.81
		Perfect forecast		600.00	1662.24	6608.83	2369.65	2295.05	26.01%	33	3.81
3	DG-PV-100kWhBB	No forecast	8823.66	286.00	1864.14	7613.25	1129.53	1129.53	12.80%	17	2.99
		1-minute ahead		600.00	1593.69	6574.74	2369.65	2279.93	25.84%	30	2.73
		Perfect forecast		600.00	1585.75	6575.72	2369.65	2310.45	26.18%	27	2.75
	DG-PV-50kWhBB	No forecast	8823.66	286.00	1873.87	7653.67	1129.53	1129.53	12.80%	16	3.01
		1-minute ahead		600.00	1602.64	6569.88	2369.65	2279.93	25.84%	29	2.73
		Perfect forecast		600.00	1596.20	6570.84	2369.65	2310.45	26.18%	26	2.75

After finalising the PV hosting capacity, the following tables represent the days for 25 February and 6 June:

25-Feb

Sl no	System configuration	Forecast strategy	Gross load demand	PV hosting capacity	Fuel consumption	Energy served by DG	Energy available from PV	PV energy used	PV penetration level	No. of DG starts	Average no. of DG online
			kWh	kW	L/day	kWh	kWh	kWh	%		
1	DG-only	N/A	8823.66	N/A	2186.72	8823.66	N/A	N/A	N/A	6	4.44
2	DG-PV	No forecast	8823.66	297.00	2051.63	8259.19	564.46	564.46	6.40%	14	4.25
		1-minute ahead forecast		600.00	1916.19	7685.61	1140.33	1131.20	12.82%	18	4.19
		Perfect forecast		600.00	1917.62	7685.70	1140.33	1140.33	12.92%	19	4.13
3	DG-PV-100kWhBB	No forecast	8823.66	279.00	2004.34	8302.15	530.25	530.25	6.01%	11	3.13
		1-minute ahead forecast		600.00	1860.13	7692.07	1140.33	1131.20	12.82%	19	2.96
		Perfect forecast		600.00	1860.66	7692.07	1140.33	1140.33	12.92%	19	2.97
	DG-PV-50kWhBB	No forecast	8823.66	279.00	2013.97	8297.78	530.25	530.25	6.01%	11	3.14
		1-minute ahead forecast		600.00	1869.72	7679.79	1140.33	1131.20	12.82%	19	2.97
		Perfect forecast		600.00	1870.24	7687.70	1140.33	1140.33	12.92%	19	2.98

6-Jun

Sl no	System configuration	Forecast strategy	Gross load demand	PV hosting capacity	Fuel consumption	Energy served by DG	Energy available from PV	PV energy used	PV penetration level	No. of DG starts	Average no. of DG online
			kWh	kW	L/day	kWh	kWh	kWh	%		
1	DG-only	N/A	8823.66	N/A	2186.72	8823.66	N/A	N/A	N/A	6	4.44
2	DG-PV	No forecast	8823.66	297.00	1785.30	7129.29	1694.37	1694.37	19.20%	19	3.95
		1-minute ahead forecast		600.00	1449.69	5733.62	3422.97	3096.78	35.10%	22	3.45
		Perfect forecast		600.00	1475.19	5754.35	3422.97	3126.88	35.44%	23	3.47
3	DG-PV-100kWhBB	No forecast	8823.66	279.00	1752.82	7240.72	1591.68	1591.68	18.04%	17	2.82
		1-minute ahead forecast		600.00	1355.71	5678.72	3422.97	3158.36	35.79%	15	2.36
		Perfect forecast		600.00	1358.97	5690.97	3422.97	3197.70	36.24%	16	2.38
	DG-PV-50kWhBB	No forecast	8823.66	279.00	1762.55	7236.35	1591.68	1591.68	18.04%	17	2.84
		1-minute ahead forecast		600.00	1365.33	5674.34	3422.97	3158.36	35.79%	16	2.37
		Perfect forecast		600.00	1368.46	5686.59	3422.97	3197.70	36.24%	17	2.38